SURFACE ELECTRON PROPERTIES AND CATALYTIC ACTIVITY OF PEROVSKITE-TYPE MIXED OXIDES (ABO_3) CONSISTING OF RARE EARTH AND 3d TRANSITION METALS

THESIS SUBMITTED TO THE
COCHIN UNIVERSITY OF SCIENCE AND TECHNOLOGY
IN PARTIAL FULFILMENT OF THE
REQUIREMENTS FOR THE DEGREE OF

DOCTOR OF PHILOSOPHY

IN

CHEMISTRY

IN THE FACULTY OF SCIENCE

By

V. MEERA

DEPARTMENT OF APPLIED CHEMISTRY
COCHIN UNIVERSITY OF SCIENCE AND TECHNOLOGY
KOCHI - 682 022, INDIA

JULY 1995

CERTIFICATE

This is to certify that the thesis bound herewith is an authentic record of research work carried out by the authour under my supervision, in partial fulfilment of the requirements for the degree of Doctor of Philosophy of Cochin University of Science and Technology, and further that, no part thereof has been presented before for any other degree.

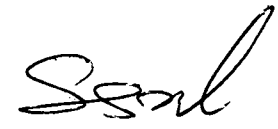

Dr.S.Sugunan
(Supervisinng Teacher)
Professor in Physical Chemistry,
Department of Applied Chemistry,
Cochin University of Science & Technology

Kochi 682 022

24-07-1995.

CONTENTS

CHAPTER 1
INTRODUCTION

INTRODUCTION

Perovskite-type oxides constitute a group of isomorphic compounds with a cubic structure and unit formula ABO_3 [1]. The larger cation A, situated at the centre of the cube, is twelve-coordinated with the oxide ions. The B cations occupy the corners of the cube and are in six-fold (octahedral) coordination with the anions. The oxygen atoms situated at the midpoints of the edges are each surrounded by two cations in position B and four cations in position A as shown in Fig.1.

The simple cubic structure and atomic arrangement was first found for the mineral perovskite $CaTiO_3$. But $CaTiO_3$ was later determined to be orthorhombic by Megaw [2]. Through the years, it has been found that very few perovskite-type oxides have the simple cubic structure at room temperature, but many assume this ideal structure at high temperatures. Apart from the idealized cubic structure, tetragonal (eg. $BaTiO_3$) rhombohedral ($LaAlO_3$, $LaNiO_3$ etc.), orthorhombic ($GdFeO_3$, $LaFeO_3$, $LaMnO_3$ etc.), monoclinic ($AgCuF_3$, $PbSnO_3$) and triclinic ($BiMnO_3$, $BiScO_3$) perovskites are also known.

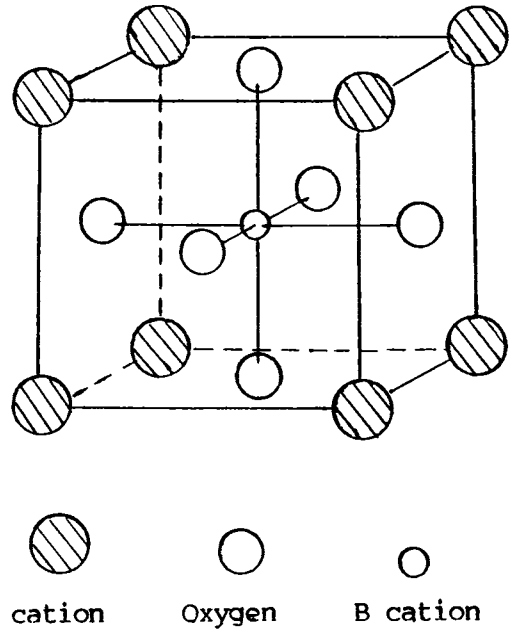

Fig.1: Perovskite structure, ABO_3

Assuming that the structure is formed by packing of spherical ions, the following relationship should hold when,

$$R_A + R_O = t\sqrt{2(R_B + R_O)}$$

R_A, R_B and R_O are the ionic radii of A, B and oxygen ions respectively; and t is a tolerance factor [3]. With simple ternary compounds, t = 0.9 to 1.0 generally yields pure

perovskite structure. When t = 0.8 to 0.9, distorted perovskite lattices result. With the more complex compounds of this process somewhat wider departure from this idealised picture may occur, particularly when ions deviating in size from the ideal are present in small proportions.

Practically all the natural metallic elements of the periodic table are stable in a perovskite oxide structure. This, together with the possibility of synthesising multicomponent perovskites by partial substitution of cations in positions A and B, accounts for the ample diversity of properties which these compounds exhibit. The position A in the structure is most frequently filled by alkaline, alkaline earth or rare earth (Ln) ions, although, other cations may have the proper size for occupation of these sites. Lanthanide cations may also be placed in B sites. Thus, interlanthanide perovskites where lanthanide cations occupy both A and B positions have been described [4].

Though the most numerous and most interesting compounds with the perovskite structure are the oxides, some hydrides, carbides, halides and nitrides also

crystallise with this structure [5]. It is interesting to remember that perovskitic materials are probably the predominant minerals in the earth's lower mantle. This is a region extending from a depth of about 670 km to about 2,900 km and constituting an important part of the total earth volume [6].

The use of perovskite-type oxides as catalysts and their central place in efforts to correlate solid state chemistry and catalysis and in attempts to tailor catalysts to meet specific demands establish these oxides as model systems in the science of catalytic materials. The properties of perovskites that are important in catalysis are primarily the stability of mixed valence states of Co, Mn, Ti etc. in the perovskite structure, the stabilization of unusual valence states, the mobility of oxygen ions and the stabilization of noble metals in high dispersion. They are very adaptable, encompassing electronic high temperature superconductors, diamagnetic, ferromagnetic, ferroelectric insulators and semiconductors [7].

Many of the perovskites are noted for their high electrical resistivities, which make them useful as dielectric materials. However, some of the perovskite type

phases such as $CaMoO_3$, $SrMoO_3$, $LaTiO_3$ and $LaVO_3$ which contain B ions in lower than their most suitable oxidation state and $La_{1-x}Sr_xMnO_3$, $SrTiO_{3-x}$, $SrVO_{3-x}$ and $Ba_{1-x}La_xTiO_3$ which contain the B ions in two valence states, are considered to be fairly good conductors or semiconductors. Probably the best conductors are the tungsten bronzes with the cubic perovskite structure [8]. Sweedler et al [9] investigated superconductivity in the tungsten bronzes. While Na, K, Rb and Cs tungsten bronzes were found to be superconductors, no perovskite bronzes were observed to be superconductors. Superconductivity has also been observed in reduced strontium titanate [10] and reduced phases in the system $(Ba_xSr_{1-x})TiO_3$ and $(Ca_ySr_{1-y})TiO_3$ when $x = 0.1$ and $y = 0.3$ [11]. Some perovskites can be used as oxygen sensors. These types of sensors utilise electrical conductivity changes due to oxygen adsorption or desorption [12].

In addition to the general well known and important properties of certain perovskitic materials they possess some other properties that can be exploited for different practical purposes and applications. They are of interest in selective oxidation and reduction processes.

Cobaltate perovskites were suggested as substitutes for noble metals in electrocatalysis [13] and automotive exhaust [14] catalysis. The preferred catalysts for the use of "catalytic afterburners" are Pt and Pt-Pd alloys. But it is recognized that this use constitutes a heavy burden on the continued availability of noble metals [15]. Substitute catalysts include primarily noble metal oxides, but these suffer from relatively low catalytic activity, low thermal stability, and often lack of chemical stability in the exhaust environment [16]. The use of perovskite-type oxides avoids several of these objections, and these oxides have been investigated widely for this purpose, particularly perovskite of Co and Mn. Thus these materials play a vital role in pollution control.

Libby and Pedersen [17,18] have reported the activity of $LnCoO_3$ perovskites (Ln = La, Nd, Dy) for cis-2-butene hydrogenation. Hydrogenolysis became important above 200°C. The hydrogenation and hydrogenolysis of several hydrocarbons on unsupported or La_2O_3 - supported $LaCoO_3$ were also reported [19-21].

Perovskite type $LaTiO_3$ has been suggested for application in the reduction of SO_2 to elemental sulphur

[22]. $SrTiO_3$ and other perovskites are being studied as photocatalysts in the decomposition of H_2O [23,24].

For the use of perovskites in fundamental and applied studies of catalytic processes, the presence of point defects and of nonstoichiometry is of great importance. These include A-cation vacancies, B-cation vacancies and anion vacancies. The presence of interstitial protons and of substitutional anion defects will be disregarded.

The existence of nonstoichiometry in the A site is effectively demonstrated by the tungsten bronzes Na_xWO_3 in which a large fraction of the A sites are vacant [25]. There are many homologues of their compounds in which other alkali ions occupy A sites [26].

The presence of B site vacancies is rare in the perovskites, but is for electrostatic reasons most likely when the charge on the B ion is low (for trivalent B ions). They have been proposed for the $(Pb,La)TiO_3$ solid solutions [27].

Nonstoichiometry due to oxygen vacancies are important in intrafacial catalysis. Small values of oxygen

deficiencies are more likely to represent isolated oxygen vacancies. These occur in the nonstoichiometric and conducting blue $BaTiO_3$ produced by reduction [28,29].

It is observed that the most frequently studied perovskites in heterogeneous catalysis are those with a lanthanide element in position A and a first row transition metal in position B. Although the lanthanide cation is generally considered to have only a modifying effect, nevertheless in some instances, it may play a more direct role in catalysis [30]. Temperature programmed reduction (TPR) studies carried out on a series of $LaMO_3$ oxides (M=Cr, Mn, Fe and Ni) showed the increased stability of transition metal cations in perovskite structure [31,32].

An interesting aspect of rare earth perovskites ($LnMO_3$) is that one is able to vary the dimensions of the unit cell by varying the lanthanide ion. Changes in the crystal dimension may be expected to produce variation in the Ln-O and M-O interactions. It would be interesting, therefore, to study the effect of the rare earth ion on the catalytic activity of rare earth transition metal mixed oxides.

To design an effective solid state catalyst, the relation should be known between the physical properties of the solid and the rate of chemical processes at its surface. However, the relation between the physical properties of the bulk and those of the surface is sparse. Attempts have been made to investigate the surface electron properties and basicity/acidity of ABO_3-type oxides with lanthanide (A=La, Pr and Sm) and transition metal cations (B=Cr, Mn, Fe, Co and Ni) and correlation of these surface properties with their catalytic activity.

REFERENCES

1. F.S. Galasso : "Strucutre, Properties and Preparation of Perovskite-type Compounds", International series of monographs in solid state Physics, vol.5, (Eds. R.Smoluchowski and N. Kurti), 1 st edn., p 3, Pergamon Press, Oxford, (1969).

2. H.D. Megaw : *Proc. Phys. Soc.*, 58, 133, 326 (1946).

3. V.M. Goldschmidt : *Skr. Nor. Videnk.-Acad., Kl 1: Mat.-Naturvidensk,* Kl.No. 8 (1926).

4. U.Berndt, D. Maier and C. Keller : *J. Solid State Chem.*, 13, 131 (1975).

5. F.S. Galasso : "Strucutre, Properties and Preparation of Perovskite-type Compounds", International series of monographs in Solid State Physics, vol.5, (Eds. R.Smoluchowski and N. Kurti), 1 st edn., p 183, Pergamon Press, Oxford, (1969).

6. R.M. Hazen : *Scient. Amer.* 75 258 (1988).

7. "Advanced Materials in Catalysis", Materials Science Series, (Eds. J.J. Burton and R.L. Garten), Academic Press, New York, p 130, (1977).

8. F.S. Galasso : "Strucutre, Properties and Preparation of Perovskite-type Compounds", International series of monographs in Solid State Physics, vol.5, (Ed. R.Smoluchowski and N. Kurti), 1 st edn., p 60, Pergamon Press, Oxford, (1969).

9. A.R. Sweedler, C.J. Raub and B.T. Matthias : *Phys. Lett.*, 15, 108 (1956).

10 J.F. Schooley, W.R. Hosler and M.L. Cohen : *Phys. Rev. Lett.*, 12, 474 (1964).

11. A.R. Mackintosh : *J. Chem. Phys.*, 38, 1991 (1963).

12. Y. Shimizu, Y. Fukuyama, T. Narikiyo, H. Arai and T. Seiyama : *Chem. Lett.*, 377 (1985).

13. D.B. Meadowcroft : *Nature*, 226, 847 (1970).

14. W.F. Libby : *Science*, 171, 499 (1971).

15. National Materials Advisory Board, Report of the panel on catalyst for automotive emission devices and petroleum refining, Rep. NMAB-297, Washington, D.C., (1973).

16. J. Wei : *Adv. Catal.* 24, 57 (1975).

17. W.F. Libby : *Science,* 171, 499 (1971).

18. L.A. Pederson and W.F. Libby : *Science,* 176, 1355 (1972).

19. M.N. Nudel, B.S. Umansky and E.A. Lombardo : *Appl. Catal.,* 31, 275, (1987).

20. M.A. Ulla, E.E. Miro and E.A. Lombardo : *Proc. Iberoam. Symp. Catal.*, 8th, La Rabida, Spain, 475 (1982).

21. J.O. Petunchi, J.L. Nicastro and E.A. Lombardo : *Chem. Commun.*, 467 (1980).

22. J. Happel, M.A. Hnatow, L. Bajars and M. Kundrath : *Ind. Eng. Chem., Prod. Res. Dev.*, 14, 155 (1975).

23. J.H. Kennedy and Fresse K.W. Jr. : *J. Electrochem Soc.,* 123, 1683 (1976).

24. J.G. Mavroides, D.I. Tehernev, J.A. Kafalas and D.F. Kolesar : *Mater. Res. Bull.,* 10, 1023 (1975).

25. P.G. Dickens and M.S. Whittingham : *Quart. Rev.* (London), 22, 30 (1968).

26. J.B. Goodenough and T.M. Longo : "Landolt-Bornstein New

Series", Vol.4, Part a, p 126-314, Springer-verlag, Berlin, (1970).

27. D. Hennings and G. Rosenstein : *Mater. Res. Bull.*, 7, 1505 (1972).

28. E.K. Weise and I.A. Lesk : *J. Chem. Phys.*, 21, 801 (1953).

29. S.A. Long and R.N. Blumenthal : *J. Am. Chem. Soc.*, 54, 515, (1971).

30. L.G. Tejuka : *J. Less Common Metals,* 146, 261, (1989).

31. J.L.G. Fierro, L.G. Tejuka : *J. Catal.*, 87, 126 (1984).

32. L. Wachowski, S. Zielinski and A. Burewicz : *Acta. Chim. Acad. Sci. Hung.*, 106, 217 (1981).

CHAPTER 2
SURFACE ELECTRON PROPERTIES OF METAL OXIDES

SURFACE ELECTRON PROPERTIES OF METAL OXIDES

2.1 ELECTRON DONOR-ACCEPTOR PROPERTIES

The adsorption of electron acceptors/donors on metal oxides has been investigated to estimate the electron donor/acceptor properties of metal oxides and their characterisation [1-4]. It is well-known that when strong electron acceptors or donors are adsorbed on metal oxides, the corresponding radicals are formed as a result of electron transfer [5,6]. By measuring the concentrations of the radicals formed, the electron donor-acceptor properties of metal oxides have been evaluated [2,3,7].

The electron donor strength of a metal oxide can be defined as the conversion power of an electron acceptor adsorbed on the surface onto its anion radical. If a strong electron acceptor is adsorbed on the metal oxide, its anion radical is formed at every donor site available on the metal oxide surface. On the other hand, if a weak electron acceptor is adsorbed, the formation of anion radical will be expected only at the strong donor sites. In the case of a very weak electron acceptor adsorption, its anion radical will not be formed even at the strongest donor sites.

The electron donating power of titania surface was evaluated by adsorption of electron acceptors with electron affinities ranging from 1.26 to 2.84 eV from acetonitrile solution onto a titania sample [8]. The concentration of radical anions formed on the titania surface, as a result of electron transfer from the surface of titania to the acceptors decreased with the decreasing electron affinity of the acceptors. The decrease was steepest between 1.26 and 1.77 eV. These results suggest that the limit of electron transfer from the titania surface to the acceptor ranged between 1.77 and 1.26 eV in terms of the electron affinity of the acceptor. Therefore, the electron donor strength on a metal oxide can be expressed as the limiting electron affinity value at which free anion radical formation is not observed at the metal oxide surface.

Adsorption of tetrachloro-p-benzoquinone (chloranil) from basic and acidic solvents on metal oxides, such as alumina and titania was carried out to understand the acid-base interaction at the interface [9]. The amount of chloranil adsorbed decreased with an increase of acid-base interaction between the basic solvent and chloranil and also, decreased with an increase of acid-base

interaction between the acidic solvent and electron donor sites of the metal oxides. Furthermore, the change in concentration of chloranil radicals formed was correlated with the acid-base interaction at the interfaces. Esumi et al. [10,11] have examined the adsorption of a strong electron acceptor such as tetracyanoquinodimethane (TCNQ) from various solvents on metal oxides and they have demonstrated that the acid-base interaction is an important factor for the adsorption.

The acid-base theory has also been applied to colloidal systems. Fowkes et al. [12,13] have studied the interaction between inorganic solids and basic adsorbates by using the Drago-correlation of the heat of acid-base interaction and have determined the Drago parameters for several solids such as silica, rutile and magnetite.

It has been reported [14-19] that the surface of metal oxides contain various types of hydroxyl groups. It should be anticipated that the various surface hydroxyl ions might have an energy distribution corresponding to those found for the electron donor sites. Flockhart et al. [20] studied the electron donor properties of alumina surface and concluded that the electron donor sites

originated from unsolvated hydroxide ions for the samples activated at lower temperatures, but from defect centres involving oxide ions, for the samples activated at higher temperatures.

Flockhart et al. [21] obtained experimental evidence for the presence of electron donor sites on the surface of alumina by electron spin resonance technique.

The presence of electron deficient centres on strongly dehydrated alumina surface sufficiently powerful to promote the formation of positive radical ions from aromatic hydrocarbons has also been demonstrated [22-27]. Chemisorption of O_2 on MgO was observed under conditions which involve different types of electron transfer processes, either from electron donor centres formed by irradiation or by addition of extrinsic impurity ions [28-31]. CO_2 was adsorbed as CO_2^- ions by electron transfer from S centres in irradiated MgO [32]. A.J.Tench and R.L.Nelson studied the adsorption of nitro compounds on the surface of MgO powder by ESR and reflectance spectroscopy [33]. They found that the negative radicals were formed on the clear MgO surfaces in vacuo whereas, this no longer occured, if the surface was contaminated with water and CO_2.

Edlund et al. [34,35] observed the ESR spectra of singly charged monomeric and dimeric cation radicals at 77 K in a γ -irradiated C_6H_6-silica gel system. The formation of cation radical of triphenylamine on surface of synthetic zeolites and anion radicals of naphthalene and biphenyl on silica gel have also been reported [36,37]. Kinell et al. detected the cation radicals of naphthalene, anthracene, pehenanthrene and biphenyl adsorbed on silica gel by ESR spectra.

M.L.Hair and W.Hertl [39] measured the adsorption isotherms by volumetric, gravimetric and spectroscopic techniques on silica surfaces which have been modified in a variety of ways. For most of the adsorbates, freely vibrating hydroxyl group on silica surface was the strongest surface adsorption site.

The effect of dehydroxylation of silica surface on the adsorption of various molecules have been studied using IR spectroscopy [40,41]. Y.A.Eltekov and co-workers [42] investigated the adsorption of a series of aromatic hydrocarbons from solutions in hydroxylated and dehydroxylated silica surfaces. They found that dehydroxylation of surfaces sharply diminishes the adsorption of aromatic hydrocarbons.

The formation of radicals of acetylene on the surface of alumina-CuO catalysts demonstrated the dual nature of alumina-CuO surface [43]. Bodrikov et al. studied the electron donor and acceptor properties of γ-alumina, silica and γ-alumina and silica supported palladium oxide [44]. It was observed that while γ-alumina had both electron donor and acceptor characteristics, γ-alumina supported Pd oxide showed better acceptor properties than donor properties. Silica supported palladium oxide showed only electron acceptor properties.

The electronic state of adsorbed species was studied by UV-vis spectroscopy in addition to ESR spectroscopy [1-3]. The band near 600 nm after the adsorption of TCNQ on metal oxide was related to the dimeric TCNQ anion radical which absorbs at 643 nm [45]. This tentative attribution was supported by the characteristic features that neutral TCNQ absorbs only at 395 nm, that TCNQ has a high electron affinity and TCNQ anion radicals are stable even at room temperature [46-49]. ESR and electronic spectra provided evidence that TCNQ anion radicals were formed as a result of electron transfer from metal oxide surface to adsorbed TCNQ.

K.Esumi and K.Meguro determined the basicity of Al_2O_3, TiO_2 and ZrO_2-TiO_2 [50]. The distribution of sites having different basicity was similar for alumina and titania with respect to Lewis and Bronsted sites. In ZrO_2-TiO_2 binary system only Lewis sites existed.

The electron donor properties of some of the rare earth oxides and supported rare earth oxides have also been investigated [51-57]. These properties have been correlated with their surface acidity/basicity and catalytic activity.

Using the ESR of adsorbed nitrobenzene radicals as a probe, the electron donor properties of several oxide powders (CaO, MgO, ZnO, Al_2O_3 and SiO_2-Al_2O_3) heated in vacuo at temperatures upto 1200 K, have been investigated [21]. The results showed the existence of a correlation between the electron donor activity of oxides and the Lewis base strength, indicating a direct connection between basic centres and donor surface sites.

Adsorption studies have also been employed for the characterisation and for the determination of the role of the adsorbed species on the catalytic activity of

perovskite type oxides. These include mainly equilibrium and kinetics of adsorption, successive or simultaneous adsorption of two gases, infrared spectroscopy (IR) and temperature programmed desorption (TPD).

It is by now well known that the surface of most oxides are covered to a greater or lesser extent, by a layer of hydroxyl groups. In principle, these should appear at all points where the surface oxygens would be coordinated to cations in the next highest layer, if they were present. In practice, lower and lower values of surface OH concentration are frequently found as the pretreatment temperature in vacuum or dry gas is increased. These result from dehydroxylation process, as H_2O is formed by condensation. In this way, coordinatively unsaturated cationic sites which may be of catalytic importance are developed as anion vacancies are introduced into the surface layers.

The surface hydroxyl concentration of $BaTiO_3$, $SrTiO_3$ and $LaCrO_3$ were determined by exchange with D_2 as a function of the dehydroxylation temperature. These results suggest that the surface chemistry of these materials resembles that of certain other oxide systems such as

alumina and titania [58]. It was observed that at 600°C, the surfaces of these perovskites were nearly completely dehydroxylated. This behaviour resembles that of alumina and is typical for such oxides.

The interaction of oxygen with perovskites has been studied mainly because of the importance of these materials as oxidation-reduction catalysts. The equilibrium and kinetics of adsorption of oxygen on $LaCrO_3$ have been studied in a wide range of temperatures (77 to 777 K). Above 350 K, activated adsorption occured [59]. In this region, rather low coverages of oxygen (below 0.20) were recorded. The exponential decrease of the isosteric heat of adsorption with coverage suggested that the surface of $LaCrO_3$ is heterogeneous.

After heating at 1270 K in H_2, only a reduction of 1.3×10^{-2} electron per molecule of $LaCrO_3$ was attained. Concentration of hydroxyl groups after adsorption of H_2O on the reduced sample was found to be higher than that on the oxidised one. In both the cases, IR spectra in the OH stretching zone obtained after H_2O adsorption at 423 K gave bands at 3680 cm^{-1} of isolated OH groups and at 3550 cm^{-1} (wide) of hydrogen bonded OH were observed. The OH band on

the latter case should be weaker and therefore, more acidic. The band intensities were stronger on the reduced sample.

It was shown that oxygen adsorption took place only on surface defects as transition metal ions in highly reactive position (corners, edges), anion vacancies etc. According to Iwamoto et al. [60] simple oxides whose metal ions has a d^0 or d^{10} configuration are poor adsorbents of oxygen. Therefore, La^{3+} ion should not play an important role as adsorption centre. The less stable oxides (and therefore those which more readily form surface defects) exhibited both higher oxygen adsorption and higher catalytic activity.

Yamazoe et al. [61] made TPD and XPS studies on thermal behaviour of adsorbed oxygen in $La_{1-x}Sr_xCoO_3$. The correlation between the amount of adsorbed oxygen and the content of Sr^{2+} suggested that the oxygen adsorption was associated with some sort of lattice defect originating from the partial substitution of Sr^{2+}. The O_{1s} spectrum obtained with lower binding energy (528.2 eV) was assigned to lattice oxygen and that with higher binding energy (530.2 - 531.4 eV) corresponds to the adsorbed oxygen.

Electron spin resonance had been used to identify oxygen species on $La_{1-x}Ca_xMnO_3$ and $LaCoO_3$ [62,63]. After adsorption of oxygen on the latter perovskite at 150°C and lowering the temperature to -196°C, a signal attributed to O_2 was found that changed rapidly into a diamagnetic species. Conductivity changes as a function of O_2 presence were associated to a part adsorption process followed by transformation of adsorbed oxygen into lattice oxygen. DTA has been used to study oxygen uptake on cobalt perovskites in order to obtain a relative measurement of the degree of non-stoichiometry [64].

NO adsorption was found to be independent of temperature for some perovskites such as $LaFeO_3$ and $LaNiO_3$ [65,66] for a wide temperature range (0-400°C). This suggests that the surface sites for NO on these oxides did not change substantially in character with the temperature.

The IR spectrum obtained after adsorbing NO on $LaMnO_3$ above room temperature included bands at 1910 cm^{-1} of dinitrosyl species at 1610, 1485, 1135 and 1045 cm^{-1} of bidentate and mono dentate nitrates; and at 1300 cm^{-1} of nitrite structure [67]. However, formation of N_2O at 100°C and higher temperature was observed, suggesting that NO

absorbs in dissociative as well as molecular forms. Voorhoeve et al. [68] found also TPD peak at 100-250°C assigned to nitrosyl groups on low valence metal ions after NO adsorption on potassium and ruthenium substituted $LaMnO_3$ pervoskites. These results indicate that NO interacts with both cations and anions on the surface of these perovskites.

IR spectra recorded after simultaneous adsorption of NO + CO on $LaMnO_3$, $LaFeO_3$ and $LaCoO_3$ at 300 to 500°C provided evidence of the presence of N_2O, isocyanate species and NO adsorbed with a donor-type or coordinate bond [66]. An additional band of nitrosyl groups was detected on $LaCoO_3$. These results may provide some evidence for the mechanism of NO + CO reaction on these oxides, as N_2O and isocyanate species have been suggested as intermediates for this reaction on simple oxides [69-71]. The chemisorption of NO seems to play an important role in this reaction catalysed on perovskites. Thus, Chien et al. [72] observed a higher NO adsorption rate for activated (reduced) than for unactivated $LaCoO_3$ and $La_{0.85}Ba_{0.15}CoO_3$.

The relative constancy of NO adsorption with temperature and the strength of its bond with perovskite surfaces have suggested the use of this molecule over CO for determining surface metallic centres [65-68,73]. However the evidence indicates that NO does not show any particular specificity for adsorption on metallic or oxide ions [65-67]. Ulla et al. [74] used the poisoning effect of NO adsorption in ethylene hydrogenation at -20°C for the estimation of metallic centres in reduced $LaCoO_3$. Active site concentration was found to be lower by one order of magnitude than the theoretical concentration of metallic cobalt.

The IR and TPD spectra obtained after CO adsorption on $LaMnO_3$ oxides in the temperature interval 25-500°C showed the presence of different types of carbonates besides linear and bridged CO [65-67, 75-77]. Thus CO, as NO, interacts with surface oxygen and metallic ions. Carbonate formation increased for increasing adsorption temperatures above 200°C. Adsorption heats determined from the TPD peaks showed that CO was slightly more stable on the Rh^{3+} cation of the $LaRhO_3$ than on metallic rhodium [78,79].

Studies on equilibrium and energetics of CO_2 adsorption have been carried out on $LaCrO_3$, $LaFeO_3$ and $LaCoO_3$ by Tejuca et al. [80-82]. Surface coverage followed the general trend $LaCoO_3 > LaFeO_3 > LaCrO_3$. The adsorption isobars on $LaCrO_3$ and $LaCoO_3$ showed activated adsorption above approximately 150°C, whereas on $LaFeO_3$, the coverage decreased continuously with temperature. In these systems, the Freundlich model of adsorption, which assumes an exponential decrease of isosteric heat with the coverage was observed.

2.2 SOLID ACIDS AND BASES

It has been seen that a surprisingly large number of solids have surface acidity and/or basicity. In general, a solid acid may be understood as a solid on which the colour of basic indicator changes or as a solid on which, a base is chemically adsorbed.

The acidic and basic properties of oxide catalysts are very important for the development of scientific criteria in catalyst applications. To describe the acidic and basic properties on a solid surface requires the determination of acidic and or basic centre, acid or base

amount and the nature of the sites. The characterisation not only depends upon the purity of the materials and the method of preparation, but also, upon heat treatment, compression and irradiation.

Solid acids and bases have found use as catalysts for many important reactions including the cracking of hydrocarbons, the isomerization, polymerization, hydration of olefines, alkylation of aromatics etc. [83,84]. Extensive investigation on solid acid and base catalysis in past several years discovered new types of solid acids and bases having a wide variety of applications.

Walling [85] defined acid strength of a solid as the ability of a surface to convert an adsorbed neutral base into its conjugate acid and can be expressed by Hammett and Deyrup acidity function, H_o [86].

If the reaction takes place by the proton transfer from surface to adsorbate, then,

$$H_o = -\log a_{H^+} \cdot f_B / f_{BH^+}$$

$$H_o = pKa + \log \frac{[B]}{[BH^+]}$$

where a_{H^+} is the activity of proton and f's are the activity coefficients for a neutral base and its conjugate acid.

If the reaction takes place with the proton transfer from adsorbate to surface,

$$H_o = -\log a_A \cdot \frac{f_B}{f_{AB}}$$

$$H_o = pKa + \log [B]/[AB]$$

where a_A is the activity of the Lewis acid or electron pair acceptor.

The strength of acid sites was expressed by H_o as usual and that of basic sites by the H_o of their conjugate acids. The strongest H_o value of the acid sites was found to be approximately equal to the strongest H_o value of the basic sites. The equal strongest H_o value was termed "$H_{o,max}$". Hence a solid of a high $H_{o,max}$ value possesses strong basic sites and weak acid sites at the same time. On the contrary, a solid of a low $H_{o,max}$ value should have strong acid sites and weak basic sites.

T.Yamanaka and K.Tanabe [87] proposed a method of determining basicity at various basic strengths by titrating solid suspended in benzene with trichloroacetic acid using a series of Hammett indicators. A correlation was found between $H_{o,max}$ and the effective negative charges on combined oxygen [88].

For the quantitative determination of acid strength, a variety of methods can be used like visual colour change method [89], spectrophotometric method using fluorescent indicators [90] and gaseous adsorption method [91]. For basic strength determination, method using indicators [92], phenol vapour adsorption method [93] and temperature programmed desorption technique [94] are generally employed.

The indicator method was originally reported by Walling [85] and is in extensive use. This method proposes the measurement of the acidic properties of a solid acid surface in a nonpolar solvent and acid strength is measured from the colour change of the indicator adsorbed on the surface by amine titration.

Benesi tried to modify the titration technique so that indicators could be added to portions of catalyst in

suspension after the catalyst sample had reached equilibrium with n-butylamine, the end point being determined by a series of approximations [95,96]. Benesi determined the acid strengths of alumina, silica, magnesia mounted acids and cracking catalysts using this method.

Hirshler proposed the use of acidity function H_R for determination of protonic surface acidity and used a series of aryl methanols and diphenylmethane as indicators [89].

J.Take et al. [97] proposed a new method which involves the titration of a solid acid with indicator itself in a nonpolar solvent. The titration of silica-alumina with 4-aniloazobenzene yielded an acid content smaller than the n-butylamine titration with the same indicator. Yoneda and co-workers [98] made a critical analysis of the conditions required for the establishment of adsorption equilibrium in n-butylamine titration of acid surfaces. Balikove found that butylamine titer is dependent upon the physical conditions of experiment [99].

The acidic properties of single oxides TiO_2, SiO_2, Al_2O_3 and binary systems TiO_2-Al_2O_3, TiO_2-ZnO, SiO_2-ZnO,

SiO_2-TiO_2, ZnO-Bi_2O_3, Al_2O_3-Mgo etc. have been studied [100-104]. Many combinations of transition metal oxides like TiO_2-MoO_3, TiO_2-V_2O_5, ZnO-Fe_2O_3 and WO_3-TiO_2 have also been found to show remarkable acid properties [105-110].

C.G.R.Nair and co-workers carried out the acidity evaluation of TiO_2-SiO_2-Al_2O_3 catalysts using butylamine titration [111]. A comparative study of the acid properties of TiO_2, SiO_2, Al_2O_3, SiO_2-Al_2O_3, SiO_2-TiO_2, Al_2O_3-TiO_2 and TiO_2-SiO_2-Al_2O_3 have also been carried out. Single oxides were found to have low acid strength and TiO_2-SiO_2-Al_2O_3 of 10% by weight of TiO_2 showed highest acid amount. Titration of dark coloured solids can be carried out however, by adding a small known amount of a white solid acid [112]. The end point of the titration is taken, when the colour change is observed on the white solid and a correction is made for the amount of butylamine used for the added white material.

J.Take, N.Nikuchi and Y.Yoneda developed a method for the determination of basic strength of solid surfaces which consist of titration of solids suspended in cyclohexane with benzoic acid using a series of H^- indicators [113]. They found that base strength of alkaline

earth oxides increased remarkably upon heat treatment in vacuum and basicity decreased in the order SrO $\simeq$ CO > MgO.

The transformation of an indicator into its conjugate acid form can be detected spectrophotometrically and spectroscopic method was introduced by Leftin, Hobson and Terenin [91,114]. Drussel and Sommers presented the use of a series of fluorescent indicators for use in spectrofluorometric titration [115]. UV-spectrophotometry has been applied for measurement of acid strength of silica-alumina catalysts using 4-benzene azodiphenylamine, 4-nitroaniline and 2,4-dinitroquinoxaline [116].

A series of UV spectroscopic studies have been made for indicators adsorbed on alkaline earth metal oxides and adsorption maxima of the spectra was correlated with the basic strength of the solid [117,118]. Pure silica gel showed neither acidic nor basic properties, while silica treated with ammonium fluoride possessed a large number of strong Bronsted acid sites [119]. Commercial ZnO had acid sites corresponding to an H_o value of +4.8 and heat treatment increased the acidity [120]. Acidic properties of Cr_2O_3 was studied and it was found that acidity in oxidised state is twice that in reduced state [121].

The adsorption of pyridine on V-Ti oxide prepared by the gas phase method (1.4-5.6 weight %) has been studied by IR spectroscopy [122]. V-Ti oxide exhibited both Bronsted and Lewis acid sites. The Lewis acid sites were converted to Bronsted sites on the introduction of water vapour. From the absorption coefficients of the 1530 cm^{-1} band (Bronsted site) and 1440 cm^{-1} (Lewis site) the number of both sites had been estimated. The acidic sites in two-dimensional or monolayer vanadia species were found to be stronger Bronsted acids than those formed from crystalline vanadia.

The surface acidities and reactivities of TiO_2, SiO_2 and a series of Ti-Si mixed oxides have been investigated with a variety of surface sensitive techniques including temperature programmed desorption (TPD), reaction of ammonia and 2-propanol and IR spectroscopy of adsorbed NH_3 [123]. Results from TPD, TPR and IR spectroscopy indicated that total acidity and relative acid strength decreased as silica was incorporated into titania. IR spectroscopy of adsorbed ammonia revealed that all the acid sites on pure titania were of the Lewis type, whereas, about 80% of the sites on the mixed oxides were of the Bronsted type. The appearance of Bronsted acidity in

titania rich mixed oxides was due to the local charge imbalance associated with tetrahedrally co-ordinated silica, chemically mixing with the octahedral titania matrix.

Zirconium dioxide modified by sulfate anions was investigated using diffuse reflectance IR spectroscopy [124]. It was found that this modification enhanced the strength of both Bronsted acid sites (terminal or bridging ZrOH groups) and Lewis acid sites (low-coordinated Zr ions). However, Bronsted acid sites with enhanced strength appeared to be weaker than bridging OH groups in zeolites. Modification also created protons with a new environment. These protons were assumed to form multicentre bonds with oxygen atom of SO_4^{2-} anions or with neighbouring basic oxygen and possess acidic properties comparable to those of protons in zeolites.

The surface acidity/basicity determination of perovskite oxides are less studied. IR spectra of pyridine adsorbed at 25°C on $LaMO_3$ (M=Cr, Mn, Fe and Co) oxides previously outgassed at 500°C showed Lewis bands at 1595, 1490 and 1440 cm^{-1} (75). Pyridine adsorbed on reduced (500°C, H_2) and outgassed $LaMO_3$ oxides yielded a spectrum

similar to that of the unreduced samples and also a weak Bronsted band at 1540-1545 cm^{-1}. The appearance of Bronsted acidity may arise from the heterolytic dissociative adsorption of H_2 on co-ordinatively unsaturated M^{3+}, O^{2-} ions as occurs on simple oxides.

$$-O-M-O + H_2 \longrightarrow \begin{matrix} & H \\ & | \\ O-M-OH & \end{matrix}$$

An increase in Bronsted acidity was observed which may be accounted for the increase in anion vacancy produced in the reduction process.

In an experiment of H_2O-pyridine adsorption on $LaCrO_3$ [60], bands of Bronsted centres were observed only on the reduced sample. Pyridine probably did not react with basic centres which were on the surface in higher concentration than the acidic centres, as observed by the stronger intensity of the 3680 cm^{-1} band. On the other hand, the pyridine molecule, because of its large size might not have access to all acidic OH groups.

It was assumed that the adsorption and dissociation of H_2O takes place on pairs of surface acid-

base centres and anion vacancy-O^{2-}, according to the scheme.

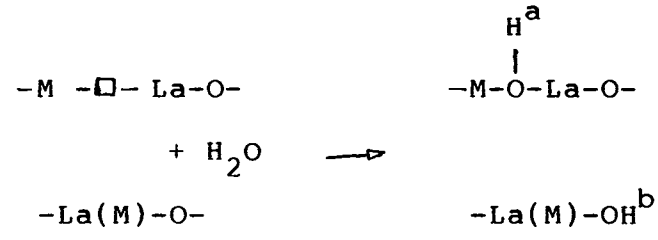

yielding an acidic OH on an anion vacancy placed between coordinatively unsaturated La^{3+} and reduced transition metal ions (M^{2+}, M^{3+}) (centre a) and a basic OH, on coordinatively unsaturated oxygen ion bonded to a La or M ion (centre b). Centres a and b should correspond to OH groups yielding bonds at 3550 and 3680 cm^{-1} respectively [59].

2.3.1 PEROVSKITES IN CATALYSIS

Perovskites offer ideal systems for establishing possible relationship between solid state chemistry and catalytic properties. The most frequently studied perovskite oxides used in heterogeneous catalysis are those with a lanthanide element in position A and a first-row transition metal in position B.

The oxidation of CO over perovskite-type oxides has been widely studied. Voorhoeve et al. [125] brought forward new ideas in explaining the role of defect chemistry of perovskites such as cobaltites, manganites, chromites and ruthenates. They suggested that two different oxidation processes should be distinguished.

(1) The catalyst participates in the reaction as a reagent, being partially consumed and regenerated in a continuous cycle, termed reagent or intrafacial catalysis.

(2) The catalyst provides the atomic orbitals of the proper symmetry and energy to activate the reactant molecules termed template or suprafacial catalysis.

$LnMO_3$ perovskites in which the lanthanide (Ln) ions are essentially inactive in catalysis and the active transition metal (M) ion are placed at relatively large distances (0.4 nm) from each other are excellent catalytic models for study of the interaction of CO and O_2 on single surface sites [126].

Voorhoeve et al., Shimizu and Tascon and Tejuca [125,127-130] have shown a suggestive correlation between

the activity data, using mixtures of CO and O_2 at atmospheric pressure, and the electronic configuration of transition metal ion.

Voorhoeve et al. [125, 127] have also stressed that the catalytic activity of perovskites is influenced by their stoichiometry. A simple way of varying the oxidation state of the ion at the position B is by substitution of the A ion by a different ion with an oxidation state other than 3. This method has been used by several authors [131-137] to understand the role of the 3d-orbital occupancy in the $LaMO_3$ series on the catalytic oxidation of CO. For M=Co, the appearance of Co^{2+} ions by introduction of Ce^{4+} in position A enhanced the rate of oxidation of CO, whereas, the presence of Co^{4+} ions by substitution with Sr^{2+} reduced the rate. The difference in behaviour was explained by assuming that CO was bonded to the transition metal ion as a carbonyl as occurs on metal [138] with donation of the carbon lone pair into the empty $3d_z^2$ orbital of M to form a σ -bond accompanied by back-donation of the t_{2g} electron of the metal to the antibonding π orbital of CO.

In the hydrogenation and hydrogenolysis reaction of C_2-C_5 alkenes and alkanes using $LaCoO_3$, it was found

that Co^{3+} plays an important role in the rupture of the C-C bond whereas La^{3+} and O^{2-} ions contribute mainly to the dissociative adsorption of hydrogen [139-141].

The adsorption of oxygen and isobutene and the catalytic activity for propene and isobutene oxidation have been studied on a series of $LaMO_3$ (M=Cr, Mn, Fe, Co and Ni) perovskite oxides [142]. Oxygen adsorption underwent a remarkable increase after isobutene had been preadsorbed on these oxides (enhanced adsorption). Activation energies for complete oxidation ranged between 16 k cal mol^{-1} ($LaMnO_3$, $LaCoO_3$ and $LaNiO_3$) and 31 k cal mol^{-1} ($LaFeO_3$). Adsorption and catalytic activity profiles showed maxima for $LaMnO_3$ and $LaCoO_3$. It was found that the activation energy for the isotopic exchange of oxygen in simple oxides with molecular O_2 [which is a measurement of the strength of the M-O bond and is proportional to the total selectivity [143] increased in the sequence $Co_3O_4 < MnO_3 < NiO < Fe_2O_3 < Cr_2O_3 < TiO_2$ [144]. Similar trend was assumed to hold for perovskites also, in consistent with the high catalytic activity for total oxidation of $LaMnO_3$ and $LaCoO_3$ and also with the higher selectivity for partial oxidation products exhibited by $LaCrO_3$ and $LaFeO_3$. The results reported that the change in crystal field stabilisation energy (ΔE_c) may

be a significant factor in the energetics of chemisorption and catalysis and showed the importance of surface metal ion M^{3+} as active-centres in the processes studied.

The spin and valence state of the ion in position B was found to influence the activity of a series of $LnCoO_3$ (Ln=La, Pr, Nd, Gd and Ho) oxides [145]. It has been shown in Mossbauer and magnetic susceptibility studies that the ratio of the concentration of Co^{3+} to that of other states was unity in $NdCoO_3$ and $HoCoO_3$, whereas it was significantly higher than unity in other cobaltites. To account for these results, it has been suggested that high-spin Co^{3+} ions facilitates CO adsorption whereas low-spin Co^{3+} favours the process

$$CO + O^{2-} \longrightarrow CO_2 + 2\ e^-$$

It has also been observed that $LaCrO_3$ and $LaFeO_3$ which only have high-spin ions, are both poor catalysts [130].

Futai et al. [146] studied the influence of binding energy between oxygen and the lanthanide cation in $LnCoO_3$ (Ln=La to Dy) oxides. A correlation was observed

between the sum of the Ln-O and Co-O binding energies, the reducibility and the catalytic activity in CO oxidation. The maximum activity corresponded to $EuCoO_3$ which exhibited the lowest oxygen binding energy and was also the oxide which was easiest to reduce.

A close relationship between the electronic configuration of the transition metal ion in position B and the catalytic activity was studied by Sazonov et al. [147]. They studied the oxygen equilibration on $LaMO_3$ (M=Cr, Mn, Fe, Co and Ni) oxides at temperatures above 500K and activity maxima was observed for $LaMnO_3$ and $LaCoO_3$. Voorhoeve and co-workers [125,127] correlated activity data on $LaMO_3$ oxides in CO oxidation with the occupancy of d levels, for the transition metals, and found maxima coincident with those of Sazonov et al. [147]. These twin-peak patterns in catalytic activity profiles resemble the twin-peak pattern which is found on going from d^o to d^{10} cations in the change in crystal field stabilization energy caused by the change in coordination of the surface M^{3+} cations upon adsorption of oxygen [148].

A distinct separation of the function of the cations of the transition and rare earth metals was

observed for $LaMO_3$ (M - first-row transition metal from chromium through Nickel) oxides [24]. The activation energy of the oxygen equilibration on these oxides above 500 K was found to be similar to those of single oxides of transition metals. However, the temperature dependence of the rate of equilibration on $LnMO_3$ (Ln=La, Nd and Sm) oxides below 500 K was found to be in identical nature to that recorded on the corresponding rare earth oxides. ie., the activity is determined by the cation of the transition metals at high temperature and by the rare earth ions at low temperature [147].

The catalytic properties and activity of $LnFeO_3$ (Ln=La-Gd) in the reaction of methanol oxidation have been studied [149]. The activity was in the following order, Gd > Eu > Sm > Nd > Pr > La, where the activity measurement was done at a temperature at which conversion of methanol to CO_2 and H_2O became 10%. Thus, it was found that the activity for $LaFeO_3$ increased, as the radius of the rare earth ion decreased.

The catalytic activities of perovskite-type mixed oxides ($LnBO_3$ and $Ln_{0.8}Sr_{0.2}CoO_3$, Ln=rare earth element, B = 3d transition metals) for the oxidation of propane and

methanol have been studied comparatively [150]. It has been found that the catalytic activity of $LnBO_3$ was principally determined by the B-site elements and was similar to those of the corresponding oxides of the B-site elements. The role of the rare-earth ions of the A-site was secondary, as long as it was trivalent. Upon the partial replacement of Ln^{3+} by Sr^{2+}, the catalytic activities of $LnCoO_3$ increased several times, the magnitude of the increase being similar among all the rare earth ions. These results demonstrate that the kind and the valence of a B-site metal are of primary importance for the control of the catalytic activity for oxidation, almost regardless of the kind of trivalent rare earth elements at the A-site. Catalytic oxidation of CO, propane and methanol have been investigated over perovskite-type mixed oxides ($La_{1-x}Sr_xCoO_{3-\delta}$, x=0, 0.1, 0.2, 0.4 and 0.6) by the use of flow and pulse method [151]. The reduction-oxidation properties as well as nonstoichiometry (δ) and desorptivity of oxygen were also measured. These properties were correlated with emphasis on the effect of the Sr substitution. Reducibility of these catalysts greatly increased with the extent of Sr substitution (x), while, the reoxidation became much slower with increasing x. The catalytic activity increased with x, when x was low, but decreased at higher x values.

2.3.2 CATALYTIC ACTIVITY AND ACID-BASE PROPERTIES

In heterogeneous catalysis by metal oxides, many close correlations between the catalytic activity, including its selectivity and the acidity of the oxides have been indicated. The nature and catalytic activity of neutral solid acid like metal oxides, sulphates etc. were elucidated through the investigation of the structure of the acid-base centres and by comparison with the kinetics of homogeneous acid-base catalysis.

Good correlation has been found in many cases between the total amount of acid (Bronsted plus Lewis type, usually measured by the amine titration method) and the catalytic activities of solid acids [152]. For example, the rates of both the catalytic decomposition of cumene and the polymerization of propylene over SiO_2-Al_2O_3 catalysts were found to increase with increasing acid amount [153].

The metal oxides show difference in the values of acidity depending upon the method of preparation. H.Pines and C.N.Pillai [154] reported that, alumina catalysts prepared from sodium aluminate were only weakly acidic while alumina catalysts prepared from aluminium isopropoxide were slightly acidic. The alumina prepared

from sodium aluminate did not cause extensive isomerization of olefines during dehydration of alcohol.

H.Pines and Haag [155] proposed that pure alumina had intrinsic acidity which was responsible for the typically acid catalysed reaction such as dehydration of alcohols and skeletal isomerization of 3,3-dimethyl butene and cyclohexene.

Involvement of surface acid-base properties was tested by studying the benzoinitrile formation from benzaldehyde and ammonia [156]. The nature of acid sites on the surface of silica gel, alumina and silica-alumina was studied by ESR and reflectance spectra of polyacenes adsorbed on the surface [157].

It was found that the acidity and activity of metal oxides depend upon the pretreatment temperature. For TiO_2-SiO_2 mixed oxide, obtained by coprecipitation method, highest activity was found at 500°C [158]. The variation in catalytic activity of rare earth oxides and their analogue scandia and yttria in ethylene hydrogenation between -12°C and 20°C was studied as a function of the pretreatment temperature [159]. By measuring the activity for the low

temperature hydrogenation of ethylene for the entire lanthanide series, Minachev et al. [159] estimated the role of pretreatment on the catalyst.

Hydrous ZrO_2 is an amorphous solid and has several catalytic activities [160]. The oxide was changed into crystalline zirconia by calcination at high temperature and the catalytic activity was lowered. The correlation between the surface property and the catalytic activity was investigated on hydrous zirconium oxide calcined at several temperatures, the best activity was obtained in the oxide calcined at 300°C. The quantity of surface acid or basic sites was measured by the butylamine or trichloroacetic acid titration methods respectively, using various Hammett indicators. Investigations were carried out to have a systematic comparison of the acidic properties and catalytic activities of single oxides TiO_2, SiO_2, Al_2O_3 and their binary and ternary oxides [161]. The activity distribution was measured by using butylamine titration technique and the test reactions selected for the catalytic activity measurement were alkylation of toluene with 2-propanol and the dehydration of 2-propanol.

The ternary oxide system MoO_3-SiO_2-Al_2O_3 was prepared by coprecipitation method [161]. The pH of

coprecipitation had been varied from 2-8 and its effect on the acidic properties of the ternary oxide was studied by butylamine titration. Its catalytic activity was found to be very high for the alkylation of toluene with 2-propanol.

It has been widely accepted that the generation of new and strong acid sites on mixing oxides is ascribed to charge imbalance, localised on M_1-O-M_2 bonds formed on the mixed oxides, where M_1 is the host metal ion and M_2 the doped metal ion [162]. The charge imbalance might be expected even on a single component metal oxides consisting of small particles. This is partially attributed to the surface imperfections of crystallographic structures in small sized particles. The relation between particle size and surface acidity of metal oxides have also been reported.

It was pointed out that the relative activities of rare earth metal oxides parallel their basicities [163]. Rare earth oxides are classified as basic catalysts and find use as catalysts in a number of reactions [164]. The acidic and basic nature and correlation with catalytic activity of rare earth oxides have been reviewed [152]. V.H.Rane and V.R.Choudhary compared the acid and base

strength distribution of rare earth oxides with the catalytic activity towards oxidative coupling of methane [94]. La_2O_3 showed highest surface basicity with highest activity and selectivity whereas SrO and CeO_2 showed lowest basicity.

The first order rate constant for the formation of benzyl benzoate from benzaldehyde over CaO calcined at various temperatures was found to change in parallel with the change in catalyst basicity. A good correlation was obtained between the catalytic activity and the amount of base per unit surface area [165].

The cis-trans isomerization of crotononitrile has been investigated using various catalysts including Al_2O_3, MgO, CaO, Na_2CO_3 and NaOH, supported on silica gel and some solid organic compounds [166]. Inorganic and organic compounds such as Al_2O_3, potassium-2-napthol-3-carboxylate, sodium-salicylate etc. which have both acidic and basic groups were found to be catalytically active. On the other hand, unmounted NaOH and Na_2CO_3, silica, and potassium biphthalate, each of which possess either only basic or only acidic properties were inactive. These observations

indicate that this isomerization undergoes by acid-base bifunctional catalysis.

Concentration of Bronsted and Lewis acid sites on sulfated zirconia catalysts were determined using the ^{31}P MAS NMR spectra of adsorbed trimethylphosphine [167]. A sample that had been calcined and exposed to air for a long period exhibited only Bronsted acidity; however, treatment of the sample at progressively higher temperatures resulted in the development of at least three types of Lewis acidity, along with a decrease in the concentration of Bronsted acid sites. In a related study, the activity of these catalysts for the alkylation of iosbutene with 2-butene was determined. The aged catalyst was inactive, but activation of the material at 100°C resulted in the most active catalyst. Thermal treatment at higher temperatures resulted in a loss in activity which paralleled the decrease in the Bronsted acid sites. These results are consistent with a model in which strong Bronsted acidity is a result of the interaction between bisulfate groups and the adjacent Lewis acid sites.

UV spctrophotometry of a Hammett indicator revealed that the acid strength of the Keggin-type

heteropolyacids ($H_{\alpha}XW_{12}O_{40}$) having W as addenda atoms increased, as the valency of the central atom increased [Co < B < Si < Ge < P]. The catalytic activity for the decomposition of isobutyl propionate in a homogenous system was correlated with the acid strength [168].

Sub-monolayer quantities of metal oxides were found to influence CO, CO_2 ethylene and acetone hydrogenation, ethylene hydroformylation and ethane hydrogenolysis over rhodium foils [169]. The metal oxides investigated include AlO_x, TiO_2, VO_x, FeO_x, ZrO_x, NbO_x, TaO_x and WO_x. Only those reactions involving the hydrogenation of C-O bonds were enhanced by the oxide overlayers. Ti, Nb and Ta oxides were the most effective promoters. The trend in promotion effectiveness was attributed to the direct relationship between oxidation state and Lewis acidity. For the oxide promoters, bonding at the metal oxide/metal inteface between the O-end of adsorbed CO and the Lewis acidic oxide was postulated to facilitate C-O bond dissociation and subsequent hydrogenation.

EPR studies of unsupported V_2O_5-Fe_2O_3 catalysts revealed that by doping with ceasium sulfate, a new phase

was formed in the solids which apparently increased their selectivity in the catalytic oxidation of polycyclic hydrocarbon. By XRD and Mossbauer spectroscopy, the new phase was found to be amorphous. A number of in situ EPR measurements performed with variation of temperature and atmosphere under mechanical stress and during treatment of the catalysts with fluorene revealed that the active centres probably consisted of oxygen lattice vacancies in the coordination spheres of Fe^{3+} ions which were occupied by an electron [170].

Using diffuse reflectance IR spectroscopy, ZrO_2 modified sulfate anions was found to have both Bronsted and Lewis acid sites. Modification also created protons with a new environment. Low-temperature ethylene and cyclopropane oligomerization and H-D exchange was shown to proceed on sulfated zirconia, presumably with participation of such sites [75].

For the study of the acidic character of layered perovskite oxide, $HLaNb_2O_7$ (HLa), the intercalation of water and alcohols was performed and further the HLa was used for dehydration of 1- and 2- butanol as a test reaction [171]. The acidic properties of the HLa was

greatly affected by the irreversible water in the interlayer removed in the temperature range of 350-400°C. With raising the heat-treatment temperature of the catalyst, its acidity decreased and was almost lost at 500°C.

Although investigations on the catalytic properties of perovskite type mixed oxides have multiplied in recent years, the primary mode of surface interactions on these materials remain largely undefined. So we have carried out an investigation on the strength and distribution of electron donor sites on ABO_3 type oxides (A = La, Pr and Sm, and B = Cr, Mn, Fe, Co and Ni) by adsorption of certain electron acceptors. The catalytic activity of these oxides for a few selected reactions (reduction of cyclohexanone, oxidation of cyclohexanol and esterification of acetic acid using 1-butanol) was correlated with their surface acidity/basicity.

REFERENCES

1. K. Meguro and K. Esumi : *J. Colloid Interface Sci.*, 59, 93, (1977).

2. K. Esumi and K. Meguro : *J. Colloid Interface Sci.*, 66, 192, (1978).

3. H. Hosaka, T. Fujiwara and K. Meguro : *Bull. Chem. Soc. Jpn.*, 44, 2616 (1971).

4. B.D. Flockhart, K.Y. Liew and R.C. Pink : *J. Chem. Soc. Faraday* I, 76, 2026 (1980).

5. B.D. Flockhart, J.A.N. Scott and R.C. Pink : *Trans. Faraday Soc.*, 62, 730 (1966).

6. B.D. Flockhart, I.R. Leith and R.C. Pink : *Trans. Faraday Soc.*, 66, 469 (1970).

7. A.J. Tench and R.L. Nelson : *Trans. Faraday Soc.*, 63, 2254 (1967).

8. K. Esumi and K. Meguro : *Bull. Chem. Soc. Jpn.*, 55, 1647, (1982).

9. K. Esumi, K. Miyata, F. Waki and K. Meguro : *Bull. Chem. Soc. Jpn.*, 59, 3363, (1986).

10. K. Esumi, K. Miyata, and K. Meguro : *Bull. Chem. Soc. Jpn.*, 58, 3524, (1985).

11. K. Esumi, K. Miyata, F. Waki and K. Meguro : *Colloids Surfaces,* 20, 81, (1986).

12. F.M. Fowkes : "Physico-chemical Aspects of Polymer Surfaces", Vol. 2, Plenum Press, p 583, (1983).

13. F.M. Fowkes : ACS Proceedings, Division of Polymeric Materials Science and Engineering, 53, 560, (1985).

14. J.B. Peri : *J. Phys. Chem.*, 69, 211 (1965).

15. J.B. Peri : *J. Phys. Chem.*, 69, 220 (1965); 69, 231 (1965).

16. P.A. Agron, E.L. Fuller Jr. and F.H. Holmes : *J. Colloid Interface Sci.*, 52, 553 (1975).

17. H.F. Holmes, E.L. Fuller Jr.and R.A. Beh : *J. Colloid Interface Sci.*, 47, 365 (1974).

18. H.P. Boehm : *Adv. Catal.*, 16, 179, (1966).

19. M. Primet, P. Pichat and M.V. Mathieu : *J. Phys. Chem.*, 75, 1216 (1971).

20. B.D. Flockhart, I.R. Leith and R.C. Pink : *Trans. Faraday Soc.*, 65, 542 (1969).

21. B.D. Flockhart, C. Naccache, J.A.N. Scott and R.C. Pink : *Chem. Commun.*, 238, (1965).

22. A.J. de Rossert, C.G. Finstorm and C.J. Adams : *J. Catal.*, 1, 235 (1962).

23. E.P. Parry : *J. Catal.* 2, 371, (1963).

24. W.K. Hall, H.P. Leftin, F.J. Cheseleke and D.E. O'Reilly : *J. Catal.*, 2, 506 (1963).

25. J.A.N. Scott, B.D. Flockhart, and R.C. Pink : *Proc. Chem. Soc.*, 139 (1964).

26. B.D. Flockhart, J.A.N. Scott and R.C. Pink : *Trans. Faraday Soc.*, 62, 730 (1966).

27. A. Terenin : *Adv. Catal.*, 15, 256 (1964).

28. R.L.Nelson and A.J. Tench : *J. Chem. Phys.*, 40, 2763 (1964).

29. A.J. Tench and R.L.Nelson : *J. Chem. Phys.*, 44, 1714 (1966).

30. R.L.Nelson, A.J. Tench and B.J. Harmsworth : *Trans. Faraday Soc.*, 63, 1427 (1967).

31. J.H. Lunsford and J.P. Jayne : *J. Chem. Phys.*, 44, 1487 (1966).

32. J.H. Lunsford and J.P. Jayne : *J. Phys. Chem.*, 69, 2182 (1965).

33. A.J. Tench and R.L.Nelson : *Trans. Faraday. Soc.*, 63, 2254 (1967).

34. O. Edlund, P.O. Kinell, A. Lund and A. Shimizu : *J. Chem. Phys.*, 46, 3678 (1967).

35. O. Edlund, P.O. Kinell, A. Lund and A. Shimizu : "Advances in Chemistry Series", No. 82, American Chemical Society, Washington, p 311, (1968).

36. D.N. Stamires and J. Turkevich : *J. Am. Chem. Soc.*, 86, 749 (1964).

37. P.K. Wong and J.E. Willard : *J. Phys. Chem.*, 72, 2623 (1968).

38. P.O. Kinell, A. Lund and A. Shimizu : *J. Phys. Chem.*, 73, 4175 (1969).

39. M.L. Hair and W. Hertl : *J. Phys. Chem.*, 73, 4269 (1969).

40. A.V. Kieselev : *Trans. Faraday Soc.*, 40, 205, (1965).

41. C. Curthoys and B.A. Elkingston : *J. Phys. Chem.*, 72, 3475 (1968).

42. Y.A. Eltekov, V.V. Khopina and A.V. Kieselev : *J. Chem. Soc. Faraday Trans.*, 68, 889 (1972).

43. R.S. Mann and K.C. Khulbe : *J. Catal.*, 42, 115 (1976).

44. I.Bodrikov, K.C. Khulbe and R.S. Mann : *J. Catal.*, 43, 339 (1976).

45. R.H. Boyd and W.D. Phillips : *J. Chem. Phys.*, 43, 2927 (1965).

46. D.S. Acker, R.J. Harder, W.R. Hertler, W.Mahler, L.R. Melby, R.E. Benson and W.E. Mochel : *J. Am. Chem. Soc.*, 82, 6408 (1960).

47. R.G. Kepler, P.E. Bierstedt and R.E. Merrifield : *Phys. Rev. Lett.*, 5, 503 (1960).

48. D.B. Chesnut, H. Fosker , W.D. Phillips : *J. Chem. Phys.*, 34, 684 (1961).

49. L.R. Melby, R.J. Harder, W.R. Hertler, D.S. Acker, W. Mahler, R.E. Benson and W.E. Mochel : *J. Am. Chem. Soc.*, 84, 3374 (1962).

50. K. Esumi, K. Magara and K. Meguro : *J. Jpn. Soc. Color. Mat*er., 58, 9 (1985).

51. S. Sugunan and K.B. Sherly : *Indian J. Chem.*, 32 A, 689 (1993).

52. S. Sugunan and G. Devika Rani : *J. Mater. Sci. Lett.*, 11, 1269 (1992).

53. S. Sugunan and G. Devika Rani : *J. Mater. Sci. Lett.*, 10, 887 (1991).

54. S. Sugunan and J.J. Malayan : *J. Adhesion Sci. Tachnol.*, 9(1), 73 (1995).

55. S.Sugunan and J.M. Jalaja : *Indian J. Chem.*, 34 A, 216, (1995).

56. S. Sugunan and G. Devika Rani : *J. Mater. Sci.*, 28, 4811 (1993).

57. S. Sugunan and G. Devika Rani and K.B. Sherly : *React. Kinet.*

Catal. Lett., 43, 375 (1991).

58. M. Crespin and W.K. Hall : *J. Catal.*, 69, 359 (1981).

59. J.L.G. Fierro and L.G. Tejuca : *J. Catal.*, 87, 126 (1984).

60. M. Iwamoto, Y. Yoda, N. Yamazoe and T. Seiyama : *J. Phys. Chem.*, 82, 2564 (1978).

61. N. Yamazoe, Y. Teraoka and T.Seiyama : *Chem. Lett.*, 1769 (1981).

62. W. Chengxian, D. Bosheng, F. Shurong, Y. Zuolong, X. Xiaofan, W. Yue : *Sci. Sin.* (Engl. Ed.) 27 B, 778 (1984).

63. J.M.D. Tascon, L.G. Tejuca : *Z. Phys. Chem.* (Wiesbaden), 121, 79 (1980).

64. D.Y. Rao, D.K. Chakrabarty : *Indian J. Chem.*, 23 A, 375 (1984).

65. M.A. Pena, J.M.D. Tascon, L.G. Tejuca : *Nouv. J. Chim.*, 9, 591 (1985).

66. J.M.D. Tascon, L.G. Tejuca and C.H. Rochester : *J. Catal.*, 95, 558 (1985).

67. M.A. Pena, J.M.D. Tascon, J.L.G. Fierro and L.G. Tejuca : *J. Colloid Interface Sci.*, 119, 100 (1987).

68. R.J.H. Voorhoeve J.P. Remeika and L.E. Trimble, "The Catalytic Chemistry of Nitrogen Oxides" (Ed. R.L. Klimisch and J.G. Larson), p 215, Plenum Press, New York (1975).

69. M. Shelef and K. Otto : *J. Catal.*, 10, 408 (1968).

70. J.W. London and A.T. Bell : *J. Catal.*, 31, 96 (1973).

71. F. Solymosi and J. Kiss : *J. Catal.*, 54, 42 (1978).

72. M.W. Chien, I.M. Pearson and K. Nobe : *Ind. Eng. Chem. Prod. Res. Dev.*, 14, 131 (1975).

73. J.M.D. Tascon, A.M.O. Olivan, L.G. Tejuca and A.T. Bell: *J. Phys. Chem.* 90, 791 (1986).

74. M.A. Ulla, E.E. Miro and E.A. Lombardo : *Proc. Iberoam. Symp. Catal.*, 8th, La Rabida, Spain, 475 (1982).

75. L.G. Tejuca, C.H. Rochester, J.L.G. Fierro and J.M.D. Tascon : *J. Chem. Soc. Faraday I*, 80, 1089 (1984).

76. L.G. Tejuca, A.T. Bell, J.L.G. Fierro and J.M.D. Tascon :

J. Chem. Soc. Faraday I, 83, 3149 (1987).

77. L.G. Tejuca, A.T. Bell, J.L.G. Fierro and M.A. Pena : *Appl. Surf. Sci.*, 31, 301 (1988).

78. P.R. Watson, G.A. Somorjai : *J. Catal.*, 74, 282 (1982).

79. G.A. Somorjai : *Chem. Soc. Rev.*, 13, 321 (1984).

80. J.L.G. Fierro, L.G. Tejuka : *J. Chem. Technol. Biotechnol.*, 34 A, 29 (1984).

81. L.G. Tejuca, M.A. Martin and J.L.G. Fierro : *Z. Phys. Chem.* (Wiesbaden) 127, 237 (1981).

82. M.A. Martin, J.M.D. Tascon, J.L.G. Fieroo, J.A. Pajares and L.G. Tejuca : *J. Catal.*, 71, 201 (1981).

83. K. Tanabe : "Solid acids and bases", Academic Press, New York (1970).

84. L. Formi : *Catal. Rev.*, 8, 65 (1973).

85. C.Walling : *J. Am. Chem. Soc.*, 72, 1164 (1950).

86. Hammett and Deyrup : *J. Am. Chem. Soc.*, 54, 2721 (1932).

87. T. Yamanaka and K. Tanabe : *J. Phys. Chem.*, 79, 2409 (1975).

88. T. Yamanaka and K. Tanabe : *J. Phys. Chem.*, 80, 1723 (1976).

89. A.E. Hirschler : *J. Catal.*, 2, 428 (1963).

90. H.P. Leftin and M.C. Hobson : *Adv. Catal.*, 14, 115 (1968).

91. A.N. Webb : *Ind. Eng. Chem.*, 267 (1957).

92. S. Malinowski and S.Sczepanska : *J. Catal.*, 2, 310 (1963).

93. C. Naccache, Y. Kodratoff, R.C. Pink and B. Imelik : *J. Chem. Phys.*, 63, 341 (1966).

94. V.R. Choudhary and V.H. Rane : *J. Catal.*, 130, 411 (1991).

95. H.A. Benesi : *J. Am. Chem. Soc.*, 78, 5490 (1956).

96. H.A. Benesi : *J. Phys. Chem.*, 61, 970 (1957).

97. J. Take, H. Kawai and Y. Yoneda : *Bull. Chem. Soc. Jpn.*, 50, 2428 (1977).

98. Y. Yoneda, J. Take and Y. Nomizo : *Bull. Chem. Soc. Jpn.*, 46, 3568 (1973).

99. M. Balikowa : *React. Kinet. Catal. Lett.*, 2, 323, (1975).

100. R. Rodenas, T. Yamaguchi, H. Hattori and K. Tanabe : *J. Catal.*, 69, 434 (1981).

101. K. Tanabe, C. Ishiya, I. Matsuzaki, I. Ichikawa and H. Hattori : *Bull. Chem. Soc. Jpn.*, 45, 47 (1972).

102. K. Tanabe, T. Sumiyoshi, and H. Hattori : *Chem. Lett.*, 723 (1972).

103. K. Tanabe, M. Ito and M. Sato : *Chem. Commun.*, 676 (1973).

104. K. Shibata, T. Kiyoura, K. Kitagawa, T. Sumiyoshi and K. Tanabe : *Bull. Chem. Soc. Jpn.*, 46, 2985 (1973).

105. T. Morimoto, J. Imai and M. Nagao : *J. Phys. Chem.*, 78, 704 (1974).

106. H.A. Benesi and B.H.C. Winquest : *Adv. Catal.*, 27, 123 (1978).

107. M. Ai. : *Bull. Chem. Soc. Jpn.*, 49, 1328 (1976).

108. H. Miyata, K. Fuji, T. Ono : *J. Chem. Soc. Faraday Trans. I*, 84, 3121 (1988).

109. T. Kotanigawa : *Bull. Chem. Soc. Jpn.*, 47, 950 (1974).

110. A. Andreini and J.C. Mol : *J. Chem. Soc. Faraday Trans. I*, 81, 1705 (1985).

111. K.R.P. Sabu, K.V.C. Rao and C.G.R. Nair : *Bull. Chem. Soc. Jpn.*, 63, 3632 (1990).

112. K. Tanabe and Y. Watanabe : *J. Res. Inst. Catal.*, 11, 65 (1963).

113. J. Take, N. Nikuchi and Y. Yoneda : *J. Catal.*, 21, 164 (1971).

114. A.N. Terenin : *Adv. Catal.*, 15, 227 (1964).

115. H.V Drussel and A.L. Sommers : *J. Anal. Chem.*, 38, 1723 (1966).

116. J. Take, T. Tsuruya, T. Sato and Y. Yoneda : *Bull. Chem. Soc. Jpn.*, 45, 3409 (1972).

117. H. Zeitlin, R. Frei and M. Mccaster : *J. Catal.*, 77, (1965).

118 H.E. Zaugg and A.D. Schaffer : *J. Am. Chem. Soc.*, 87, 1857 (1965).

119. I.D. Chapman and M.L. Hair : *J. Catal.*, 2, 145 (1963).

120. E. Marihari and G. Parravano : *J. Am. Chem. Soc.*, 75, 5233 (1953).

121. S.E. Voltz, A.E. Hirschler and A. Smith : *J. Phys. Chem.*, 64, 1594 (1960).

122. H. Miyata, K. Fujii and T. Ono : *J. Chem. Soc. Faraday Trans. I*, 84 (9), 3121 (1988).

123. Z. Lui, J. Tabora and R.J. Davis : *J. Catal.*, 149, 112 (1994).

124. L.M. Kustov, V.B. Kazansky, F. Figueras and D. Tichit : *J. Catal.*, 150, 143 (1994).

125. R.J.H. Voorhoeve, J.P. Remeika and L.E. Trimble : *Ann. N. Y. Acad. Sci.*, 272, 3, (1976).

126. L.G. Tejuca and J.L.G. Fierro : "Advances in catalysis" Academic Press, Vol. 36, New York (1989).

127. R.J.H. Voorhoeve : "Advanced Materials in Catalysis" (Eds. J.J. Burton and R.L. Garten), p 129, Academic Press, New York (1977).

128. R.J.H. Voorhoeve, D.W. Johnson Jr., J.P. Remeika and P.K. Gallagher : *Science*, 195, 827 (1977).

129. T.Schimizu : *Chem. Lett.*, p 1, (1980).

130. J.M.D. Tascon and L.G. Tejuka : *React. Kinet. Catal. Lett.*, 15, 185 (1980).

131. R.J.H. Voorhoeve, J.P. Remeika, P.E. Freeland and B.T. Matthias : *Science*, 177, 353 (1972).

132. P.K. Gallagher, D.W. Johnson Jr., F. Schrey : *Mater. Res. Bull.*, 9, 1345 (1974).

133. P.K. Gallagher, D.W. Johnson Jr. and E.M. Vogel : *J. Am. Chem. Soc.*, 60, 28 (1977).

134. T. Nakamura, M. Misono and Y. Yoneda : *J. Catal.*, 83, 151 (1983).

135. P.K. Gallagher, D.W. Johnson Jr., J.P. Remeika, F. Schrey, L.E. Trimble, E.M. Vogel and R.J.H. Voorhoeve : *Mater. Res. Bull.*, 10, 529 (1975).

136. S. George and B. Viswanathan : *React. Kinet. Catal. Lett.*, 22, 411 (1983).

137. Y.F.Y. Yao : *J. Catal.*, 36, 266 (1975).

138. G. Blyholder : *J. Phys. Chem.*, 68, 2772 (1964).

139. K. Ichimura, Y. Inoue and I. Yasumori : *Bull. Chem. Soc. Jpn.*, 53, 3044 (1980).

140. K. Ichimura, Y. Inoue, I. Kojima, E. Miyasaki and I. Yasumori : "New Horizons in Catalysis" (Ed. T. Seiyama and K. Tanabe), Vol B, p 1281, Elsevier-Kodansha, Tokyo (1981).

141. K. Ichimura, Y. Inoue and I. Yasumori : *Bull. Chem. Soc. Jpn.*, 54, 1787 (1981).

142. G. Kremenic, J.M.L. Nieto, J.M.D. Tascon and L.G. Tejuka : *J. Chem. Soc. Faraday Trans.I*, 81, 939 (1985).

143. T. Seiyama, N. Yamazoe and M. Egashira : Proc. 5th Int. Congr. Catal., (Ed. J.W. Hightower), Vol 2, p 997, North Holland, Amsterdam (1973).

144. A.I. Gelbshtein, S.S. Stroeva, Y.M. Bakshi and Y.A. Mischenko *Proc. 4th Int. Congr. Catal.*, (Akademiai Kiado, Budapest), Vol 1, p 297,(1971).

145. O. Parkash, P. Ganguly, G.R. Rao, C.N.R. Rao, D.S. Rajoria and

V.G. Bhide : *Mater. Res. Bull.*, 9, 1173 (1974).

146. M. Futai, C. Yonghua and L. Hui : *React. Kinet. Catal. Lett.*, 31, 47 (1986).

147. L.A. Sazonov, Z.V. Moskvina and E.V. Artamonov : *Kinet. Catal.*, 15, 100 (1974).

148. A. Clark : "The Theory of Adsorption and Catalysis" Academic Press, New York p 360, (1970).

149. T. Arakawa, S. Tsuchi-Ya and J. Shiokawa : *J. Catal.*, 74, 317 (1982).

150. T. Nitadori, T. Ichiki and M. Misono : *Bull. Chem. Soc. Jpn.*, 61, 621 (1988).

151. T. Nakamura, M. Misono and Y.Yoneda : *J. Catal.*, 83, 151 (1983).

152. K. Tanabe, M. Misono, Y. Ono and H. Hattori : "New Solid Acids and Bases", Kodansha, New York (1989).

153. O. Johnson : *J. Phys. Chem.*, 59, 827 (1955).

154. H. Pines and C.N. Pillai : *J. Am. Chem. Soc.*, 83, (1961).

155. H. Pines and W.O. Haag : *J. Am. Chem. Soc.*, 82, 2471, (1960).

156. S.I. Mikiniwa, and Y. Murakami : *J. Phys. Chem.*, 89, 2590 (1985).

157. K. Takimoto and M. Miura : *Bull. Chem. Soc. Jpn.*, 44, 1534 (1971).

158. M. Itoh, H. Hattori and K. Tanabe : *J. Catal.*, 35, 225 (1974).

159. K.M. Minachev, Y.S. Klaodakov and V.S. Nakhshriov : *J. Catal.*, 49, 207 (1977).

160. M. Shibagaki, K. Takahashi, H. Kuno and H. Matsushita : *Bull. Chem. Soc. Jpn.*, 63, 258 (1990).

161. K.R.P. Sabu, K.V.C. Rao and C.G.R. Nair : *Bull. Chem. Soc. Jpn.*, 64, 1926 (1991).

162. K. Tanabe " Catalysis, Science and Technology", (Eds. J.R. Anderson and M. Boudart), Springer-Verlag, Berlin-Heidelberg-New York (1981), Vol 2, p 231; K. Tanabe and T. Takeshita : Adv. Catal., 17, 315 (1967).

163. K.D. Camphbell, H. Zhang and J.H. Lunsford : *J. Phys. Chem.*, 92, 750 (1988).

164. H. Nakabayashi : *Bull. Chem Soc. Jpn.*, 65 (3), 914 (1992).

165. K. Saito, and K. Tanabe : *J. Polym. Sci.*, 11, 206 (1969).

166. M. Ichikawa, M. Soma, T. Ohnishi and K Tamaru : *Trans. Faraday Soc.*, 63, 2012 (1967).

167. J.H. Lunsford, H. Sang, S.M. Camphbell, C.H. Liang and R.G. Anthony : *Catal. Lett.*, 27, 305 (1994).

168. T. Okuhara, C.Hu, M. Hashimoto and M. Misono : *Bull. Chem. Soc. Jpn.*, 67, 1186 (1994).

169. A.B. Boffa, C. Lin, A.T. Bell and G.A. Somorjai : *Catal. Lett.*, 27, 243 (1994).

170. A. Bruckner, G.U. Wolf, M. Meisel, R. Stosser and H. Mehner : *J. Chem. Soc. Faraday Trans.*, 90 (20), 3159 (1994).

171. T. Matsuda, T. Fujita and N. Miyame : Catalysis Today, 16, 455 (1993).

CHAPTER 3
EXPERIMENTAL

EXPERIMENTAL

3.1 MATERIALS

3.1.1 ABO_3 type oxides

The ABO_3 type oxides (A = La, Pr and Sm, B = Cr, Mn, Fe, Co and Ni) were prepared by n-butylamine precipitation method from their nitrate solutions. The rare earth nitrates (purity 99.9%) were obtained from Indian Rare Earths Ltd., Udyogamandal, Kerala.

3.1.2 n-Butylamine precipitation

All ABO_3 type oxides were prepared by the same procedure. As an example, the procedure for $LaCoO_3$ is described. n-Butylamine was added to an aqueous solution (250 ml) containing lanthanum nitrate (9g) and cobalt nitrate (6g, SQ grade obtained from Qualigens Fine Chemicals Ltd.) until the precipitation was complete. The precipitate obtained was filtered and washed with water containing a few drops of n-butylamine till no NO_3^- ions were detected. It was then decomposed in air at 300°C for 3h and calcined in air at 850°C for 10h [1]. The duration of calcination depends upon the oxides under preparation and it is given in Table 1 for other oxides.

Table-1 Surface area of the oxides determined by BET method

Oxide	Surface area ($m^2 g^{-1}$)	Calcination time (h)
$LaCrO_3$	3.03	10
$PrCrO_3$	3.01	10
$SmCrO_3$	3.83	10
$LaMnO_3$	10.24	10
$PrMnO_3$	15.81	10
$SmMnO_3$	13.66	10
$LaFeO_3$	14.36	5
$PrFeO_3$	18.13	5
$SmFeO_3$	14.55	5
$LaCoO_3$	10.61	10
$PrCoO_3$	7.26	10
$SmCoO_3$	6.07	10
$LaNiO_3$	15.65	10
$PrNiO_3$	5.95	10
$SmNiO_3$	11.50	10
Cr_2O_3	7.48	2
MnO_2	8.40	2
Fe_2O_3	3.98	2
Co_3O_4	18.19	2
NiO	9.42	2
La_2O_3	35.14	2
Pr_6O_{11}	14.15	2
Sm_2O_3	30.01	2

3.1.3 Single oxides

The component rare earth and transition metal oxides were prepared from the corresponding nitrate solutions by the same method as described above and were activated at 850°C for 2h before each experiment.

3.1.4 Characterisation of the oxides

Powder X-ray diffraction patterns of the ABO_3 type oxides were recorded on a powdered X-ray diffractometer (Rigaku model D/max III VC Japan) using Ni filtered Cu K_α radiation (λ = 1.5418 A^o). The XRD patterns of these samples are given in Figs.2-9. The perovskite structure of the oxides were confirmed by comparing the 2θ (position) and intensity of the peaks obtained with those of the standard values (Tables 2-10) [2].

Elemental analysis of the perovskite oxides was carried out using a Perkin-Elmer 23-80 atomic absorption spectrometer.

Electronic spectra of the samples were scanned on a Shimadzu (UV-160 A) UV-visible spectrophotometer.

The radical concentrations of electron acceptors adsorbed on the oxides were determined based on the ESR

Fig-2

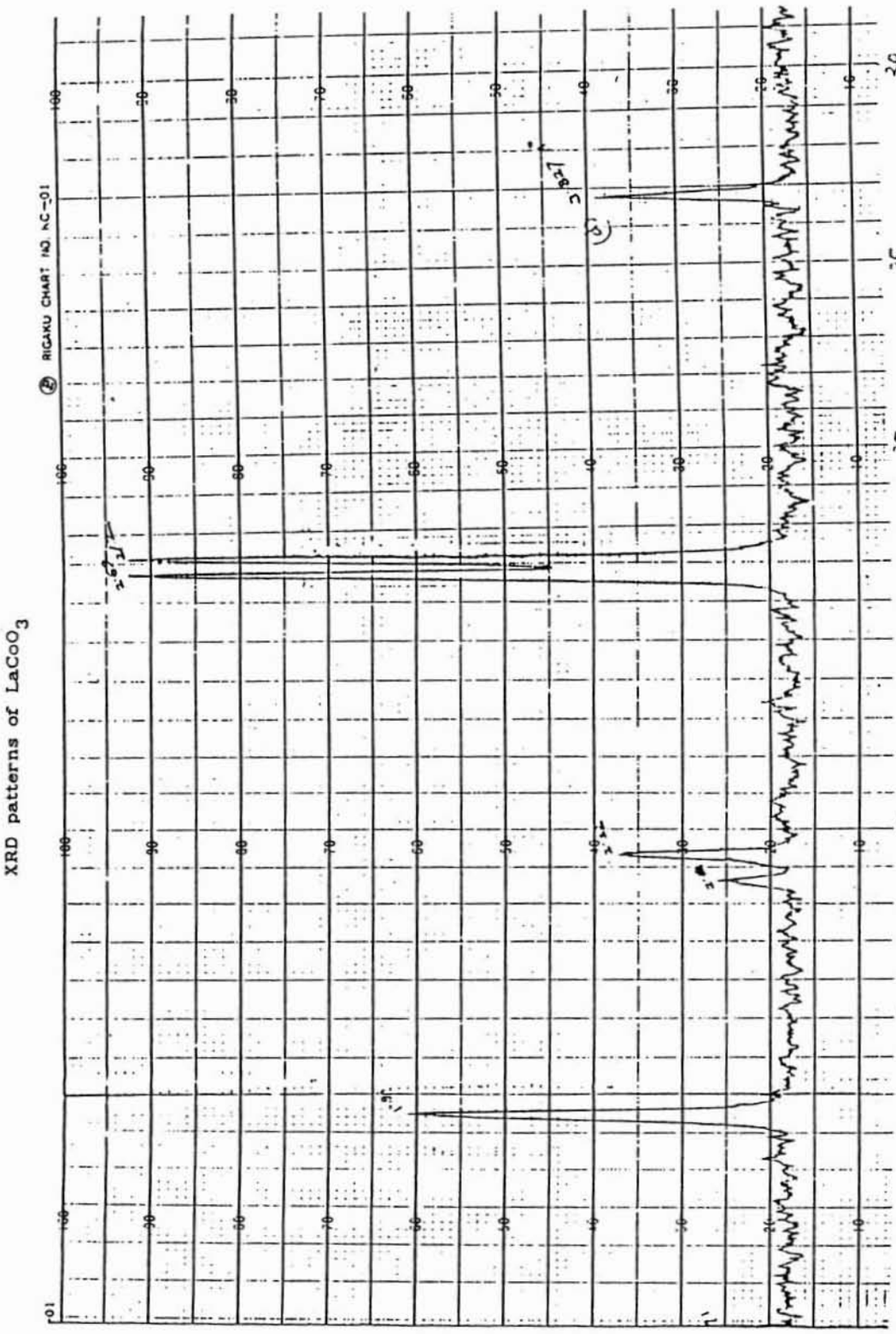

XRD patterns of $LaCoO_3$

Table-2 XRD data for $LaCoO_3$.

JCPDS data			Observed data		
2θ	d (A^o)	I/I_o	2θ	d (A^o)	I/I_o
32.93	2.720	100	32.30	2.120	100
33.39	2.686	100	33.4	2.691	100
33.03	2.714	100			
33.30	2.695	95			
59.07	1.544	80	55.18	1.661	50
47.61	1.910	80	23.2	3.827	30
47.51	1.913	80	40.8	2.212	28
40.75	2.215	60	41.4	2.180	14
59.98	1.542	60	47.8	1.902	59
69.18	1.359	60			
70.14	1.343	60			
78.79	1.215	60			
79.59	1.204	60			
23.29	3.835	60			
58.77	1.571	55			
41.41	2.183	30			
40.66	2.219	35			
69.93	1.345	25			
68.96	1.362	20			
78.79	1.214	20			
79.48	1.206	20			
23.29	3.835	20			
59.78	1.547	20			
53.27	1.720	10			
53.86	1.705	10			
74.30	1.278	10			

Table-3 XRD data for La_2O_3 and Co_3O_4

La_2O_3			Co_3O_4		
2θ	d (A^o)	I/I_o	2θ	d (A^o)	I/I_o
29.90	2.999	100	36.80	2.447	100
27.2	3.280	100	65.18	1.432	50
46.00	1.976	63	31.20	2.866	40
39.40	2.287	58	59.30	1.560	35
26.10	3.426	34			
52.08	1.760	52			
55.45	1.657	24			
28.08	3.185	45			
45.11	2.012	45			
49.05	1.866	35			
24.82	3.602	25			
31.50	2.844	35			
53.86	1.705	25			

Fig-3

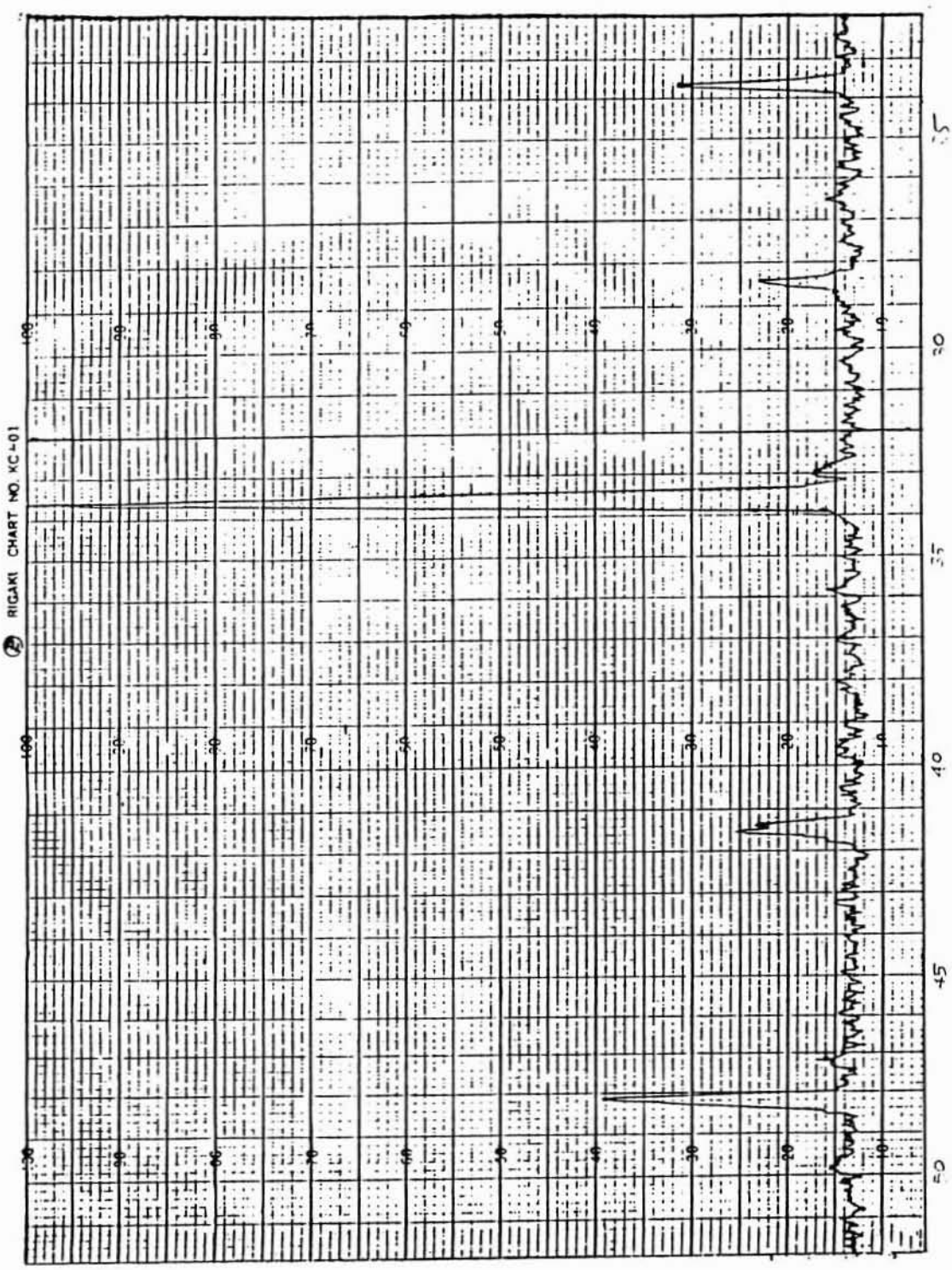

XRD patterns of $PrCoO_3$

Table- 4 XRD data for $PrCoO_3$.

JCPDS data			Observed data		
2θ	d (A^o)	I/I_o	2θ	d (A^o)	I/I_o
33.48	2.676	100	33.4	2.682	100
47.99	1.895	40	23.8	3.738	23
59.78	1.547	40	28.4	3.142	14
41.22	2.190	14	41.4	2.181	16
23.55	3.778	12	48.0	1.895	33
80.06	1.198	12	41.6	2.170	16
54.16	1.694	10	54.4	1.686	9
70.25	1.340	10			
89.63	1.093	5	60.0	1.5418	27
55.55	1.654	4			
75.19	1.263	4			
26.26	3.396	3			
49.64	1.839	3			
84.87	1.143	3			
71.55	1.320	2			
81.22	1.186	2			
79.48	1.206	20			
23.29	3.385	20			
59.78	1.547	20			
53.27	1.720	10			
53.86	1.705	10			

Fig-4

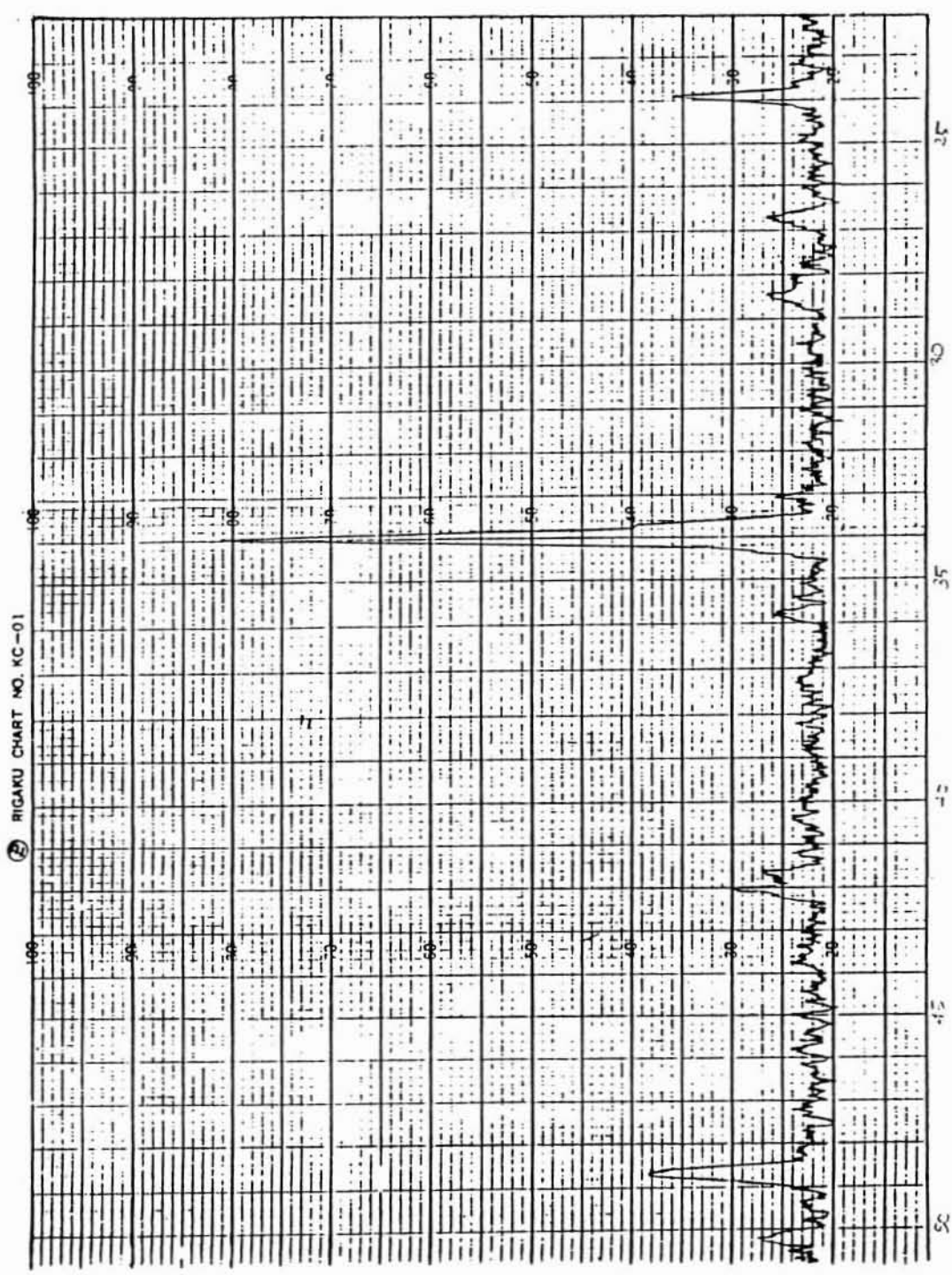

XRD patterns of $SmCoO_3$

Table-5 XRD data for $SmCoO_3$.

JCPDS data			Observed data		
2θ	d (A^o)	I/I_o	2θ	d (A^o)	I/I_o
33.85	2.648	100	34.0	2.636	100
48.48	1.877	35	24.0	3.707	26
60.50	1.532	35	26.8	3.326	10
33.48	2.676	30	28.4	3.142	11
59.99	1.542	18	41.6	2.171	10
60.19	1.537	18	42.0	2.151	16
23.73	3.760	16	48.8	1.866	29
71.01	1.329	15	50.2	1.817	10
80.98	1.187	15	56.0	1.642	10
41.78	2.165	12			
41.41	2.183	10			
49.93	2.159	10			
55.65	1.651	10			
54.75	1.676	8			
81.56	1.180	8			
86.80	1.122	8			
26.54	3.366	6			
43.49	2.083	6			

Fig.6

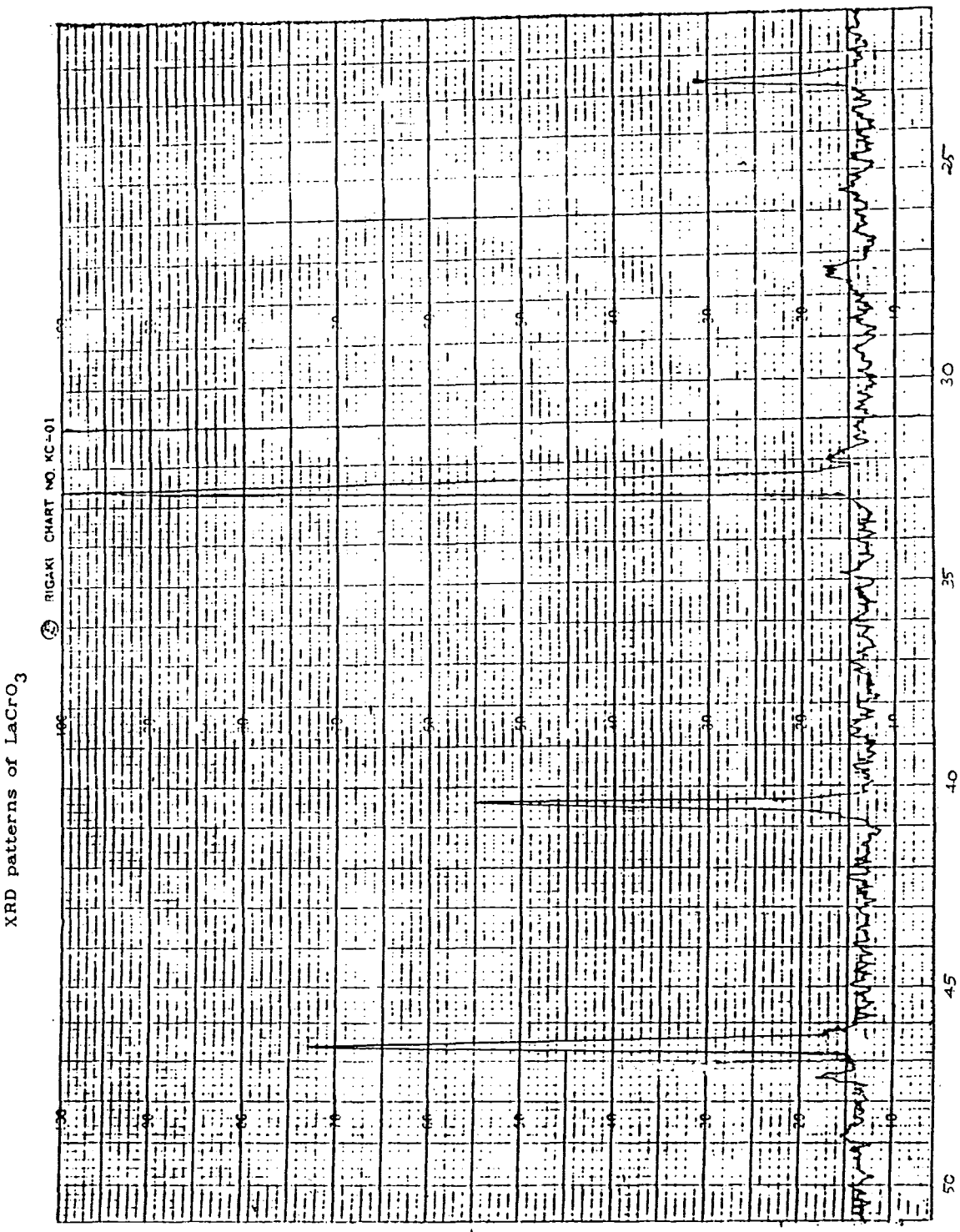

XRD patterns of $LaCrO_3$

Table-6 XRD data for $LaCrO_3$.

JCPDS data			Observed data		
2θ	d (A^o)	I/I_o	2θ	d (A^o)	I/I_o
32.28	2.744	100	32.3	2.771	100
32.65	2.743	100	22.8	3.90	26
40.37	2.234	50	40.4	2.232	50
95.10	1.045	40	46.4	1.948	70
96.42	1.034	30			
77.20	1.237	50			
22.83	3.913	30			
86.19	1.128	20			
39.90	2.260	70			
77.65	1.231	50			
52.28	1.750	30			
95.63	1.040	20			
46.64	1.951	70			
67.78	1.384	40			
52.67	1.740	30			

Fig-7

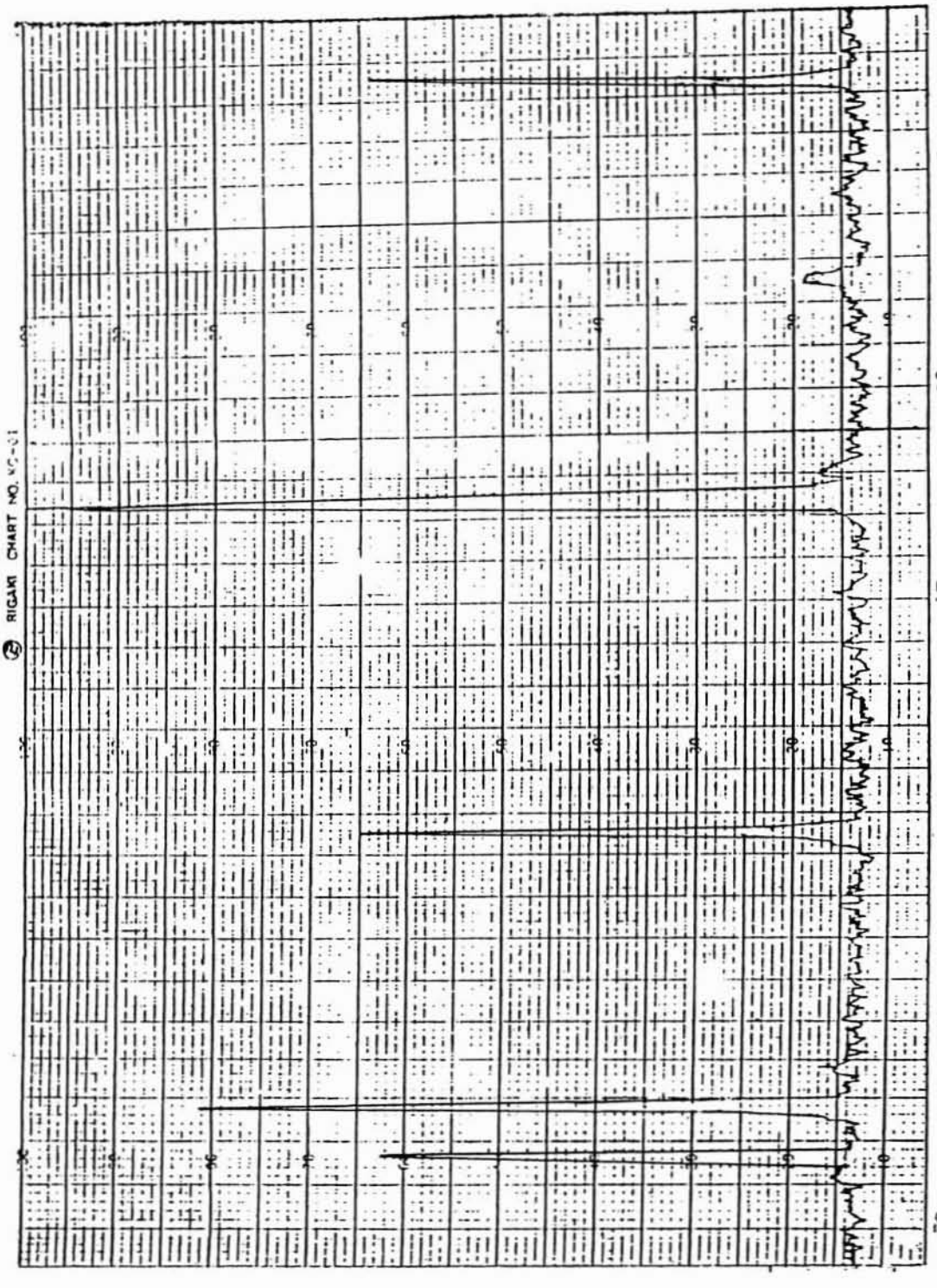

XRD patterns of $PrCrO_3$

Table- 7 XRD data for $PrCrO_3$.

JCPDS data			Observed data		
2θ	d (A^o)	I/I_o	2θ	d (A^o)	I/I_o
32.65	2.743	100	32.6	2.746	100
40.37	2.234	60	22.8	3.900	60
64.62	1.443	40	40.4	2.232	60
77.76	1.229	20	47.2	1.925	80
47.03	1.936	80	48.4	1.880	60
48.67	1.871	60	58.3	1.582	60
68.42	1.371	40			
78.67	1.217	20			
54.25	1.690	80			
58.36	1.582	60			
69.49	1.352	40			
82.14	1.173	20			
23.37	3.806	60			
42.16	2.143	40			
52.87	1.732	20			

Fig-8

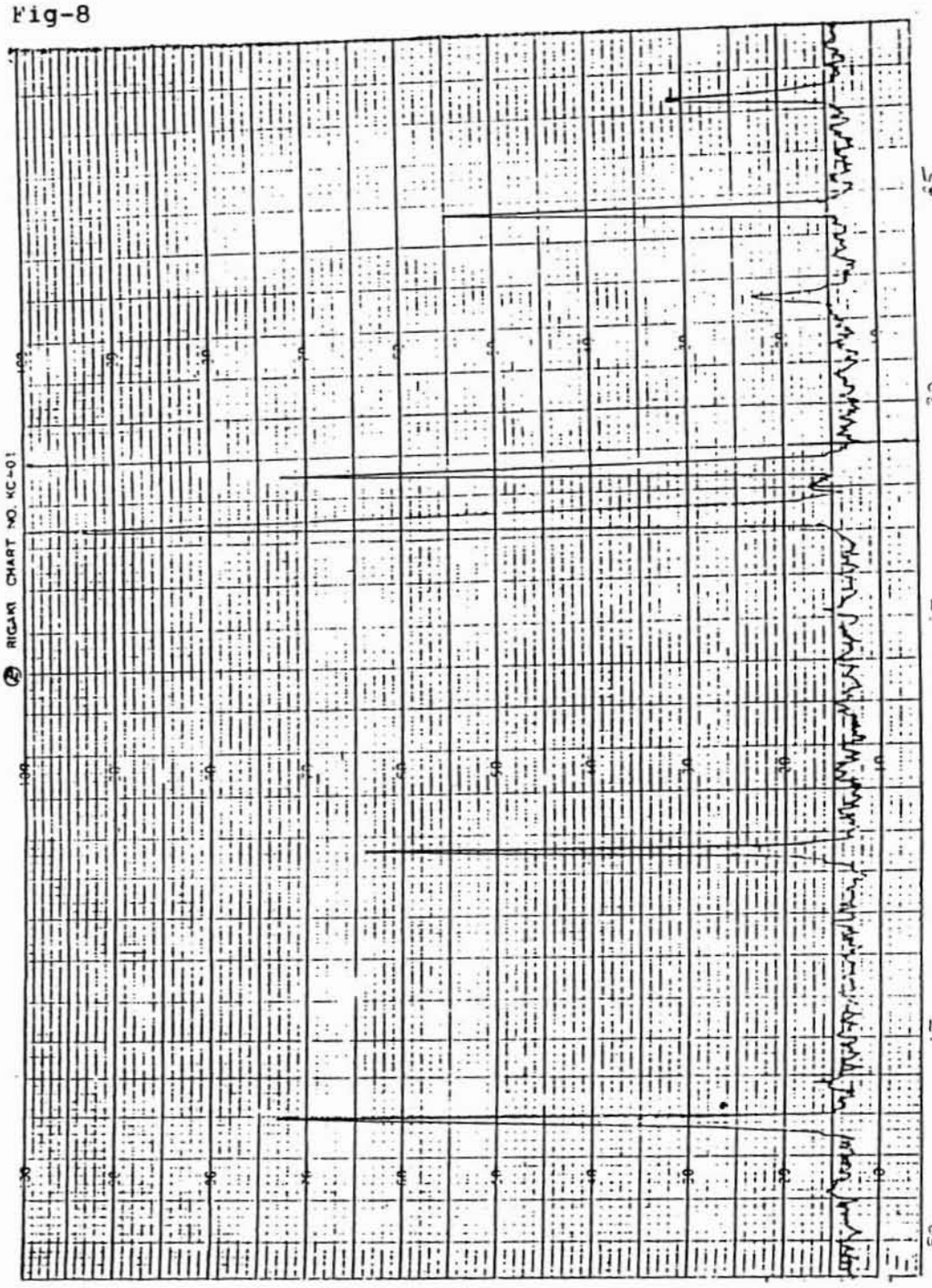

XRD patterns of $LaMnO_3$

Table-8 XRD data for $LaMnO_3$.

JCPDS data			Observed data		
2θ	d (A^o)	I/I_o	2θ	d (A^o)	I/I_o
32.38	2.773	100	32.6	2.746	100
31.37	2.852	70	31.4	2.848	70
40.18	2.247	60	22.8	3.90	24
25.27	3.536	50	25.4	3.506	50
57.75	1.599	90	27.6	3.231	13
47.31	1.922	70	40.4	2.232	60
52.08	1.756	60	47	1.933	70
33.39	2.686	50			
67.78	1.382	90			
56.35	1.633	70			
62.96	1.476	60			
39.34	2.290	50			
45.68	1.986	80			
58.46	1.579	70			
76.41	1.247	60			

Fig-9

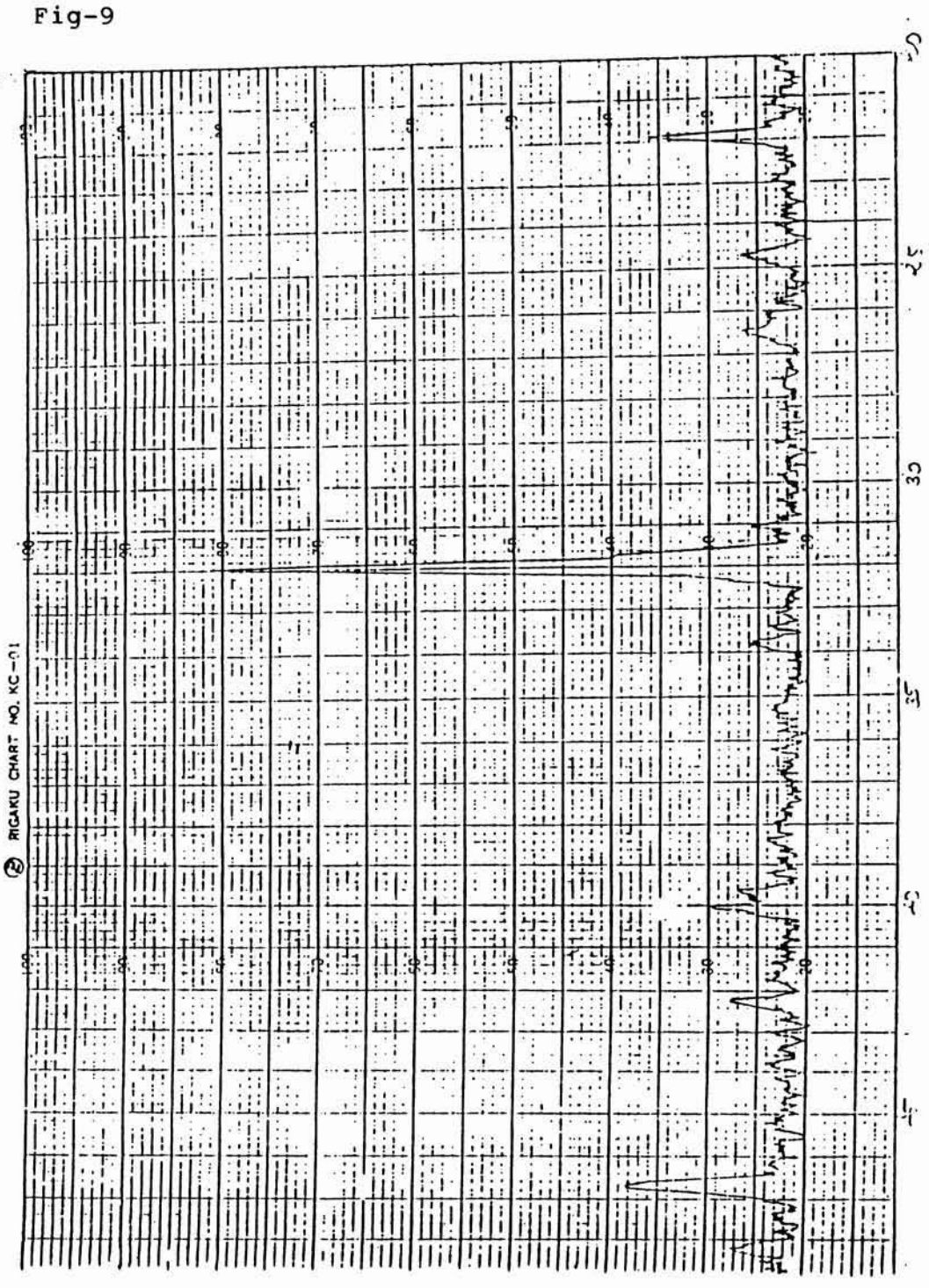

XRD patterns of $SmMnO_3$

Table-9 XRD data for $SmMnO_3$.

JCPDS data			Observed data		
2θ	d (A^o)	I/I_o	2θ	d (A^o)	I/I_o
32.93	2.720	100	32.2	2.779	100
48.57	1.873	14	22.0	4.040	26
42.82	2.112	10	24.8	3.590	10
63.06	1.474	8	40.0	2.253	16
33.39	2.686	25	42.4	2.131	11
45.97	1.976	12	46.8	1.733	29
47.99	1.895	10			
69.17	1.358	8			
59.57	1.552	20			
47.60	1.910	12			
51.30	1.781	10			
58.66	1.573	6			
25.54	3.488	18			
22.47	3.973	10			
60.29	1.535	10			

Table-10 XRD data for Pr_6O_{11} and Sm_2O_3

Pr_6O_{11}			Sm_2O_3		
2θ	d (A^o)	I/I_o	2θ	d (A^o)	I/I_o
29.90	2.999	100	28.24	3.155	100
46.00	1.976	63	32.75	2.731	35
39.40	2.287	58	34.79	2.575	8
26.10	3.414	34	36.72	2.444	2
52.08	1.760	52	47.03	1.931	40
55.45	1.657	24	48.53	1.873	4
28.08	3.185	45	48.66	1.873	4
45.11	2.012	45	50.04	1.821	2
49.05	1.857	35	51.57	1.772	6
24.82	3.602	25	55.80	1.647	30
27.20	3.280	100			
31.50	2.840	35			
53.86	1.810	25			

Table-10a XRD data for Cr_2O_3 and MnO_2

Cr_2O_3			MnO_2		
2θ	d (A^o)	I/I_o	2θ	d (A^o)	I/I_o
29.90	2.999	100	28.60	3.110	100
46.00	1.976	63	37.32	2.407	55
39.40	2.287	58	40.97	2.199	8
26.10	3.426	34	42.81	2.110	16
52.08	1.760	52	56.58	1.623	55
55.45	1.657	24	59.33	1.555	14
28.08	3.185	45	72.31	1.306	20
45.11	2.012	45	72.45	1.304	20
49.05	1.857	35	64.82	1.437	8
24.82	3.587	25	67.28	1.391	8
27.20	3.280	100			
31.50	2.840	35			
53.86	1.705	25			

Due to the absorption to Cu K_α (λ = 1.5418 A^o) by Fe and Ni, the XRD patterns of oxides containing Fe and Ni are not included.

spectra measured at room temperature using a Varian E-112 X/Q band ESR spectrophotometer.

The reflectance spectra of the adsorbed samples were measured with a Hitachi 200-20 UV-visible spectrophotometer equipped with a 200-0531 reflectance attachment.

The surface area of the samples was determined by the BET method using Carlo Erba Strumentazione Sorptomatic Series 1800. Data print out from the instrument are also attached (pages 96-118).

The oxides used and their surface area, alongwith the calcination temperature are also given in Table 1.

3.1.5 Electron acceptors

Electron acceptors employed for the study are 7,7,8,8-tetracyanoquinodimethane (TCNQ) 2,3,5,6-tetra-chloro-1,4-benzoquinone (chloranil), p-dinitrobenzene (PDNB) and m-dinitrobenzene (MDNB).

TCNQ was obtained from Merck Schuchandt and was purified by repeated recrystallisation from acetonitrile [3].

Carlo Erba Strumentazione Microstructure Lab.

Mi. Le. S. TO. NE. 1 0 0

Calculation parameters of Sorptomatic

Surface area of $LaCrO_3$

Sample	: DR.S.SUGUNAN/MI1/CUS63R		
Comment	: OUTGASSED AT 120 C		
Operator	: DOROTHY SAMUEL		
Date (mm/dd/yy)	: 08-25-1994		
Monolayer thickness (a)	4.3	Total introduction	: 9
Satur/Limit pressure (torr)	760	Reduced introduction	: 9
Mol.mass. gas ads. (g/mol)	28	Reduction factor	: .25
Gas ads. density (g/cm3)	.808	Constant bur.(cm3/torr)	: .11593
Burette temperature (c)	-195.82	Sample weight (g)	: 1.587
Operating pressure (torr)	800	Sample Density (g/mm3)	: 1.8356

Initial point (P/PO) for linear regression of B.E.T. region : .05

Final point (P/PO) for linear regression of B.E.T. region : .33

Correlation factor = .9870775

Monolayer Volume (CM3/G) = .6949994

Specific surface area (M2/G) = 3.036894

C value of B. E. T equation = 43.7213

Pore specific volume (CM3/G) = 1.540331E-03

Total volume introduced (CM3) = 35.71574

Corrected Burette Constant = .1119168

Adsorption values

P.ADS (Torr)	P/PO ADS	VI (CM3)	V.ADS(CM3/G)	T(A)	P/(PO-P)Va/g
29.5	0.0388	3.97	0.42	5.0	0.096103087
62.6	0.0824	7.94	0.59	5.4	0.153036162
97.1	0.1278	11.91	0.65	5.8	0.223922446
130.5	0.1717	15.87	0.80	6.1	0.259354560
165.8	0.2182	19.84	0.81	6.4	0.344266980
199.2	0.2621	23.81	0.96	6.7	0.371678650
235.3	0.3096	27.78	0.91	7.0	0.492554010
269.2	0.3542	31.75	1.02	7.3	0.537543710
305.0	0.4013	35.72	1.00	7.6	

Carlo Erba Strumentazione — Microstructure Lab.
MI. Le. S. TO. NE. 1 0 0

Calculation parameters of Sorptomatic

Sample : DR.S.SUGUNAN/M12/CUS64
Comment : OUTGASSED AT 120 C
Operator : DOROTHY SAMUEL
Date (mm/dd/yy) : 08-26-1994

Surface area of $PrCrO_3$

Monolayer thickness (a):	4.3	Total introduction :	9
Satur/Limit pressure (torr):	760	Reduced introduction :	9
Mol.mass. gas ads. (g/mol):	28	Reduction factor :	.25
Gas ads. density (g/cm3):	.808	Constant bur.(cm3/torr):	.11593
Burette temperature (c):	-195.82	Sample weight (g):	1.66
Operating pressure (torr):	800	Sample Density (g/mm3):	1.8444

Initial point (P/PO) for linear regression of B.E.T. region : .05

Final point (P/PO) for linear regression of B.E.T. region : .33

Correlation factor = .9902084

Monolayer Volume (CM3/G) = .6899586

Specific surface area (M2/G) = 3.014868

C value of B. E. T equation = 63.90827

Pore specific volume (CM3/G) = 1.508932E-03

Total volume introduced (CM3) = 35.71574

Corrected Burette Constant = .1117522

Adsorption values

P.ADS (Torr)	P/PO ADS	VI (CM3)	V.ADS(CM3/G)	T(A)	P/(PO-P)Va/g
28.9	0.0380	3.97	0.45	5.0	0.088821083
61.8	0.0813	7.94	0.62	5.4	0.142577186
96.2	0.1266	11.91	0.70	5.8	0.208344996
130.3	0.1714	15.87	0.79	6.1	0.261739940
165.3	0.2175	19.84	0.82	6.4	0.336931620
198.7	0.2614	23.81	0.97	6.7	0.366055760
234.9	0.3091	27.78	0.92	7.0	0.485888720
269.1	0.3541	31.75	1.01	7.3	0.543332340
305.1	0.4014	35.72	0.98	7.6	

Carlo Erba Strumentazione — Microstructure Lab.
MI. Le. S. TO. NE. 1 0 0

Calculation parameters of Sorptomatic

Sample : DR.S.SUGUNAN/M13/CUS65
Comment : OUTGASSED AT 120 C
Operator : DOROTHY SAMUEL
Date (mm/dd/yy) : 08-26-1994

Surface area of $SmCrO_3$

Monolayer thickness (a):	4.3	Total introduction :	11
Satur/Limit pressure (torr):	760	Reduced introduction :	11
Mol.mass. gas ads. (g/mol):	28	Reduction factor :	.25
Gas ads. density (g/cm3):	.808	Constant bur.(cm3/torr):	.167179
Burette temperature (c):	-195.82	Sample weight (g):	1.756
Operating pressure (torr):	800	Sample Density (g/mm3):	1.953

Initial point (P/PO) for linear regression of B.E.T. region : .05

Final point (P/PO) for linear regression of B.E.T. region : .3

Correlation factor = .9720756

Monolayer Volume (CM3/G) = .876489

Specific surface area (M2/G) = 3.829938

C value of B. E. T equation = 70.8293

Pore specific volume (CM3/G) = 1.980305E-03

Total volume introduced (CM3) = 43.65257

Corrected Burette Constant = .1630054

Adsorption values

P.ADS (Torr)	P/PO ADS	VI (CM3)	V.ADS(CM3/G)	r(A)	P/(PO-P)Va/g
19.0	0.0250	3.97	0.50	4.8	0.051675562
41.9	0.0551	7.94	0.63	5.2	0.092564091
63.8	0.0839	11.91	0.86	5.4	0.104887959
86.7	0.1141	15.87	0.99	5.7	0.129870847
111.8	0.1471	19.84	0.92	5.9	0.187179074
133.9	0.1762	23.81	1.13	6.1	0.189279139
160.5	0.2112	27.78	0.92	6.3	0.290817860
181.9	0.2393	31.75	1.19	6.5	0.263528790
206.9	0.2722	35.72	1.13	6.7	0.330097770
231.5	0.3046	39.68	1.11	6.9	0.394775480
254.0	0.3342	43.65	1.28	7.1	0.391902800

Carlo Erba Strumentazione — Microstructure Lab.
MI. Le. S. TO. NE. 1 0 0

Calculation parameters of Sorptomatic

Sample : DR.SUGUNAN/CUSAT/M14
Comment : OUTGASSED AT 120 C
Operator : A.NARAYANAN
Date (mm/dd/yy) : 12-07-1994

Surface area of $LaMnO_3$

Monolayer thickness (a):	4.3	Total introduction :	8
Satur/Limit pressure (torr):	760	Reduced introduction :	8
Mol.mass. gas ads. (g/mol):	28	Reduction factor :	.25
Gas ads. density (g/cm3):	.808	Constant bur.(cm3/torr):	.16778
Burette temperature (c):	-195.82	Sample weight (g):	1.36
Operating pressure (torr):	800	Sample Density (g/cm3):	.68

Initial point (P/PO) for linear regression of B.E.T. region : .05

Final point (P/PO) for linear regression of B.E.T. region :

Correlation factor .9941368

Monolayer Volume (CM3/G) 2.343533

Specific surface area (M2/G) = 10.24039

C value of B. E. T equation = 54.57

Pore specific volume (CM3/G) = 4.451043E-03

Total volume introduced (CM3) = 31.74733

Corrected Burette Constant .1584963

Adsorption values

P.ADS (Torr)	P/PO ADS	VI (CM3)	V.ADS(CM3/G)	T(A)	P/(PO-P)Va/g
22.1	0.0291	3.97	0.34	4.8	0.087473489
34.8	0.0458	7.94	1.78	5.1	0.026954839
57.9	0.0762	11.91	2.01	5.4	0.041107833
79.5	0.1046	15.87	2.41	5.6	0.048540510
105.3	0.1386	19.84	2.32	5.9	0.069387488
127.2	0.1674	23.81	2.68	6.1	0.074902287
152.2	0.2003	27.78	2.69	6.3	0.093156599
175.6	0.2311	31.75	2.88	6.5	0.104371011

Carlo Erba Strumentazione — Microstructure Lab.

MI. Le. S. TO. NE. 1 0 0

Calculation parameters of Sorptomatic

Sample : DR,SUGUNAN/CUSAT/M15
Comment : OUTGASSED AT 120 C
Operator : A.NARAYANAN
Date (mm/dd/yy) : 12-07-1994

Surface area of $PrMnO_3$

Monolayer thickness (a):	4.3	Total introduction :	6
Satur/Limit pressure (torr):	760	Reduced introduction :	6
Mol.mass. gas ads. (g/mol):	28	Reduction factor :	.25
Gas ads. density (g/cm3):	.808	Constant bur.(cm3/torr):	.11478
Burette temperature (c):	-195.82	Sample weight (g):	1.318
Operating pressure (torr):	800	Sample Density (g/cm3):	.88

Initial point (P/PO) for linear regression of B.E.T. region : .05

Final point (P/PO) for linear regression of B.E.T. region : .33

Correlation factor = .9993954

Monolayer Volume (CM3/G) = 3.619741

Specific surface area (M2/G) = 15.81695

C value of B. E. T equation = 43.13878

Pore specific volume (CM3/G) = 6.44300E-03

Total volume introduced (CM3) = 23.8105

Corrected Burette Constant = .1078278

Adsorption values

P.ADS (Torr)	P/PO ADS	VI (CM3)	V.ADS(CM3/G)	T(A)	P/(PO-P)Va/g
9.0	0.0118	3.97	2.27	4.5	0.005268552
40.0	0.0526	7.94	2.75	5.1	0.020206366
70.8	0.0932	11.91	3.24	5.5	0.031700760
103.5	0.1362	15.87	3.58	5.8	0.044083752
134.8	0.1774	19.84	4.03		0.053548325
168.3	0.2214	23.81	4.30	6.4	0.066198058

Carlo Erba Strumentazione Microstructure Lab.
MI. Le. S. TO. NE. 1 0 0

Calculation parameters of Sorptomatic

Surface area of $SmMnO_3$

Sample	: DR.SUGUNAN/CUSAT/M16		
Comment	: OUTGASSED AT 120 C		
Operator	: A.NARAYANAN		
Date (mm/dd/yy)	: 12-07-1994		
Monolayer thickness (a)	4.3	Total introduction	: 11
Satur/Limit pressure (torr)	760	Reduced introduction	: 11
Mol.mass. gas ads. (g/mol)	28	Reduction factor	: .25
Gas ads. density (g/cm3)	.808	Constant bur.(cm3/torr)	: .167013
Burette temperature (c)	-195.82	Sample weight (g)	: 1.394
Operating pressure (torr)	,800	Sample Density (g/cm3)	: .66

Initial point (P/PO) for linear regression of B.E.T. region : .05

Final point (P/PO) for linear regression of B.E.T. region : .33

Correlation factor = .9961588

Monolayer Volume (CM3/G) = 3.128061

Specific surface area (M2/G) = 13.66849

C value of B. E. T equation = 40.5617

Pore specific volume (CM3/G) = ~~6.5859246-05~~

Total volume introduced (CM3) = 43.65257

Corrected Burette Constant = .1572089

Adsorption values

P.ADS (Torr)	P/PO ADS	VI (CM3)	V.ADS(CM3/G)	T(A)	P/(PO-P)Va/a
8.7	0.0114	3.97	1.87	4.5	0.006206955
29.5	0.0388	7.94	2.37	5.0	0.017063174
53.2	0.0700	11.91	2.54	5.3	0.029625224
75.3	0.0991	15.87	2.90	5.6	0.037986033
99.5	0.1309	19.84	3.01	5.8	0.050001692
123.2	0.1621	23.81	3.19	6.0	0.060709454
144.0	0.1895	27.78	3.69	6.2	0.063388564
169.3	0.2228	31.75	3.68	6.4	0.077853374
193.3	0.2543	35.72	3.82	6.6	0.089235877
214.6	0.2824	39.68	4.27	6.8	0.092229486
239.9	0.3157	43.65	4.26	7.0	0.108281426

Carlo Erba Strumentazione Microstructure Lab.

NI. Le. S. TO. NE. 1 0 0

Calculation parameters of Sorptomatic

Sample : DR.SUGUNAN/CUSAT/M8

Comment : OUTGASSED AT 120 C

Operator : A.NARAYANAN

Date (mm/dd/yy) : 10-21-1993

Surface area of $LaFeO_3$

Monolayer thickness (a):	4.3	Total introduction :	7
Satur/Limit pressure (torr):	760	Reduced introduction :	7
Mol.mass. gas ads. (g/mol):	28	Reduction factor :	.25
Gas ads. density (g/cm3):	.808	Constant bur.(cm3/torr):	.10785
Burette temperature (c):	-195.82	Sample weight (g):	.867
Operating pressure (torr):	800	Sample Density (g/cm3):	1.1

Initial point (P/PO) for linear regression of B.E.T. region : .05

Final point (P/PO) for linear regression of B.E.T. region : .33

Correlation factor = .9974249

Monolayer Volume (CM3/G) = 3.286411

Specific surface area (M2/G) = 14.30042

C value of B. E. T equation = 13.9659

Pore specific volume (CM3/G) =

Total volume introduced (CM3) = 27.77891

Corrected Burette Constant = .1041914

Adsorption values

P.ADS (Torr)	P/PO ADS	VI (CM3)	V.ADS(CM3/G)	T(A)	P/(PO-P)Va/g
26.3	0.0346	3.97	1.42	4.9	0.025304241
59.7	0.0786	7.94	1.98	5.4	0.043056481
93.6	0.1232	11.91	2.48	5.7	0.056562562
128.1	0.1686	15.87	2.91	6.1	0.069559753
163.8	0.2155	19.84	3.20	6.4	0.085821249
197.2	0.2595	23.81	3.76	6.7	0.093073830
232.6	0.3061	27.78	4.09	7.0	0.107893459

Carlo Erba Strumentazione Microstructure Lab.
MI. Le. S. TO. NE. 1 0 0

Calculation parameters of Sorptomatic

Sample : DR.SUGUNAN/CUSAT/M9
Comment : OUTGASSED AT 120 C
Operator : A.NARAYANAN
Date (mm/dd/yy) : 10-21-1993

Surface area of $PrFeO_3$

Monolayer thickness (a):	4.3	Total introduction :	8
Satur/Limit pressure (torr):	760	Reduced introduction :	8
Mol.mass. gas ads. (g/mol):	28	Reduction factor :	.25
Gas ads. density (g/cm3):	.808	Constant bur.(cm3/torr):	.11112
Burette temperature (c):	-195.82	Sample weight (g):	.756
Operating pressure (torr):	800	Sample Density (g/cm3):	.99

Initial point (P/PO) for linear regression of B.E.T. region : .05

Final point (P/PO) for linear regression of B.E.T. region : .33

Correlation factor = .9945926

Monolayer Volume (CM3/G) = 4.150209

Specific surface area (M2/G) = 18.1349

C value of B. E. T equation = 20.29986

Pore specific volume (CM3/G) =

Total volume introduced (CM3) = 31.74733

Corrected Burette Constant = .1075753

Adsorption values

P.ADS (Torr)	P/PO ADS	VT (CM3)	V.ADS(CM3/G)	T(A)	P/(PO-P)Va/g
21.4	0.0282	3.97	2.20	4.8	0.013145343
53.5	0.0704	7.94	2.89	5.3	0.026242051
87.1	0.1146	11.91	3.35	5.7	0.038595468
120.2	0.1582	15.87	3.89	6.0	0.048258647
155.4	0.2045	19.84	4.13	6.3	0.062182985
187.5	0.2467	23.81	4.81	6.6	0.068019159
220.6	0.2903	27.78	5.35	6.8	0.076383151
254.0	0.3342	31.75	5.85	7.1	0.085796252

Carlo Erba Strumentazione Microstructure Lab.

MI. Le. S. TO. NE. 1 0 0

Calculation parameters of Sorptomatic

Sample : DR.SUGUNAN/CUSAT/M10

Comment : OUTGASSED AT 120 C

Operator : A.NARAYANAN Surface area of $SmFeO_3$

Date (mm/dd/yy) : 10-21-1993

Monolayer thickness (a):	4.3	Total introduction :	10
Satur/Limit pressure (torr):	760	Reduced introduction :	10
Mol.mass. gas ads. (g/mol):	28	Reduction factor :	.25
Gas ads. density (g/cm3):	.808	Constant bur.(cm3/torr):	.11263
Burette temperature (c):	-195.82	Sample weight (g):	.748
Operating pressure (torr):	800	Sample Density (g/cm3):	.88

Initial point (P/PO) for linear regression of B.E.T. region : .05

Final point (P/PO) for linear regression of B.E.T. region : .33

Correlation factor = .9941173

Monolayer Volume (CM3/G) = 3.329813

Specific surface area (M2/G) = 14.55007

C value of B. E. T equation = 15.56386

Pore specific volume. (CM3/G) =

Total volume introduced (CM3) = 39.68416

Corrected Burette Constant = .1086844

Adsorption values

P.ADS (Torr)	P/PO ADS	VI (CM3)	V.ADS(CM3/G)	T(A)	P/(PO-P)Va/g
26.1	0.0343	3.97	1.51	4.9	0.023504650
58.8	0.0774	7.94	2.07	5.4	0.040567193
91.4	0.1203	11.91	2.64	5.7	0.051866472
125.1	0.1646	15.87	3.04	6.0	0.064720884
160.4	0.2111	19.84	3.22	6.3	0.083059624
193.5	0.2546	23.81	3.72	6.6	0.091902763
226.4	0.2979	27.78	4.24	6.9	0.100028776
260.1	0.3422	31.75	4.65	7.2	0.111883447
295.1	0.3883	35.72	4.87	7.5	0.130333483
329.1	0.4330	39.68	5.24	7.8	

Carlo Erba Strumentazione Microstructure Lab.
MI. Le. S. TO. NE. 1 0 0

Calculation parameters of Sorptomatic

Sample : DR.SUGUNAN/CUSAT/M1
Comment : OUTGASSED AT 120 C Surface area of $LaCoO_3$
Operator : A.NARAYANAN
Date (mm/dd/yy) : 07-22-1993

Monolayer thickness (a):	4.3	Total introduction	: 12
Satur/Limit pressure (torr):	760	Reduced introduction	: 12
Mol.mass. gas ads. (g/mol):	28	Reduction factor	: .25
Gas ads. density (g/cm3):	.808	Constant bur.(cm3/torr):	.11478
Burette temperature (c):	-195.82	Sample weight (g):	1.084
Operating pressure (torr):	800	Sample Density (g/cm3):	.9

Initial point (P/P0) for linear regression of B.E.T. region : .05

Final point (P/P0) for linear regression of B.E.T. region : .33

Correlation factor = .9991796

Monolayer Volume (CM3/G) = 2.428625

Specific surface area (M2/G) = 10.61221

C value of B. E. T equation = 22.63492

Pore specific volume (CM3/G) =

Total volume introduced (CM3) = 47.62099

Corrected Burette Constant = .1091892

Adsorption values

P.ADS (Torr)	P/P0 ADS	VI (CM3)	V.ADS(CM3/G)	T(A)	P/(P0-P)Va/g
24.9	0.0328	3.97	1.15	4.9	0.029383875
55.4	0.0729	7.94	1.74	5.3	0.045149319
89.0	0.1171	11.91	2.02	5.7	0.065730348
122.1	0.1607	15.87	2.34	6.0	0.081634432
156.2	0.2055	19.84	2.57	6.3	0.100628600
189.5	0.2493	23.81	2.88	6.6	0.115437321
223.4	0.2939	27.78	3.12	6.9	0.133280843
256.5	0.3375	31.75	3.45	7.2	0.147641852
290.6	0.3824	35.72	3.68	7.5	0.168388680
323.4	0.4255	39.68	4.03	7.7	
358.1	0.4712	43.65	4.20	8.1	
390.6	0.5139	47.62	4.59	8.4	

Carlo Erba Strumentazione Microstructure Lab.

MI. Le. S. TO. NE. 1 0 0

Calculation parameters of Sorptomatic

Sample : DR.SUGUNAN/CUSAT/M2
Comment : OUTGASSED AT 120 C
Operator : A.NARAYANAN
Date (mm/dd/yy) : 07-22-1993

Surface area of $PrCoO_3$

Monolayer thickness (a):	4.3	Total introduction	: 13
Satur/Limit pressure (torr):	760	Reduced introduction	: 13
Mol.mass. gas ads. (g/mol):	28	Reduction factor	: .25
Gas ads. density (g/cm3):	.808	Constant bur.(cm3/torr):	.112155
Burette temperature (c):	-195.82	Sample weight (g):	1.06
Operating pressure (torr):	800	Sample Density (g/cm3):	1.12

Initial point (P/P0) for linear regression of B.E.T. region : .05

Final point (P/P0) for linear regression of B.E.T. region : .33

Correlation factor = .9987022

Monolayer Volume (CM3/G) = 1.662556

Specific surface area (M2/G) = 7.264764

C value of B. E. T equation = 19.96683

Pore specific volume (CM3/G) =

Total volume introduced (CM3) = 51.5894

Corrected Burette Constant = .1077618

Adsorption values

P.ADS (Torr)	P/P0 ADS	VI (CM3)	V.ADS(CM3/G)	T(A)	P/(P0-P)Va/g
29.7	0.0391	3.97	0.72	5.0	0.056138676
62.0	0.0816	7.94	1.18	5.4	0.074987896
96.9	0.1275	11.91	1.38	5.8	0.105868928
131.0	0.1724	15.87	1.66	6.1	0.125657380
166.7	0.2193	19.84	1.77	6.4	0.158572778
201.4	0.2650	23.81	1.99	6.7	0.181361496
236.3	0.3109	27.78	2.18	7.0	0.206621036
269.9	0.3551	31.75	2.51	7.3	0.219254553
306.9	0.4038	35.72	2.49	7.6	
340.5	0.4480	39.68	2.82	7.9	
375.7	0.4943	43.65	2.99	8.3	
409.0	0.5382	47.62	3.35	8.6	
445.0	0.5855	51.59	3.43	9.1	

Carlo Erba Strumentazione Microstructure Lab.

MI. Le. S. TO. NE. 1 0 0

Calculation parameters of Sorptomatic

Sample : DR.SUGUNAN/CUSAT/CODE[M3]
Comment : OUTGASSED AT 120 C
Operator : A.NARAYANAN
Date (mm/dd/yy) : 07-27-1993

Surface area of $SmCoO_3$

Monolayer thickness (a):	4.3	Total introduction :	5
Satur/Limit pressure (torr):	760	Reduced introduction :	5
Mol.mass. gas ads. (g/mol):	28	Reduction factor :	.25
Gas ads. density (g/cm3):	.808	Constant bur.(cm3/torr):	.112155
Burette temperature (c):	-195.82	Sample weight (g):	1.218
Operating pressure (torr):	800	Sample Density (g/mm3):	1.11

Initial point (P/PO) for linear regression of B.E.T. region : .05

Final point (P/PO) for linear regression of B.E.T. region : .33

Correlation factor = .9988291

Monolayer Volume (CM3/G) = 1.390828

Specific surface area (M2/G) = [6.077417]

C value of B. E. T equation = 59.45795

Pore specific volume (CM3/G) = ~~9.586611E-03~~

Total volume introduced (CM3) = 19.84208

Corrected Burette Constant = .1070615

Adsorption values

P.ADS (Torr)	P/PO ADS	VI (CM3)	V.ADS(CM3/G)	T(A)	P/(PO-P)Va/g
26.8	0.0353	3.97	0.90	4.9	0.040503807
59.6	0.0784	7.94	1.28	5.4	0.066611208
95.4	0.1255	11.91	1.39	5.8	0.103357777
130.3	0.1714	15.87	1.58	6.1	0.131025210
166.3	0.2188	19.84	1.67	6.4	0.167425483

Carlo Erba Strumentazione Microstructure Lab.
MI. Le. S. TO. NE. 1 0 0

Calculation parameters of Sorptomatic

Sample	: DR.SUGUNAN/CUSAT/MS		
Comment	: OUTGASSED AT 120 C		
Operator	: A.NARAYANAN	Surface area of $LaNiO_3$	
Date (mm/dd/yy)	: 10-21-1993		
Monolayer thickness (a)	4.3	Total introduction	: 6
Satur/Limit pressure (torr)	760	Reduced introduction	: 6
Mol.mass. gas ads. (g/mol)	28	Reduction factor	: .25
Gas ads. density (g/cm3)	.808	Constant bur.(cm3/torr)	: .10785
Burette temperature (c)	-195.82	Sample weight (g)	: .586
Operating pressure (torr)	800	Sample Density (g/cm3)	: .73

Initial point (P/PO) for linear regression of B.E.T. region : .05

Final point (P/PO) for linear regression of B.E.T. region : .33

Correlation factor = .9974258

Monolayer Volume (CM3/G) = 3.582845

Specific surface area (M2/G) = 15.65573

C value of B. E. T equation = 16.31274

Pore specific volume (CM3/G) =

Total volume introduced (CM3) = 23.8105

Corrected Burette Constant = .1041238

Adsorption values

P.ADS (Torr)	P/PO ADS	VI (CM3)	V.ADS(CM3/G)	T(A)	P/(PO-P)Va/g
27.7	0.0364	3.97	1.85	4.9	0.020444870
62.7	0.0825	7.94	2.40	5.4	0.037416212
98.3	0.1293	11.91	2.85	5.8	0.052132104
133.5	0.1757	15.87	3.37	6.1	0.063284971
169.6	0.2232	19.84	3.72	6.4	0.077123486
204.6	0.2692	23.81	4.28	6.7	0.086116046

Carlo Erba Strumentazione Microstructure Lab.
MI. Le. S. TO. NE. 1 0 0

Calculation parameters of Sorptomatic

Sample : DR.SUGUNAN/CUSAT/M6
Comment : OUTGASSED AT 120 C
Operator : A.NARAYANAN
Date (mm/dd/yy) : 10-21-1993

Surface area of $PrNiO_3$

Monolayer thickness (a):	4.3	Total introduction :	8
Satur/Limit pressure (torr):	760	Reduced introduction :	8
Mol.mass. gas ads. (g/mol):	28	Reduction factor :	.25
Gas ads. density (g/cm3):	.808	Constant bur.(cm3/torr):	.11112
Burette temperature (c):	-195.82	Sample weight (g):	.702
Operating pressure (torr):	800	Sample Density (g/cm3):	2.2

Initial point (P/PO) for linear regression of B.E.T. region : .05

Final point (P/PO) for linear regression of B.E.T. region : .33

Correlation factor = .9993954

Monolayer Volume (CM3/G) = 1.362195

Specific surface area (M2/G) = 15.952298

C value of B. E. T equation = 77.91014

Pore specific volume (CM3/G) =

Total volume introduced (CM3) = 31.74733

Corrected Burette Constant = .1096388

Adsorption values

P.ADS (Torr)	P/PO ADS	VI (CM3)	V.ADS(CM3/G)	T(A)	P/(PO-P)Va/g
29.5	0.0388	3.97	1.05	5.0	0.038619012
63.9	0.0841	7.94	1.33	5.4	0.069224276
99.6	0.1311	11.91	1.40	5.8	0.107462205
134.6	0.1771	15.87	1.59	6.1	0.135348082
170.3	0.2241	19.84	1.67	6.4	0.173187584
205.5	0.2704	23.81	1.82	6.7	0.203298256
241.0	0.3171	27.78	1.93	7.0	0.240403891
274.6	0.3613	31.75	2.34	7.3	0.242080808

Carlo Erba Strumentazione Microstructure Lab.
MI. Le. S. TO. NE. 1 0 0

Calculation parameters of Sorptomatic

Sample : DR.SUGUNAN/CUSAT/M7
Comment : OUTGASSED AT 120 C
Operator : A.NARAYANAN
Date (mm/dd/yy) : 10-21-1993

Surface area of $SmNiO_3$

Monolayer thickness (a):	4.3	Total introduction :	7
Satur/Limit pressure (torr):	760	Reduced introduction :	7
Mol.mass. gas ads. (g/mol):	28	Reduction factor :	.25
Gas ads. density (g/cm3):	.808	Constant bur.(cm3/torr):	.11263
Burette temperature (c):	-195.82	Sample weight (g):	.771
Operating pressure (torr):	800	Sample Density (g/cm3):	1.3

Initial point (P/PO) for linear regression of B.E.T. region : .05

Final point (P/PO) for linear regression of B.E.T. region : .33

Correlation factor = .9994005

Monolayer Volume (CM3/G) = 2.633138

Specific surface area (M2/G) = 11.50585

C value of B. E. T equation = 17.65742

Pore specific volume (CM3/G) =

Total volume introduced (CM3) = 27.77891

Corrected Burette Constant = .109877

Adsorption values

P.ADS (Torr)	P/PO ADS	VI (CM3)	V.ADS(CM3/G)	T(A)	P/(PO-P)Va/g
26.9	0.0354	3.97	1.31	4.9	0.027935237
60.0	0.0789	7.94	1.74	5.4	0.049163215
93.6	0.1232	11.91	2.10	5.7	0.066815481
127.0	0.1671	15.87	2.49	6.1	0.080596395
161.4	0.2124	19.84	2.73	6.4	0.098620042
195.1	0.2567	23.81	3.08	6.6	0.112189747
229.5	0.3020	27.78	3.32	6.9	0.130181596

Carlo Erba Strumentazione Microstructure Lab.
MI. Le. S. TO. NE. 1 0 0

Calculation parameters of Sorptomatic

Sample : DR.SUGUNAN/CUSAT/CODE NO. V1
Comment : OUTGASSED AT 120 C
Operator : A.NARAYANAN
Date (mm/dd/yy) : 01-24-1994

Surface area of La_2O_3

Monolayer thickness (a):	4.3	Total introduction :	12
Satur/Limit pressure (torr):	760	Reduced introduction :	12
Mol.mass. gas ads. (g/mol):	28	Reduction factor :	.25
Gas ads. density (g/cm3):	.808	Constant bur.(cm3/torr):	.11436
Burette temperature (c):	-195.82	Sample weight (g):	1.339
Operating pressure (torr):	800	Sample Density (g/cm3):	.605

Initial point (P/PO) for linear regression of B.E.T. region : .05

Final point (P/PO) for linear regression of B.E.T. region : .33

Correlation factor = .9995769

Monolayer Volume (CM3/G) = 8.041904

Specific surface area (M2/G) = 35.14019

C value of B. E. T equation = 68.16414

Pore specific volume (CM3/G) = 1.935006E-02

Total volume introduced (CM3) = 47.62099

Corrected Burette Constant = .1040856

Adsorption values

P.ADS (Torr)	P/PO ADS	VI (CM3)	V.ADS(CM3/G)	T(A)	P/(PO-P)Va/g
1.3	0.0017	3.97	2.86	4.0	0.000598554
7.4	0.0097	7.94	5.35	4.4	0.001837111
29.5	0.0388	11.91	6.60	5.0	0.006120555
57.9	0.0762	15.87	7.35	5.4	0.011213829
87.4	0.1150	19.84	8.02	5.7	0.016193181
115.8	0.1524	23.81	8.78	6.0	0.020472074
144.5	0.1901	27.78	9.51	6.2	0.024677733
176.6	0.2324	31.75	9.98	6.5	0.030325990
206.5	0.2704	35.72	10.70	6.7	0.034639154
237.1	0.3120	39.68	11.21	7.0	0.040462315
264.7	0.3483	43.65	12.02	7.2	0.044444412
296.1	0.3896	47.62	12.55	7.5	0.050869875

Carlo Erba Strumentazione Microstructure Lab.
MI. Le. S. TO. NE. 1 0 0

Calculation parameters of Sorptomatic

Sample : DR.SUGUNAN/CUSAT/CODE NO.'Y5'
Comment : OUTGASSED AT 120 C
Operator : A.NARAYANAN
Date (mm/dd/yy) : 01-24-1994 Surface area of Pr_6O_{11}

Monolayer thickness (a):	4.3	Total introduction	: 10
Satur/Limit pressure (torr):	760	Reduced introduction	: 10
Mol.mass. gas ads. (g/mol):	28	Reduction factor	: .25
Gas ads. density (g/cm3):	.808	Constant bur.(cm3/torr):	.16209
Burette temperature (c):	-195.82	Sample weight (g):	1.115
Operating pressure (torr):	800	Sample Density (g/cm3):	1.03

Initial point (P/PO) for linear regression of B.E.T. region : .05

Final point (P/PO) for linear regression of B.E.T. region : .33

Correlation factor = .9966384

Monolayer Volume (CM3/G) = 3.239369

Specific surface area (M2/G) = 14.15407

C value of B. E. T equation = 66.53358

Pore specific volume (CM3/G) = 6.680834E-03

Total volume introduced (CM3) = 39.68416

Corrected Burette Constant = .1570471

Adsorption values

P.ADS (Torr)	P/PO ADS	VI (CM3)	V.ADS(CM3/G)	T(A)	P/(PO-P)Va/g
8.4	0.0111	3.97	2.37	4.5	0.004720678
32.5	0.0428	7.94	2.53	5.0	0.017646726
56.1	0.0738	11.91	2.77	5.3	0.028816035
76.6	0.1008	15.87	3.44	5.6	0.032629952
102.5	0.1349	19.84	3.35	5.8	0.046583787
125.9	0.1657	23.81	3.61	6.0	0.055017743
150.0	0.1974	27.78	3.77	6.3	0.065176137
173.9	0.2288	31.75	3.97	6.5	0.074831381
198.4	0.2584	35.72	4.35	6.6	0.080042347
221.9	0.2920	39.68	4.32	6.9	0.095431328

Carlo Erba Strumentazione Microstructure Lab.
MI. Le. S. TO. NE. 1 0 0

Calculation parameters of Sorptomatic

Sample : DR.SUGUNAN/CUSAT/CODE NO. V21
Comment : OUTGASSED AT 120 C
Operator : A.NARAYANAN
Date (mm/dd/yy) : 01-24-1994 Surface area of Sm_2O_3

Monolayer thickness (a):	4.3	Total introduction :	14
Satur/Limit pressure (torr):	760	Reduced introduction :	14
Mol.mass. gas ads. (g/mol):	28	Reduction factor :	.25
Gas ads. density (g/cm3):	.808	Constant bur.(cm3/torr):	.16209
Burette temperature (c):	-195.82	Sample weight (g):	1.378
Operating pressure (torr):	800	Sample Density (g/cm3):	1.05

Initial point (P/PO) for linear regression of B.E.T. region : .05

Final point (P/PO) for linear regressic of B.E.T. region : .33

Correlation factor = .9996225

Monolayer Volume (CM3/G) = 6.86906

Specific surface area (M2/G) = 30.01529

C value of B. E. T equation = 148.8526

Pore specific volume (CM3/G) = 1.0[illegible]4E-02

Total volume introduced (CM3) = 55.55782

Corrected Burette Constant = .1559981

Adsorption values

P.ADS (Torr)	P/PO ADS	VI (CM3)	V.ADS(CM3/G)	T(A)	P/(PO-P)Va/g
1.1	0.0014	3.97	2.76	3.9	0.000526063
7.4	0.0097	7.94	4.92	4.4	0.001997701
25.0	0.0329	11.91	5.81	4.9	0.005854968
43.2	0.0568	15.87	6.63	5.2	0.009091763
64.5	0.0849	19.84	7.10	5.4	0.013066643
88.7	0.1167	23.81	7.24	5.7	0.018256191
110.0	0.1447	27.78	7.71	5.9	0.021960395
131.3	0.1728	31.75	8.17	6.1	0.025547478
156.1	0.2054	35.72	8.25	6.3	0.031342912
176.8	0.2336	39.68	8.78	6.5	0.034514077
198.2	0.2608	43.65	9.24	6.7	0.038178179
221.3	0.2912	47.62	9.51	6.9	0.043217421
242.9	0.3196	51.59	9.94	7.0	0.047256589
263.4	0.3466	55.56	10.50	7.2	0.050518744

Carlo Erba Strumentazione Microstructure Lab.
MI. Le. S. TO. NE. 1 0 0

Calculation parameters of Sorptomatic

Surface area of Cr_2O_3

Sample	: DR.S.SUGUNAN/VZ/CU362		
Comment	: OUTGASSED AT 120 C		
Operator	: DOROTHY SAMUEL		
Date (mm/dd/yy)	: 08-24-1994		
Monolayer thickness (a):	4.3	Total introduction	: 9
Satur/Limit pressure (torr):	760	Reduced introduction	: 9
Mol.mass. gas ads. (g/mol):	28	Reduction factor	: .25
Gas ads. density (g/cm3):	.808	Constant bur.(cm3/torr):	.11593
Burette temperature (c):	-195.82	Sample weight (g):	1.645
Operating pressure (torr):	800	Sample Density (g/mm3):	.7948

Initial point (P/PO) for linear regression of B.E.T. region : .05

Final point (P/PO) for linear regression of B.E.T. region : .33

Correlation factor = .999249

Monolayer Volume (CM3/G) = 4.162902

Specific surface area (M2/G) = 18.19037

C value of B. E. T equation = 31.80638

Pore specific volume (CM3/G) = 8.84545E-03

Total volume introduced (CM3) = 35.71574

Corrected Burette Constant = .1063228

Adsorption values

P.ADS (Torr)	P/PO ADS	VI (CM3)	V.ADS(CM3/G)	T(A)	P/(PO-P)Va/g
5.3	0.0070	3.97	2.07	4.3	0.003392832
29.5	0.0388	7.94	2.92	5.0	0.013838796
60.0	0.0789	11.91	3.36	5.4	0.025516281
91.2	0.1200	15.87	3.76	5.7	0.036314897
121.2	0.1595	19.84	4.23	6.0	0.044870302
152.5	0.2007	23.81	4.62	6.3	0.054361168
182.8	0.2405	27.78	5.07	6.5	0.062443569
214.6	0.2824	31.75	5.43	6.8	0.072478041
247.4	0.3255	35.72	5.72	7.1	0.084358416

Carlo Erba Strumentazione — Microstructure Lab.
MI. Le. S. TO. NE. 1 0 0

Calculation parameters of Sorptomatic

Surface area of MnO_2

Sample	: DR.SUGUNAN/CUSAT/V8		
Comment	: OUTGASSED AT 120 C		
Operator	: A.NARAYANAN		
Date (mm/dd/yy)	: 12-07-1994		
Monolayer thickness (a):	4.3	Total introduction	: 13
Satur/Limit pressure (torr):	760	Reduced introduction	: 13
Mol.mass. gas ads. (g/mol):	28	Reduction factor	: .25
Gas ads. density (g/...):	.808	Constant bur.(cm3/torr):	.16778
Burette temperature (c):	-195.82	Sample weight (g):	1.541
Operating pressure (torr):	800	Sample Density (g/cm3):	.57

Initial point (P/PO) for linear regression of B.E.T. region : .05

Final point (P/PO) for linear regression of B.E.T. region : .33

Correlation factor = .990489

Monolayer Volume (CM3/G) = 2.157194

Specific surface area (M2/G) = 9.426151

C value of B. E. T equation = 15.09514

Pore specific volume (CM3/G) = ~~4.927657E-03~~

Total volume introduced (CM3) = 51.5894

Corrected Burette Constant = .1552307

Adsorption values

P.ADS (Torr)	P/PO ADS	VI (CM3)	V.ADS(CM3/G)	T(A)	P/(PO-P)Va/g
24.2	0.0318	3.97	0.14	4.9	0.239257500
40.8	0.0537	7.94	1.04	5.1	0.054521292
62.1	0.0817	11.91	1.47	5.4	0.060527414
87.2	0.1147	15.87	1.52	5.7	0.085442327
109.5	0.1441	19.84	1.85	5.9	0.091199301
133.5	0.1757	23.81	2.00	6.1	0.106365025
158.8	0.2089	27.78	2.03	6.3	0.130115643
180.1	0.2370	31.75	2.46	6.5	0.126267821
205.7	0.2707	35.72	2.46	6.7	0.151095361
228.6	0.3008	39.68	2.72	6.9	0.157896340
253.1	0.3330	43.65	2.83	7.1	0.176327556
276.8	0.3642	47.62	3.02	7.3	0.189713106
300.7	0.3957	51.59	3.19	7.5	0.205411091

Carlo Erba Strumentazione — Microstructure Lab.
MI. Le. S. TO. NE. 1 0 0

Calculation parameters of Sorptomatic

Sample : DR.SUGUNAN/CUSAT/CODE V3.
Comment : OUTGASSED AT 120 C;REPEAT ANALYSIS WITH MORE SAMPLE Wt.
Operator : A.NARAYANAN
Date (mm/dd/yy) : 04-11-1994 Surface area of Fe_2O_3

Monolayer thickness (a):	4.3	Total introduction :	10
Satur/Limit pressure (torr):	760	Reduced introduction :	10
Mol.mass. gas ads. (g/mol):	28	Reduction factor :	.25
Gas ads. density (g/cm3):	.808	Constant bur.(cm3/torr):	.15916
Burette temperature (c):	-195.82	Sample weight (g):	6.266
Operating pressure (torr):	800	Sample Density (g/cm3):	2.35

Initial point (P/PO) for linear regression of B.E.T. region : .05

Final point (P/PO) for linear regression of B.E.T. region : .33

Correlation factor = .9975885

Monolayer Volume (CM3/G) = 1.712048

Specific surface area (M2/G) = 7.481028

C value of B. E. T equation = 50.25988

Pore specific volume (CM3/G) = ~~5.525247E-03~~

Total volume introduced (CM3) = 39.68416

Corrected Burette Constant = .1467831

Adsorption values

P.ADS (Torr)	P/PO ADS	VI (CM3)	V.ADS(CM3/G)	T(A)	P/(PO-P)Va/g
2.1	0.0028	3.97	0.58	4.1	0.004743471
8.1	0.0107	7.94	1.08	4.4	0.010003394
27.0	0.0355	11.91	1.27	4.9	0.029061269
45.7	0.0601	15.87	1.46	5.2	0.043738239
68.8	0.0905	19.84	1.55	5.5	0.064012438
92.2	0.1213	23.81	1.64	5.7	0.084179118
111.6	0.1468	27.78	1.82	5.9	0.094620645
134.7	0.1772	31.75	1.91	6.1	0.112712085
159.4	0.2097	35.72	1.97	6.3	0.135000303
178.6	0.2350	39.68	2.15	6.5	0.142912820

Carlo Erba Strumentazione Microstructure Lab.
MI. Le. S. TO. NE. 1 0 0

Calculation parameters of Sorptomatic

Sample : DR.SUGUNAN/CUSAT/CODE NO. V6
Comment : OUTGASSED AT 120 C
Operator : A.NARAYANAN
Date (mm/dd/yy) : 01-24-1994

Surface area of Co_3O_4

Monolayer thickness (a):	4.3	Total introduction :	12
Satur/Limit pressure (torr):	760	Reduced introduction :	12
Mol.mass. gas ads. (g/mol):	28	Reduction factor :	.25
Gas ads. density (g/cm3):	.808	Constant bur.(cm3/torr):	.16103
Burette temperature (c):	-195.82	Sample weight (g):	1.417
Operating pressure (torr):	800	Sample Density (g/cm3):	.925

Initial point (P/PO) for linear regression of B.E.T. region : .05

Final point (P/PO) for linear regression of B.E.T. region : .33

Correlation factor = .9623302

Monolayer Volume (CM3/G) = 1.923532

Specific surface area (M2/G) = 8.405133

C value of B. E. T equation = 11.34003

Pore specific volume (CM3/G) = 4.347851E-03

Total volume introduced (CM3) = 47.62099

Corrected Burette Constant = .1539192

Adsorption values

P.ADS (Torr)	P/PO ADS	VI (CM3)	V.ADS(CM3/G)	T(A)	P/(PO-P)Va/g
21.5	0.0283	3.97	0.47	4.8	0.062585130
42.2	0.0555	7.94	1.02	5.2	0.057793837
66.6	0.0876	11.91	1.17	5.5	0.082274280
92.6	0.1218	15.87	1.14	5.7	0.121305086
115.1	0.1514	19.84	1.50	5.9	0.118957862
139.8	0.1839	23.81	1.62	6.2	0.139321432
163.6	0.2153	27.78	1.83	6.4	0.149630859
189.1	0.2488	31.75	1.86	6.6	0.177704468
210.1	0.2764	35.72	2.38	6.8	0.160302430
235.8	0.3103	39.68	2.39	7.0	0.188024759
259.6	0.3416	43.65	2.61	7.2	0.198941499
283.5	0.3730	47.62	2.81	7.4	0.211564541

Carlo Erba Strumentazione Microstructure Lab.
MI. Le. S. TO. NE. 1 0 0

Calculation parameters of Sorptomatic

Sample : DR.SUGUNAN/CUSAT/CODE NO. V4
Comment : OUTGASSED AT 120 C
Operator : A.NARAYANAN
Date (mm/dd/yy) : 01-24-1994

Surface area of NiO

Monolayer thickness (a):	4.3	Total introduction :	11
Satur/Limit pressure (torr):	760	Reduced introduction :	11
Mol.mass. gas ads. (g/mol):	28	Reduction factor :	.25
Gas ads. density (g/cm3):	.808	Constant bur.(cm3/torr):	.11436
Burette temperature (c):	-195.82	Sample weight (g):	1.335
Operating pressure (torr):	800	Sample Density (g/cm3):	3.2

Initial point (P/PO) for linear regression of B.E.T. region : .05

Final point (P/PO) for linear regression of B.E.T. region : .33

Correlation factor = .9948471

Monolayer Volume (CM3/G) = .9116001

Specific surface area (M2/G) = 3.983361

C value of B. E. T equation = 137.1744

Pore specific volume (CM3/G) = 2.550175E-03

Total volume introduced (CM3) = 43.65257

Corrected Burette Constant = .1124235

Adsorption values

P.ADS (Torr)	P/PO ADS	VI (CM3)	V.ADS(CM3/G)	T(A)	P/(PO-P)Va/g
26.2	0.0345	3.97	0.77	4.9	0.046597511
59.8	0.0787	7.94	0.91	5.4	0.093923517
94.4	0.1242	11.91	0.97	5.8	0.146493673
128.2	0.1687	15.87	1.09	6.1	0.185415879
163.6	0.2153	19.84	1.09	6.4	0.252626750
196.7	0.2588	23.81	1.27	6.7	0.274736050
232.1	0.3054	27.78	1.26	6.9	0.348253790
265.1	0.3488	31.75	1.46	7.2	0.367881120
300.3	0.3951	35.72	1.46	7.5	0.446088310
334.1	0.4396	39.68	1.59	7.8	
368.7	0.4851	43.65	1.65	8.2	

Chloranil was obtained from Sisco Research Laboratories Ltd., and was purified by recrystallisation from benzene [4].

p-Dinitrobenzene was supplied by Koch-Light Laboratories Ltd. and was purified by recrystallisation from chloroform [5].

m-Dinitrobenzene was obtained from Loba-Chemie Industrial Company and was purified by recrystallisation from CCl_4 [6].

3.1.6 Solvents

Acetonitrile

SQ grade acetonitrile obtained from Qualigens Fine Chemicals was first dried by passing through a column filled with silica gel (60-120 mesh) activated at 110°C for 2h. It was then distilled with anhydrous phosphorous pentoxide and the fraction between 79-82°C was collected [7].

1,4-Dioxane

SQ grade 1,4-dioxane was obtained from Qualigens Fine Chemicals. It was dried by keeping over potassium

hydroxide pellets for 2-3 days, filtered and refluxed with sodium metal for 6-7 h till the surface of sodium metal got shining appearance. The refluxed solvent was then distilled and the fraction at 101°C was collected [8].

3.1.7 Reagents for acidity/basicity measurements

Benzene

Benzene used for the acidity/basicity measurements was purified by the following procedure [9]. SQ grade benzene obtained from Qualigens Fine Chemicals was shaken repeatedly with about 15% of its volume of concentrated sulphuric acid in a stoppered separating funnel until the acid layer was colourless on standing. After shaking, the mixture was allowed to settle and the lower layer was drawn off. It was then washed twice with water to remove most of the acid, then with 10% sodium carbonate solution and finally with water. It was dried with anhydrous $CaCl_2$, then filtered and distilled. The distillate was kept over sodium wire for one day. Finally, it was distilled and the fraction boiling at 80°C was collected.

3.1.8 Hammett indicators

Hammett indicators used for the study are the following:

Methyl red (E.Merck India Pvt. Ltd.)

Dimethyl yellow (Loba Chemie Industrial Company).

Crystal violet (Romali)

Bromothymol blue (Qualigens Fine Chemicals).

Thymol blue (Qualigens Fine Chemicals)

4-Nitroaniline (Indian Drug and Pharmaceuticals Ltd.)

Trichloroacetic acid (SQ Grade, Qualigens Fine Chemicals) and n-butylamine (S.d-Fine Chemicals Pvt. Ltd.) were used without further purification.

3.1.9 Reagents used for catalytic activity measurements

Cyclohexanone

Commercial cyclohexanone obtained from BDH was purified by the bisulphite method [10]. A saturated solution of sodium bisulphite was prepared from 40g of finely powdered sodium bisulphite. The volume of the resulting solution was measured and it was then treated

with 70% of its volume of rectified spirit. Sufficient water was added to dissolve the precipitate which was separated. 20g of cyclohexanone was introduced into the aqueous alcoholic bisulphite solution with stirring and the mixture was allowed to stand for 30 minutes. The crystalline bisulphite compound was filtered at the pump and washed it with a little rectified spirit.

The bisulphite compound was transferred to a separating funnel and decomposed with 80 ml of 10% NaOH solution. The liberated cyclohexanone was removed. The aqueous solution layer was saturated with salt and extracted with 30 ml of ether. The ether extract was combined with the ketone layer and dried with 5g of anhydrous magnesium sulphate. The dried etherial solution was filtered into a 50 ml distilling flask, attached with a condenser and ditilled off the ether using a water bath. The resultant cyclohexanone was distilled and the fraction at 153°C was collected.

Benzophenone

Benzophenone was supplied by Sisco Research Laboratories Pvt. Ltd., and was purified by recrystallisation from ethanol [11].

2-Propanol

LR grade reagent obtained from Merck was further purified by adding about 200g of quick lime to1litre of 2-propanol. It was kept for 3-4 days, refluxed for 4 h and distilled. The fraction distilling at 82°C was collected [12].

Cyclohexanol

Cyclohexanol obtained from Merck was refluxed with freshly ignited CaO and then fractionally distilled. The fraction distilling at 161.1°C was collected [13].

1-Butanol

LR grade reagent obtained from Merck was further purified by drying with anhydrou s potassium carbonate and fractionally distilled. The fraction distilling at 116.5°C was collected [14].

Acetic acid

LR grade reagent obtained from Merck was purified by adding some acetic anhydride to react with the water present. It was then heated for 1h just below boiling in the presence of 2g CrO_3 per 100 ml and then fractionally distilled. The fraction at 116-118°C was collected [15].

Toluene

SQ grade toluene obtainbed from Qualigens Fine Chemicals was shaken twice with cold concentrated H_2SO_4 (100 ml of acid for 1 litre of toluene), then with water, aq. 5% $NaHCO_3$ and again with water. Then it was dried successively with $CaSO_4$ and P_2O_5, distilled and fraction distilling at 110°C was collected [16].

n-Decane

LR grade reagent obtained from S.d-Fine Chemicals Pvt. Ltd. was further purified by shaking with conc. H_2SO_4. It was washed with water and aq. $NaHCO_3$. Finally, it was washed with more water, then dried with $MgSO_4$, refluxed with sodium and distilled. The fraction distilling at 174°C was collected [17].

3.2 METHODS

3.2.1 Adsorption studies [18]

The oxide (0.5g) was placed in a 25 ml test tu be and outgassed at 10^{-5} torr for 1 hour. Into the test tube which was fitted with a mercury sealed stirrer, 20 ml of a solution of an electron acceptor in the organic solvent was added, and the solution was stirred at 28°C for 4 hours in

a thermostated bath. The oxide was then collected by centrifuging the solution and dried at room temperature in vacuo. The reflectance and ESR spectra of the dried samples were taken. Radical concentrations were calculated by comparison of peak area obtained by double integration of the first derivative curve for the sample and standard solution of 1,1-diphenyl-2-picryl-hydrazyl in benzene. The amount of electron acceptor adsorbed was determined from its difference in concentration before and after adsorption. The absorbance of electron acceptors was measured at the λ_{max} of the electron acceptor in the solvent. The λ_{max} values of TCNQ, chloranil PDNB and MDNB were 393.5 nm, 288 nm, 262 nm and 237 nm respectively in acetonitrile. The corresponding values in dioxan are 403 nm, 286 nm, 261 nm and 218 nm respectively.

3.2.2 Acidity/basicity measurements

The oxides were sieved to prepare powders of 100-200 mesh size. The acidity of colourless rare earth oxides (La_2O_3 and Sm_2O_3) at various acid strengths was measured by titrating 0.1 g of solid suspended in 5 ml of benzene with a 0.1N solution of n-butylamine in benzene. At the end point, basic colour of indicators appeared [19].

The basicity was measured by titrating 0.1 g of solid suspended in 5 ml of benzene with a 0.1N solution of trichloroacetic acid in benzene, using the same indicators as those for acidity measurements. The colours of indicators on the surface at the end point of titration were the same as the colours which appeared by adsorption of respective indicators on the acid sites. The colour of the benzene solution was the basic colour of the indicator at the end point, but it turned to be the acidic colour by adding and excess of the acid. As the results for a titration lasting 1 hour were the same as those for a titration lasting 20h, titer for 1h was accepted.

For the coloured ABO_3 type oxides and the component transition metal oxides (Cr_2O_3, MnO_2, Fe_2O_3, Co_3O_4 and NiO), the titration was carried out by adding a small known amount of basic alumina the basicity of which was already determined. The values in 10^{-3} mol m^{-2} are 9.0 ($H_o \geqslant 3.3$), 4.9 ($H_o \geqslant 4.8$) and 0.40 ($H_o \geqslant 7.2$). The end point of the titration was taken when the colour change was observed on the white solid [20]. The sharp colour change was observed for a mixture with the proportion of 0.02 g of the coloured oxide to about 0.2 g of alumina. The

difference in basicity between the pure alumina and that of the mixture gave the acidic or basic strength of the added oxides.

3.2.3 Catalytic activity measurements

a) Oxidation of cyclohexanol

In a round bottomed flask (20 ml) equipped with a reflux condenser were placed catalyst (100-200 mesh, 1.5g), 10 cm^3 of a toluene solution of cyclohexanol (0.25 m mol), benzophenone (14.6 m mol) and n-decane (0.20 m mol) as an internal standard. The contents were heated under gentle reflux at 110°C. The amount of cyclohexanone formed was determined by GC method at various time intervals [21].

b) Reduction of cyclohexanone

To 1.5g of the catalyst placed in a round bottomed flask (20 cm^3) equipped with a reflux condenser, 5 m mol of ketone, 10 cm^3 of 2-propanol and 0.2 m mol of n-decane were added. The contents were heated under gentle reflux at 80°C. The amount of cyclohexanol formed at various time intervals was determined by GC method [22].

c) Esterification of acetic acid using 1-butanol

The esterification was carried out in a 25 ml round bottomed flask equipped with a reflux condenser in

which the catalyst (1.5g), acetic acid (2 m mol) and n-butanol (32 m mol) was used as the internal standard. The reaction temperature was maintained 98°C and stirred continuously on a magnetic stirrer for 5h [23].

The reaction was followed by product analysis by means of a CHEMITO-8510 Gas Chromatograph, by comparison of its retention time with that of the standard samples. From the peak area of the product, the concentration of the product formed was calculated with reference to that of the internal standard.

REFERENCES

1. T. Nitadori, T. Ichiki and M. Misono : *Bull. Chem. Soc. Jpn.*, 61, 621 (1988).

2. "Selected Powder Diffraction Data for Metals and Alloys", JCPDS International Centre for Diffraction Data, First ed., (1978).

3. D.S. Acker and W.R. Hertler : *J. Am. Chem. Soc.*, 84, 3370 (1962).

4. L.F. Flesser and M. Flesser : "Reagents for Organic Synthesis" p 125, (John Wiley, New York , 1967).

5. B.S. Furness, A.J. Hannaford, V. Rogers, P.W.G. Smith and A.R. Tatchell : "Vogel's Text Book of Practical Organic Chemistry", 4th ed., p 708 (ELBS, London 1978).

6. ibid, p 626.

7. A.I. Vogel : "A Text Book of Practical Organic Chemistry", 3rd ed., p 407 (ELBS, London 1973).

8. ibid, p 177.

9. ibid, p 172.

10. ibid, p 342.

11. D.D. Perrin, W.L.F. Armarego and D.R. Perrin : "Purification of Laboratory Chemicals", 2nd ed., Pergamon Press, p 123 (1983).

12. A.I. Vogel : "A Text Book of Practical Organic Chemistry", 3rd ed., p 886 (ELBS, London 1973).

13. ibid, p 185.

14. ibid, p 170.

15. D.D. Perrin, W.L.F. Armarego and D.R. Perrin : "Purification of Laboratory Chemicals", 2nd ed., Pergamon Press, p 77 (1983).

16. A.I. Vogel : "A Text Book of Practical Organic Chemistry", 3rd ed., p 487 (ELBS, London 1973).

17. ibid p 190.

18. K. Esumi, K. Miyata and K. Meguro : *Bull. Chem. Soc. Jpn.*, 59, 3363 (1986).

19. Y. Yamanaka and K. Tanabe : *J. Phys. Chem.*, 79, 2409 (1978).

20. K. Tanabe and Y. Watanabe : *J. Res. Inst. Catalysis,* Hokkaido Univ., 11, 65 (1963).

21. H. Kuno, K. Takahashi, M. Shibagaki and H. Matsushita : *Bull. Chem. Soc. Jpn.*, 63, 1943 (1990).

22. M. Shibagaki, T. Takahashi, and H. Matsushita : *Bull. Chem. Soc. Jpn.*, 61, 328 (1988).

23. K. Takahashi, M. Shibagaki and H. Matsushita : *Bull. Chem. Soc. Jpn.*, 62, 2353 (1989).

CHAPTER 4
RESULTS AND DISCUSSION

RESULTS AND DISCUSSION

Perovskite-type oxides serve as suitable model compounds for studying the relationship between the solid state chemistry of mixed metal oxides and their catalytic effects [1,2]. The catalytic activity of some transition metal oxides have been correlated with their surface acid-base properties [3-5]. The surface electron donor and acid-base properties of some of the rare earth and supported rare earth oxides have also been correlated with their catalytic activities [6-8]. However, no attempts have so far been made to study the electron donor and acid-base properties of perovskite-type mixed oxides involving rare earth and 3d transition metals. These properties were correlated with the catalytic activity of the mixed oxides for the reduction (Meerwein-Ponndorf-Verley reduction), oxidation (Oppenauer oxidation) and esterification reactions.

The ABO_3 type oxides selected for the study are those with La, Pr and Sm as the rare earth elements (site A) and with Cr, Mn, Fe, Co and Ni (site B) as 3d transition metals. The behaviour of the component oxides are also studied.

4.1 ADSORPTION STUDIES

The electron donor properties are studied in accetonitrile and dioxan by the adsorption of different electron acceptors on the oxide surface. The electron donor properties obviously depend on the basicity of the solvent. The electron donor properties of some of the metal oxides as a function of the basicity of the solvents (using three solvents, acetonitrile, ethyl acetate and 1,4-dioxan, in order of increasing basicity) are reported by earlier workers [9-11]. It was found that the amount of electron acceptor adsorbed decreased with the increase in basicity of the solvents. The solvent effect on the electron donor properties of $LaCoO_3$, $PrCoO_3$, $SmCoO_3$, La_2O_3, Pr_6O_{11}, Sm_2O_3 and Co_3O_4 were also studied in dioxan (by increasing the basicity of medium). Since the results were as expected from earlier reports [10] the solvent effect on other oxides are not included in the thesis.

On the surface of metal oxides, the electron donor sites are distributed from low electron affinity to a high electron affinity. To study the distribution of electron donor sites, adsorption of electron acceptors of various electron affinity are studied. They are listed in Table 11.

Table 11: Electron acceptor used

Electron acceptor	Electron affinity (eV)
1. 7,7,8,8-tetracyanoquino dimethane (TCNQ)	2.84
2. 2,3,5,6-tetrachloro-1,4-benzoquinone (Chloranil)	2.40
3. p-dinitrobenzene (PDNB)	1.77
4. m-dinitrobenzene (MDNB)	1.26

With the mixed oxides and the component 3d metal oxides, the adsorption of chloranil, PDNB and MDNB was so low that the amount could hardly be estimated. The component rare earth oxides exhibited adsorption of TCNQ and chloranil, but not of PDNB and MDNB. The adsorption isotherm of TCNQ and chloranil from acetonitrile and dioxan may be classified as Langmuir type. It is verified by the linear plot of C_{eq}/C_{ads} against C_{eq}, where C_{eq} is the equilibrium concentration in mol dm^{-3} and C_{ads} is the amount adsorbed in mol m^{-2} of the electron acceptor

(Fig.10). The limiting amount of electron acceptor adsorbed is determined from the Langmuir plots (Figs.11-13). Data are given in Tables 12-46.

Visible colour change was observed in the case of colourless oxides like La_2O_3 and Sm_2O_3 when electron acceptors were adsorbed. Chloranil gave light pink colour and TCNQ gave green colour to the oxide surface. The characteristic colouration is due to the interaction between the electron acceptor adsorbed and the oxide surface [12]. The rest of the oxides studied were all coloured.

To study the nature of interaction during adsorption, reflectance spectra (Fig.14) of adsorbed samples were measured. The bands appearing below 400 nm correspond to physically adsorbed state of neutral TCNQ radical which has the absorption band at 395 nm [13]. The band near 600 nm is attributed to the dimeric TCNQ radical which absorbs at 643 nm [14]. The broad band extending upto 700 nm corresponds to chloranil anion radical [15].

The electronic state of adsorbed species was studied by ESR spectroscopy in addition to the electronic

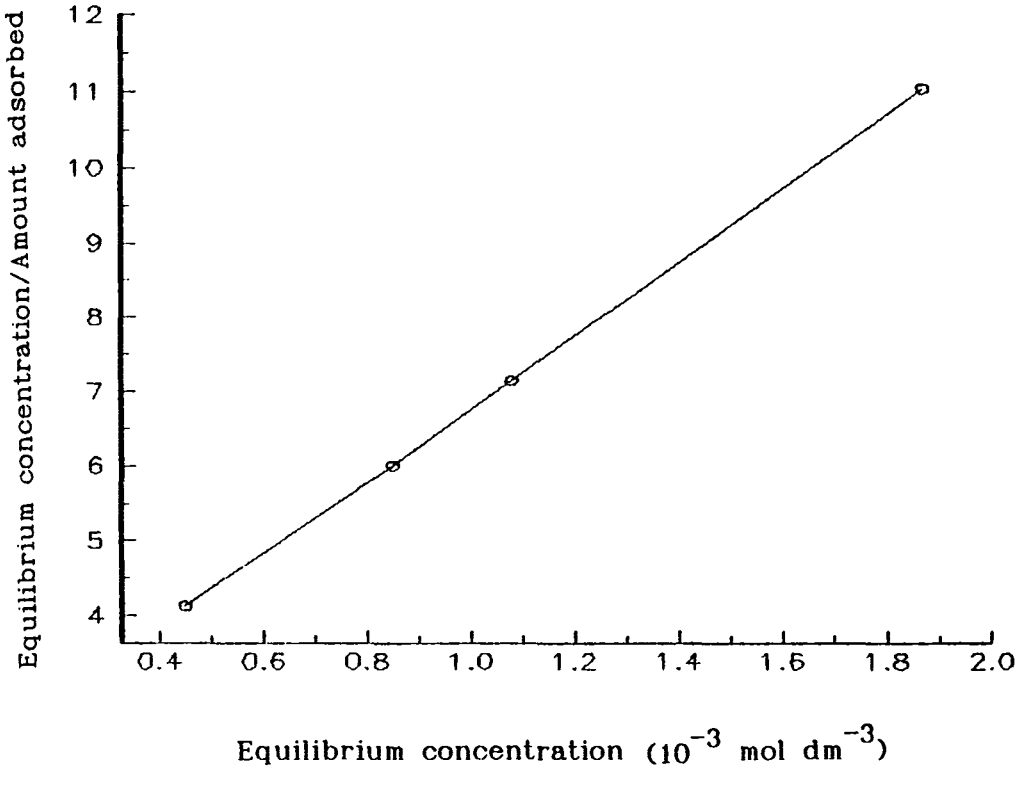

Fig-10

Linear form of Langmuir isotherm obtained for adsorption of TCNQ on $LaCrO_3$.

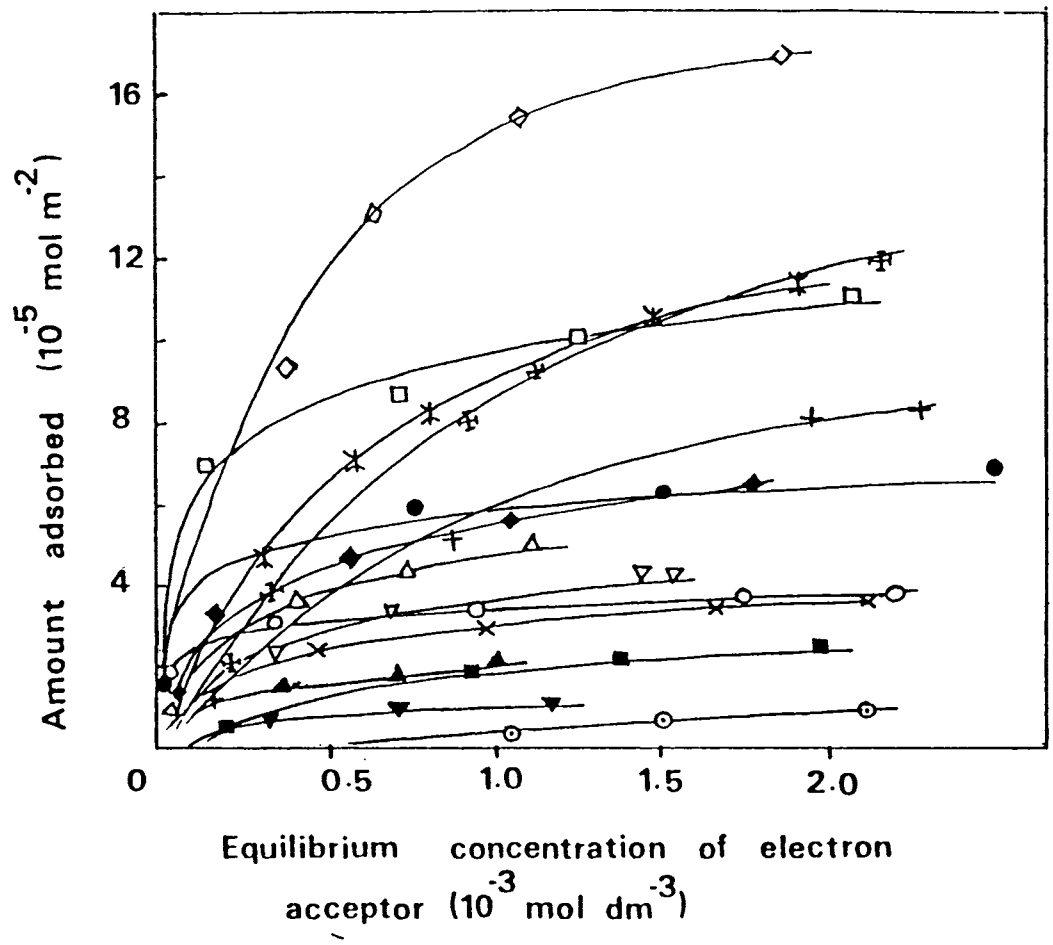

Fig-11 Amount of electron acceptor (TCNQ) adsorbed vs equilibrium concentration of the electron acceptor for the mixed oxides in acetonitrile.

◇ $LaCrO_3$
+ $PrCrO_3$
+ $SmCrO_3$
✳ $LaMnO_3$
× $PrMnO_3$
⊙ $SmMnO_3$
△ $LaFeO_3$
▽ $PrFeO_3$
◆ $SmFeO_3$
● $LaCoO_3$
○ $PrCoO_3$
■ $SmCoO_3$
▲ $LaNiO_3$
▼ $PrNiO_3$
□ $SmNiO_3$

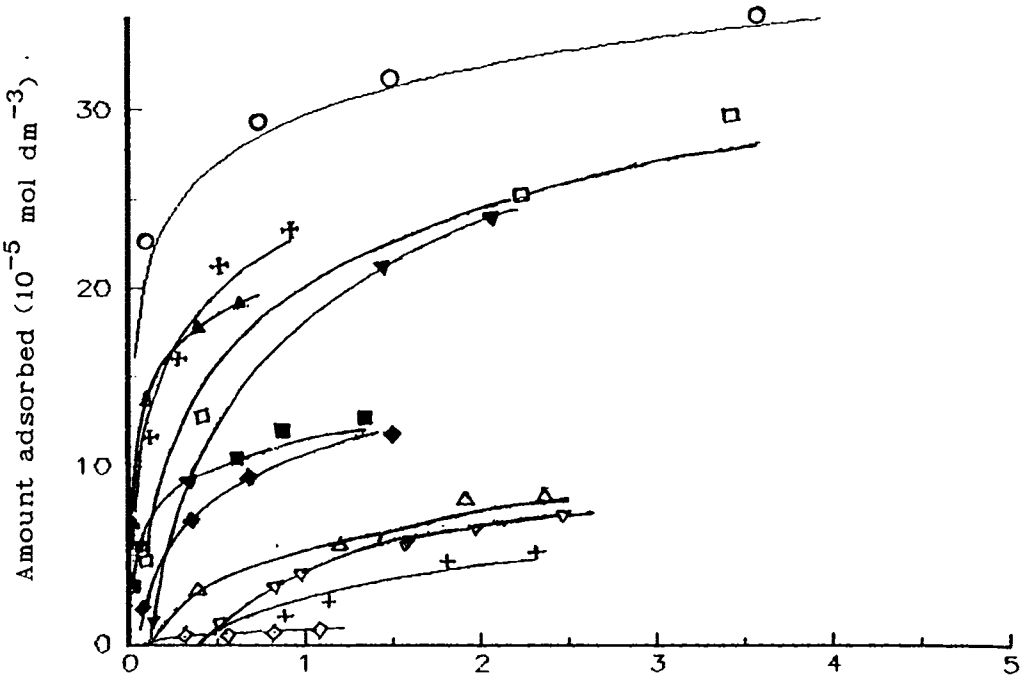

Fig-12

Amount of electron acceptors adsorbed against its equilibrium concentration in Acetonitrile medium for pure oxides.

- o TCNQ / La_2O_3
- ▽ TCNQ / Cr_2O_3
- \+ TCNQ / Co_3O_4
- ■ Chloranil / La_2O_3
- ▲ Chloranil / Sm_2O_3
- ▼ TCNQ / Pr_6O_{11}
- ◆ TCNQ / MnO_2
- ✣ TCNQ / NiO
- △ Chloranil / Pr_6O_{11}
- □ TCNQ / Sm_2O_3
- ◇ TCNQ / Fe_2O_3

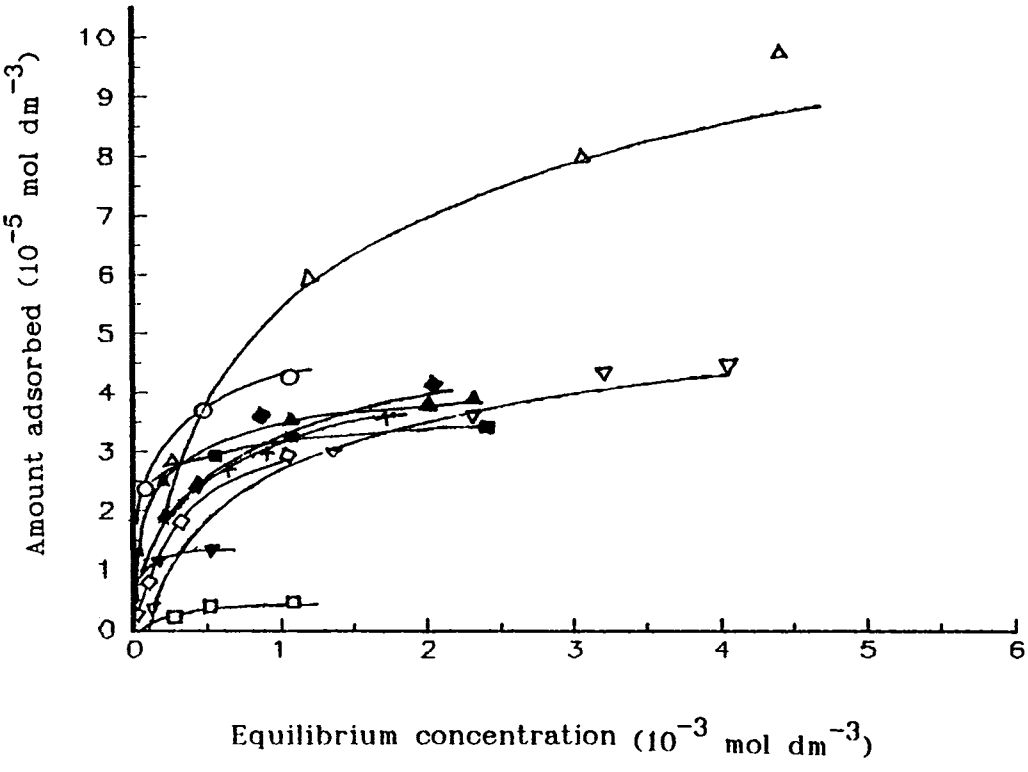

Fig-13

Amount of electron acceptors adsorbed against its equilibrium concentration in Dioxan medium.

▲ TCNQ / La_2O_3
o TCNQ / $LaCoO_3$
\+ TCNQ / Co_3O_4
▼ Chloranil / La_2O_3
△ TCNQ / Pr_6O_{11}
■ TCNQ / $PrCoO_3$
▽ Chloranil / Pr_6O_{11}
◇ Chloranil / Sm_2O_3
◆ TCNQ / Sm_2O_3
□ TCNQ / $SmCoO_3$

Table-12 Adsorption of TCNQ on $LaCrO_3$

Solvent: Acetonitrile

Initial concentration 10^{-3} mol dm^{-3}	Equilibrium concentration 10^{-3} mol dm^{-3}	Amount adsorbed 10^{-5} mol m^{-2}	Radical concentration 10^{18}spins m^{-2}
0.260	0.247	0.858	0.391
0.595	0.449	9.526	5.162
1.047	0.852	12.86	6.969
1.290	1.077	15.08	8.173
2.125	1.867	16.89	9.154

Table-13 Adsorption of TCNQ on $PrCrO_3$

Solvent: Acetonitrile

Initial concentration 10^{-3} mol dm^{-3}	Equilibrium concentration 10^{-3} mol dm^{-3}	Amount adsorbed 10^{-5} mol m^{-2}	Radical concentration 10^{18}spins m^{-2}
0.249	0.230	1.243	0.673
0.581	0.504	5.043	2.733
0.950	0.872	5.178	2.806
2.076	1.949	8.171	4.428
2.398	2.272	8.392	4.548

Table-14 Adsorption of TCNQ on $SmCrO_3$

Solvent: Acetonitrile

Initial concentration 10^{-3} mol dm^{-3}	Equilibrium concentration 10^{-3} mol dm^{-3}	Amount adsorbed 10^{-5} mol m^{-2}	Radical concentration 10^{18}spins m^{-2}
0.333	0.291	2.237	1.212
0.470	0.364	5.434	2.945
1.128	0.981	7.668	4.155
1.308	1.117	10.02	5.430
2.389	2.158	12.07	6.541

Table-15 Adsorption of TCNQ on $LaMnO_3$

Solvent: Acetonitrile

Initial concentration 10^{-3} mol dm^{-3}	Equilibrium concentration 10^{-3} mol dm^{-3}	Amount adsorbed 10^{-5} mol m^{-2}	Radical concentration 10^{18}spins m^{-2}
0.567	0.324	4.714	2.554
0.704	0.378	6.362	3.448
0.973	0.613	6.963	3.773
1.208	0.796	8.004	4.338
2.027	1.480	10.65	5.148
2.517	1.911	11.71	5.239

Table-16 Adsorption of TCNQ on $PrMnO_3$

Solvent: Acetonitrile

Initial concentration 10^{-3} mol dm^{-3}	Equilibrium concentration 10^{-3} mol dm^{-3}	Amount adsorbed 10^{-5} mol m^{-2}	Radical concentration 10^{18} spins m^{-2}
0.245	0.139	1.339	0.725
0.573	0.398	2.194	1.189
0.693	0.472	2.597	1.407
1.189	0.963	2.837	1.537
2.047	1.756	3.644	1.974
2.478	2.177	3.762	2.038

Table-17 Adsorption of TCNQ on $SmMnO_3$

Solvent: Acetonitrile

Initial concentration 10^{-3} mol dm^{-3}	Equilibrium concentration 10^{-3} mol dm^{-3}	Amount adsorbed 10^{-5} mol m^{-2}	Radical concentration 10^{18} spins m^{-2}
0.586	0.575	0.152	0.082
0.761	0.633	0.202	0.109
1.045	1.031	0.223	0.120
2.180	2.048	0.801	0.434
2.521	2.110	1.130	0.612

Table-18 Adsorption of TCNQ on $LaFeO_3$

Solvent: Acetonitrile

Initial concentration 10^{-3} mol dm^{-3}	Equilibrium concentration 10^{-3} mol dm^{-3}	Amount adsorbed 10^{-5} mol m^{-2}	Radical concentration 10^{18}spins m^{-2}
0.177	0.084	1.296	0.702
0.414	0.198	3.013	1.632
0.673	0.409	3.698	2.004
1.025	0.725	4.180	2.265
1.479	1.112	5.098	2.736

Table-19 Adsorption of TCNQ on $PrFeO_3$

Solvent: Acetonitrile

Initial concentration 10^{-3} mol dm^{-3}	Equilibrium concentration 10^{-3} mol dm^{-3}	Amount adsorbed 10^{-5} mol m^{-2}	Radical concentration 10^{18}spins m^{-2}
0.076	0.039	0.416	0.225
0.229	0.112	1.278	0.692
0.534	0.345	2.071	1.122
0.916	0.676	2.643	1.432
1.841	1.451	4.317	2.339
1.935	1.517	4.610	2.498

Table-20 Adsorption of TCNQ on $SmFeO_3$

Solvent: Acetonitrile

Initial concentration 10^{-3} mol dm^{-3}	Equilibrium concentration 10^{-3} mol dm^{-3}	Amount adsorbed 10^{-5} mol m^{-2}	Radical concentration 10^{18} spins m^{-2}
0.178	0.073	1.441	0.781
0.416	0.171	3.360	1.821
0.912	0.570	4.681	2.537
1.161	0.744	5.725	3.102
1.478	1.046	5.942	3.220
2.240	1.799	6.061	3.284

Table-21 Adsorption of TCNQ on $LaCoO_3$

Solvent: Acetonitrile

Initial concentration 10^{-3} mol dm^{-3}	Equilibrium concentration 10^{-3} mol dm^{-3}	Amount adsorbed 10^{-5} mol m^{-2}	Radical concentration 10^{18} spins m^{-2}
0.081	0.004	1.440	0.780
0.405	0.021	3.581	1.909
0.973	0.709	4.690	2.645
1.011	0.744	6.014	3.509
2.487	2.114	7.021	3.744

Table-22 Adsorption of TCNQ on $PrCoO_3$

Solvent: Acetonitrile

Initial concentration 10^{-3} mol dm^{-3}	Equilibrium concentration 10^{-3} mol dm^{-3}	Amount adsorbed 10^{-5} mol m^{-2}	Radical concentration 10^{18}spins m^{-2}
0.093	0.027	1.811	0.965
0.279	0.189	2.490	1.328
0.466	0.348	3.221	1.717
1.068	0.943	3.453	1.840
2.331	2.193	3.792	2.021

Table-23 Adsorption of TCNQ on $SmCoO_3$

Solvent: Acetonitrile

Initial concentration 10^{-3} mol dm^{-3}	Equilibrium concentration 10^{-3} mol dm^{-3}	Amount adsorbed 10^{-5} mol m^{-2}	Radical concentration 10^{18}spins m^{-2}
0.083	0.079	0.092	0.048
0.248	0.239	0.043	0.074
0.578	0.552	0.851	0.453
0.992	0.934	1.890	1.001
2.066	1.989	2.554	1.361
2.180	2.101	2.651	1.413

Table-24 Adsorption of TCNQ on $LaNiO_3$

Solvent: Acetonitrile

Initial concentration 10^{-3} mol dm^{-3}	Equilibrium concentration 10^{-3} mol dm^{-3}	Amount adsorbed 10^{-5} mol m^{-2}	Radical concentration 10^{18}spins m^{-2}
0.048	0.018	0.380	0.205
0.144	0.087	0.732	0.396
0.516	0.445	0.914	0.495
0.832	0.701	1.790	0.970
1.204	1.019	2.361	1.279

Table-25 Adsorption of TCNQ on $PrNiO_3$

Solvent: Acetonitrile

Initial concentration 10^{-3} mol dm^{-3}	Equilibrium concentration 10^{-3} mol dm^{-3}	Amount adsorbed 10^{-5} mol m^{-2}	Radical concentration 10^{18}spins m^{-2}
0.083	0.079	0.142	0.066
0.147	0.140	0.245	0.118
0.352	0.327	0.857	0.464
0.742	0.715	0.902	0.488
1.197	1.169	0.956	0.518

Table-26 Adsorption of TCNQ on $SmNiO_3$

Solvent: Acetonitrile

Initial concentration 10^{-3} mol dm^{-3}	Equilibrium concentration 10^{-3} mol dm^{-3}	Amount adsorbed 10^{-5} mol m^{-2}	Radical concentration 10^{18}spins m^{-2}
0.033	0.012	0.432	0.234
0.544	0.111	7.511	4.071
1.197	0.725	8.210	4.449
1.837	1.258	10.07	5.457
2.722	2.075	11.18	6.059

Table-27 Adsorption of TCNQ on La_2O_3

Solvent: Acetonitrile

Initial concentration 10^{-3} mol dm^{-3}	Equilibrium concentration 10^{-3} mol dm^{-3}	Amount adsorbed 10^{-5} mol m^{-2}	Radical concentration 10^{18}spins m^{-2}
2.365	0.029	13.29	7.201
4.058	0.083	22.62	10.16
5.901	0.713	29.53	16.01
7.043	1.462	31.77	17.21
11.14	5.120	34.34	18.61

Table-28 Adsorption of Chloranil on La_2O_3

Solvent: Acetonitrile

Initial concentration 10^{-3} mol dm^{-3}	Equilibrium concentration 10^{-3} mol dm^{-3}	Amount adsorbed 10^{-5} mol m^{-2}	Radical concentration 10^{17} spins m^{-2}
0.524	0.011	2.934	0.177
1.295	0.413	5.042	0.305
2.437	0.601	10.46	0.634
2.982	0.821	12.31	0.746
3.703	1.320	13.68	0.829

Table-29 Adsorption of TCNQ on Sm_2O_3

Solvent: Acetonitrile

Initial concentration 10^{-3} mol dm^{-3}	Equilibrium concentration 10^{-3} mol dm^{-3}	Amount adsorbed 10^{-5} mol m^{-2}	Radical concentration 10^{18} spins m^{-2}
1.263	0.091	7.81	4.232
2.947	1.063	12.55	6.801
5.656	2.138	23.45	12.71
8.121	3.392	31.52	17.08
9.403	4.542	32.41	17.56

Table-30 Adsorption of Chloranil on Sm_2O_3

Solvent: Acetonitrile

Initial concentration 10^{-3} mol dm^{-3}	Equilibrium concentration 10^{-3} mol dm^{-3}	Amount adsorbed 10^{-5} mol m^{-2}	Radical concentration 10^{17} spins m^{-2}
0.280	0.032	1.672	0.101
1.015	0.011	6.701	0.406
2.299	0.200	13.99	0.848
3.099	0.309	18.59	1.127
3.530	0.626	19.36	1.174

Table-31 Adsorption of TCNQ on Pr_6O_{11}

Solvent: Acetonitrile

Initial concentration 10^{-3} mol dm^{-3}	Equilibrium concentration 10^{-3} mol dm^{-3}	Amount adsorbed 10^{-5} mol m^{-2}	Radical concentration 10^{18} spins m^{-2}
0.168	0.110	0.831	0.450
1.027	0.384	9.094	4.928
1.637	0.850	11.12	6.027
3.113	1.410	24.07	13.04
3.958	2.121	25.96	14.07

Table-32 Adsorption of Chloranil on Pr_6O_{11}

Solvent: Acetonitrile

Initial concentration 10^{-3} mol dm^{-3}	Equilibrium concentration 10^{-3} mol dm^{-3}	Amount adsorbed 10^{-5} mol m^{-2}	Radical concentration 10^{17} spins m^{-2}
0.080	0.071	0.130	0.007
0.032	0.776	0.456	0.027
1.588	1.236	4.868	0.295
2.480	1.901	8.232	0.489
3.153	2.486	9.424	0.572

Table-33 Adsorption of TCNQ on Cr_2O_3

Solvent: Acetonitrile

Initial concentration 10^{-3} mol dm^{-3}	Equilibrium concentration 10^{-3} mol dm^{-3}	Amount adsorbed 10^{-5} mol m^{-2}	Radical concentration 10^{18} spins m^{-2}
0.561	0.476	0.930	0.504
1.104	0.814	3.190	1.728
1.289	0.977	3.431	1.859
2.347	1.965	7.120	3.980
3.092	2.353	8.134	4.408

Table-34 Adsorption of TCNQ on MnO_2

Solvent: Acetonitrile

Initial concentration 10^{-3} mol dm^{-3}	Equilibrium concentration 10^{-3} mol dm^{-3}	Amount adsorbed 10^{-5} mol m^{-2}	Radical concentration 10^{18}spins m^{-2}
0.132	0.063	1.470	0.796
0.219	0.120	2.134	1.156
0.660	0.335	6.900	3.739
1.119	0.657	9.810	5.316
2.055	1.503	11.72	6.352

Table-35 Adsorption of TCNQ on Fe_2O_3

Solvent: Acetonitrile

Initial concentration 10^{-3} mol dm^{-3}	Equilibrium concentration 10^{-3} mol dm^{-3}	Amount adsorbed 10^{-5} mol m^{-2}	Radical concentration 10^{18}spins m^{-2}
0.084	0.080	0.110	0.059
0.299	0.291	0.239	0.129
0.509	0.494	0.410	0.222
0.839	0.810	0.790	0.428
1.111	1.079	0.854	0.462

Table-36 Adsorption of TCNQ on Co_3O_4

Solvent: Acetonitrile

Initial concentration 10^{-3} mol dm^{-3}	Equilibrium concentration 10^{-3} mol dm^{-3}	Amount adsorbed 10^{-5} mol m^{-2}	Radical concentration 10^{18}spins m^{-2}
0.435	0.400	0.840	0.455
0.930	0.878	1.240	0.672
1.215	1.115	2.381	1.290
1.999	1.810	4.500	2.438
2.516	2.300	5.134	2.782

Table-37 Adsorption of TCNQ on NiO

Solvent: Acetonitrile

Initial concentration 10^{-3} mol dm^{-3}	Equilibrium concentration 10^{-3} mol dm^{-3}	Amount adsorbed 10^{-5} mol m^{-2}	Radical concentration 10^{18}spins m^{-2}
0.143	0.021	6.201	3.361
0.429	0.195	11.76	6.373
0.660	0.336	16.30	8.834
0.933	0.510	21.30	11.54
1.379	0.890	24.58	13.32

Table-38 Adsorption of TCNQ on $LaCoO_3$

Solvent: 1,4-dioxane

Initial concentration 10^{-3} mol dm^{-3}	Equilibrium concentration 10^{-3} mol dm^{-3}	Amount adsorbed 10^{-5} mol m^{-2}
0.008	0.001	0.124
0.012	0.004	0.135
0.058	0.044	0.266
0.315	0.219	1.802
0.725	0.526	3.746
1.322	1.097	4.250

Table-39 Adsorption of TCNQ on $PrCoO_3$

Solvent: 1,4-dioxane

Initial concentration 10^{-3} mol dm^{-3}	Equilibrium concentration 10^{-3} mol dm^{-3}	Amount adsorbed 10^{-5} mol m^{-2}
0.043	0.024	0.521
0.055	0.034	0.561
0.307	0.251	1.523
0.736	0.631	2.885
1.146	1.028	3.258

Table-40 Adsorption of TCNQ on $SmCoO_3$

Solvent: 1,4-dioxane

Initial concentration 10^{-3} mol dm^{-3}	Equilibrium concentration 10^{-3} mol dm^{-3}	Amount adsorbed 10^{-5} mol m^{-2}
0.039	0.035	0.023
0.138	0.126	0.080
0.301	0.298	0.081
0.517	0.504	0.413
1.077	1.065	0.421

Table-41 Adsorption of TCNQ on La_2O_3

Solvent: 1,4-dioxane

Initial concentration 10^{-3} mol dm^{-3}	Equilibrium concentration 10^{-3} mol dm^{-3}	Amount adsorbed 10^{-5} mol m^{-2}
0.248	0.003	1.651
0.497	0.127	2.438
0.995	0.549	2.993
1.244	0.774	3.156
2.487	1.988	3.349
2.860	2.355	3.385

Table-42 Adsorption of Chloranil on La_2O_3

Solvent: 1,4-dioxane

Initial concentration 10^{-3} mol dm^{-3}	Equilibrium concentration 10^{-3} mol dm^{-3}	Amount adsorbed 10^{-5} mol m^{-2}
0.020	0.002	0.069
0.060	0.004	0.373
0.120	0.014	0.713
0.300	0.120	1.210
0.602	0.419	1.220

Table-43 Adsorption of TCNQ on Pr_6O_{11}

Solvent: 1,4-dioxane

Initial concentration 10^{-3} mol dm^{-3}	Equilibrium concentration 10^{-3} mol dm^{-3}	Amount adsorbed 10^{-5} mol m^{-2}
1.201	1.010	2.710
2.412	1.641	3.765
3.622	3.078	8.021
4.830	4.411	9.860
6.031	5.620	9.961

Table-44 Adsorption of Chloranil on Pr_6O_{11}

Solvent: 1,4-dioxane

Initial concentration 10^{-3} mol dm^{-3}	Equilibrium concentration 10^{-3} mol dm^{-3}	Amount adsorbed 10^{-5} mol m^{-2}
0.851	0.798	0.135
1.701	1.534	2.498
2.564	2.379	3.497
3.418	3.202	4.532
4.260	4.064	4.540

Table-45 Adsorption of TCNQ on Sm_2O_3

Solvent: 1,4-dioxane

Initial concentration 10^{-3} mol dm^{-3}	Equilibrium concentration 10^{-3} mol dm^{-3}	Amount adsorbed 10^{-5} mol m^{-2}
0.538	0.269	1.771
0.840	0.501	2.252
0.951	0.532	2.781
1.409	0.859	3.683
1.596	1.036	3.686

Table-46 Adsorption of Chloranil on Sm_2O_3

Solvent: 1,4-dioxane

Initial concentration 10^{-3} mol dm^{-3}	Equilibrium concentration 10^{-3} mol dm^{-3}	Amount adsorbed 10^{-5} mol m^{-2}
0.293	0.143	0.994
0.585	0.300	1.905
0.999	0.527	3.125
1.175	0.673	3.178
1.292	0.808	3.178

Table-46 a Adsorption of TCNQ on Co_3O_4

Solvent: 1,4-dioxane

Initial concentration 10^{-3} mol dm^{-3}	Equilibrium concentration 10^{-3} mol dm^{-3}	Amount adsorbed 10^{-5} mol m^{-2}
0.307	0.271	0.896
0.625	0.572	1.320
0.948	0.840	2.591
1.220	1.100	2.870
1.409	1.273	3.321

spectroscopy. Fig.15 shows the ESR spectrum of the sample adsorbed with TCNQ (C_{ads} = $3.241x10^{-4}$ mol m^{-2}) on Sm_2O_3 surface. Samples after TCNQ adsorption gave unresolved ESR spectra with a g value of 2.003. These spectra have been identified as those of TCNQ anion radicals [16]. The samples obtained by the adsorption of chloranil gave unresolved ESR spectra having a g value of 2.011 [17]. The radical concentration of TCNQ on the surface is calculated by a standard method and are given in Tables 12-37. Fig.16 shows the radical concentration of TCNQ against its equilibrium concentration in acetonitrile. The isotherm obtained is also of Langmuir type and its shape is the same as in Fig.11. Limiting radical concentrations are calculated from the such Langmuir plots.

The electron donating capacity of the oxide is found to depend on the electron affinity of the electron acceptor adsorbed. The amount of electron acceptor adsorbed increased with increase in electron affinity of the electron acceptor. Strong electron acceptor like TCNQ is capable of forming anions even from weak donor sites, whereas, weak electron acceptor like MDNB is capable of forming anions only at strong donor sites. Hence the limiting radical concentration of the weak electron

Fig-14

Electronic spectrum obtained from the adsobption of TCNQ on Sm_2O_3

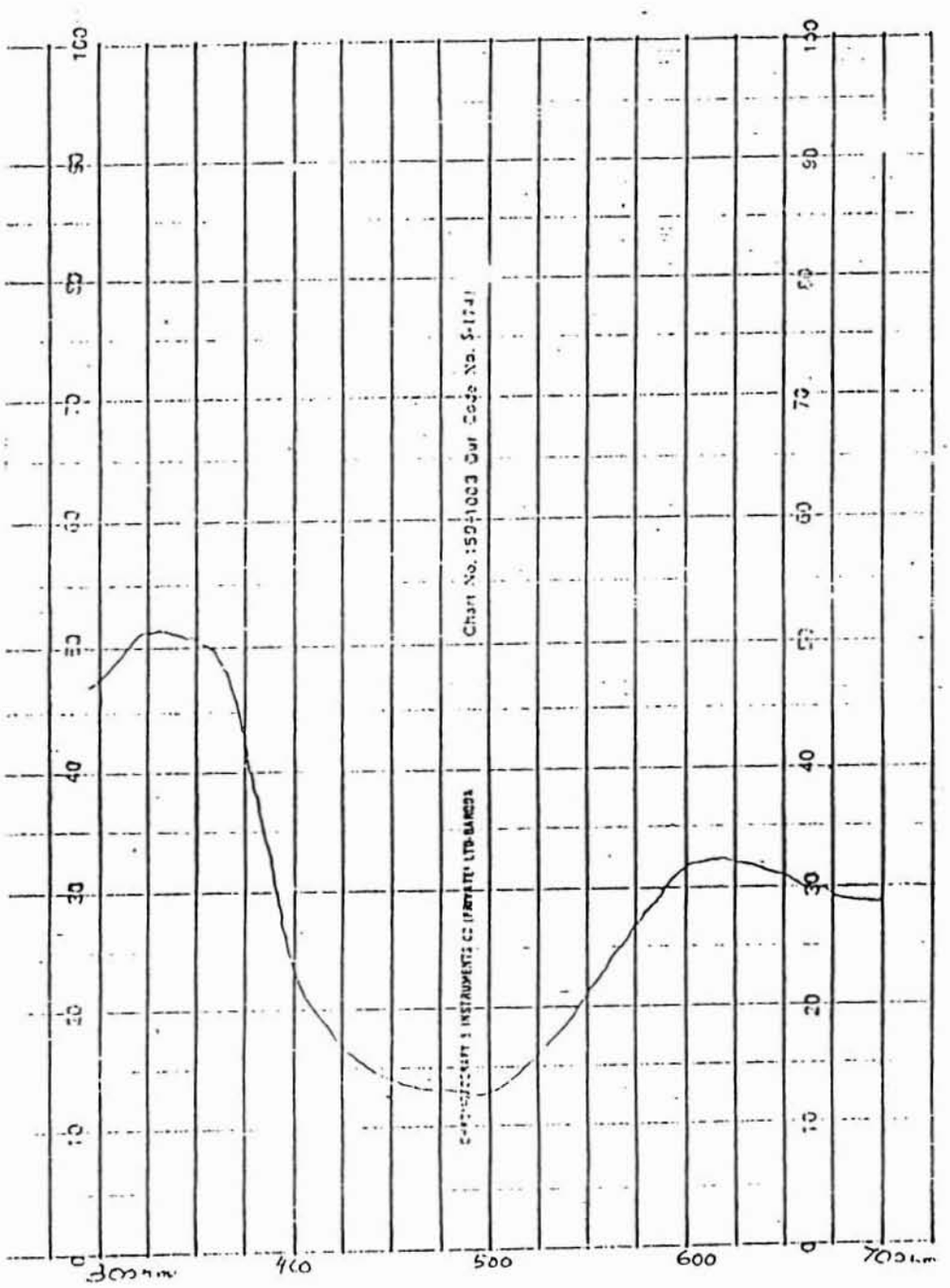

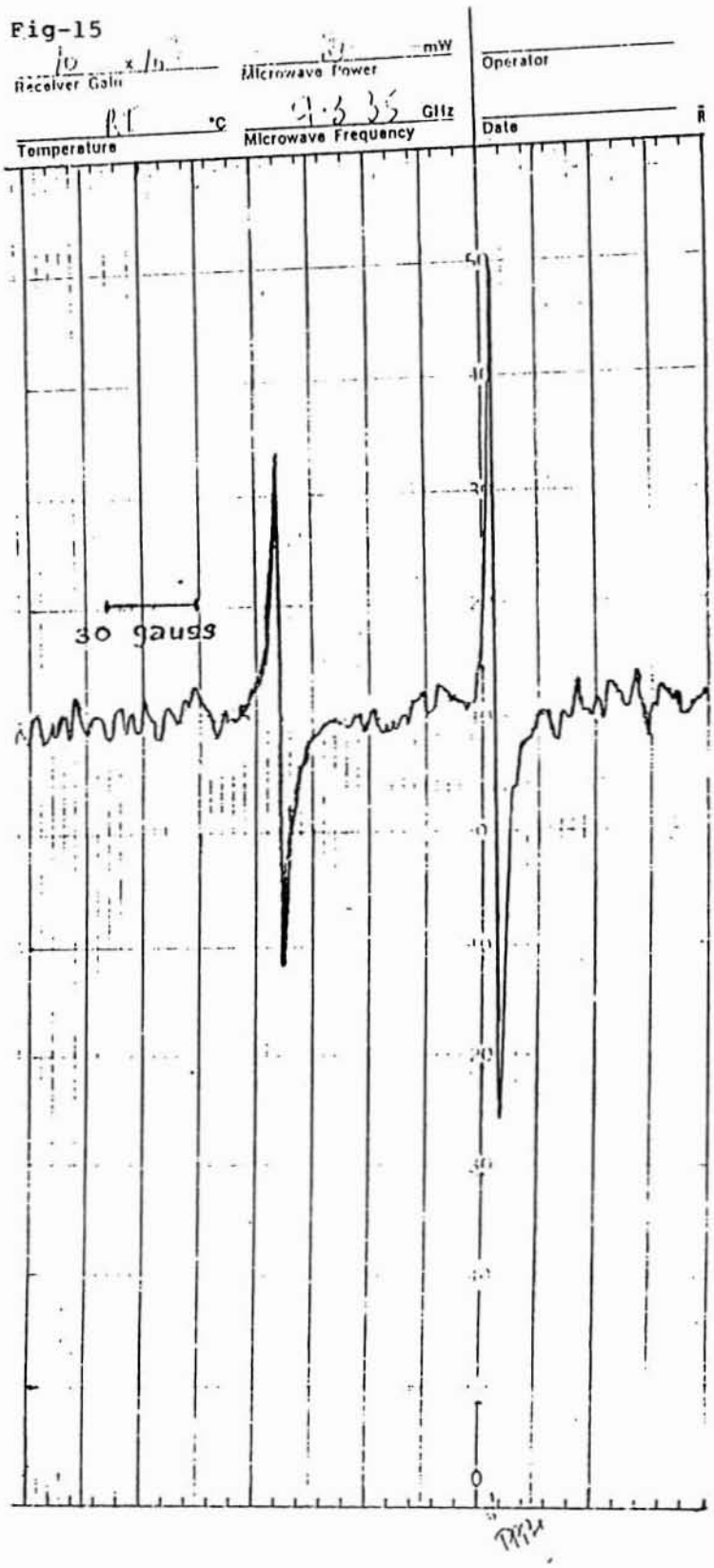

E.S.R spectrum obtained from the adsorption of TCNQ on Sm_2O_3

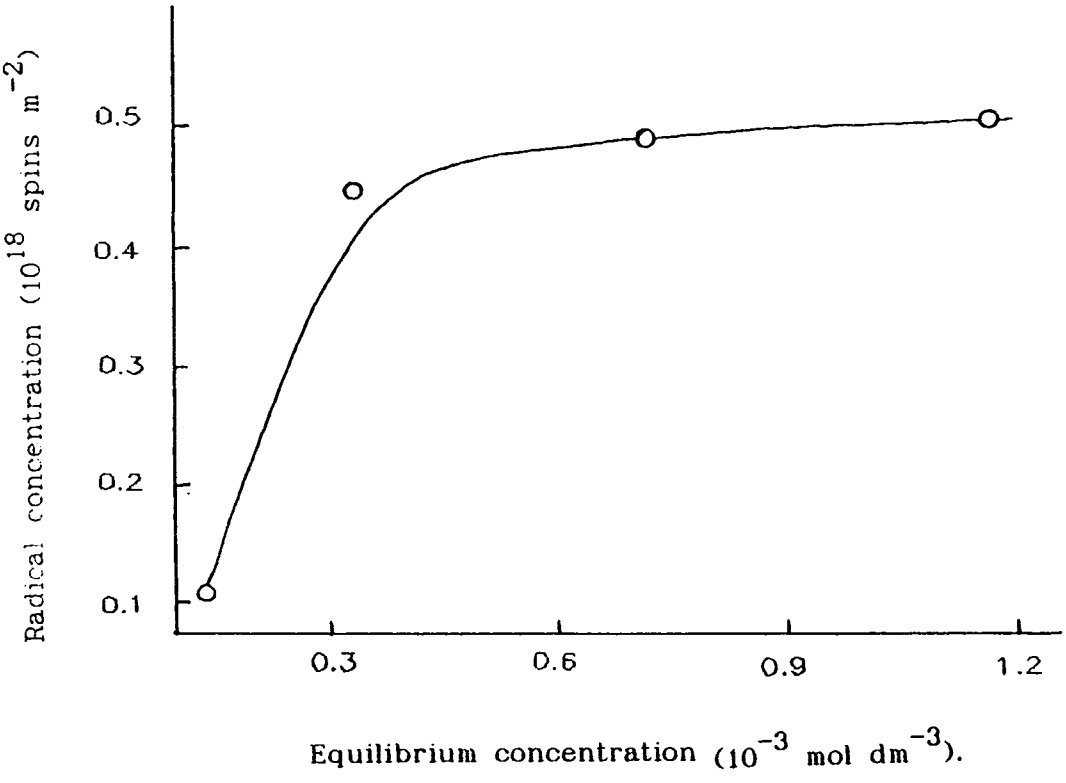

Fig-16

Radical concentration of TCNQ vs its equilibrium concentration on $PrNiO_3$

acceptor is a measure of the number of strong donor sites on the surface and that for a strong acceptor is related to the total number of sites (weak and strong donor sites) on the surface. Accordingly, the limit of electron transfer in terms of the electron affinity (eV) of the acceptors is between 2.40 and 2.84 for the mixed and transition metal oxides and between 1.77 and 2.40 for the rare earth oxides.

Two possible electron sources exist on oxide surface, responsible for electron transfer. One of these has electrons trapped in intrinsic defects and the other has hydroxyl ions [18]. The surface hydroxyl concentrations of $BaTiO_3$, $SrTiO_3$ and $LaCoO_3$ perovskite oxides were determined by exchange with D_2 as a function of the dehydroxylation temperature by earlier workers [19]. These results suggested that the surface chemistry of these materials resembles that of certain other oxide systems such as alumina and titania. It was observed that at 600°C the surface of these pervoskites were almost dehydroxylated. This behaviour resembles that of alumina and is typical of such oxides. It is reported that free electron defect site on metal oxide surface is created at an activation temperature of above 500°C [20]. Therefore, surface sites may be associated with the presence of

unsolvated hydroxyl ions at lower activation temperature and with the electron defect centres at higher activation temperature. Fomin et al. have shown that electron transfer from OH^- ions can and does occur in certain solvent systems, provided a suitable electron acceptor is present [21]. Surface hydroxyls on metal oxides are shown to differ in chemical properties and difference in acidity between hydroxyl groups on several oxide surfaces have been reported [22]. These suggest that hydroxyl ions on metal oxide surfaces have electron donor sites of varying electron donicity.

It might be expected that the trapped electron centres are solely responsible for the adsorption of electron acceptor on the surface of the mixed and the component oxides, as the activation temperature is 850°C. It is found that these centres are stronger reducing agents than hydroxyl ions.

A strong electron acceptor (TCNQ) can accept electron from both strong and weak donor sites whereas, a weak electron acceptor such as MDNB can accept electrons from strong donor sites only. The difference between the limiting amounts of TCNQ and chloranil adsorbed on the

metal oxides can tell the number of stronger donor sites. The rare earth oxides are found to have greater number of strong donor sites than the mixed oxides and 3d transition metal oxides as indicated by the results.

4.2 ACID-BASE STRENGTH DISTRIBUTION

Acidity and basicity of the perovskite-type oxides and component oxides were estimated by titration method using Hammett indicators. The following indicators were used (Table 47). Visible colour change was obtained only for the following Hammett indicators, dimethyl yellow, methyl red and bromothymol blue.

Table 47: Hammett indicators used

Indicators	pKa	Acidic colour	Basic colour
1. Crystal violet	0.8	Yellow	Blue
2. p-Nitroaniline	1.1	Yellow	Orange
3. p-Dimethyl amino-azobenzene (Dimethyl Yellow)	3.3	Red	Yellow
4. Methyl red	4.8	Red	Yellow
5. Neutral Red	6.8	Red	Yellow
6. Bromothymol Blue	7.2	Yellow	Blue

Figures 17-22 show the acid base distribution curves for the different mixed and component oxides. The data are given in Tables 48-53.

The strength of an acidic or basic site can be expressed in terms of the Hammett acidity function H_o [23]. It is measured by using indicators that are adsorbed on the solid surface. If acid sites of $H_o \leqslant$ Pka of the indicator exist on a solid surface, the colour of the indicator changes to that of its conjugate acid. When a neutral acid indicator is adsorbed on a basic solid, the colour of the indicator changes to that of its conjugate base, provided, the solid oxide has sufficient basic strength. Both acidity and basicity were determined on a common H_o scale. The acidity measured with an indicator shows the number of acidic sites whose acid strength $H_o \leqslant$ pKa of the indicator, and the basicity shows the number of basic sites whose basic strength $H_o \geqslant$ pKa of the indicator.

The acid-base strength distribution curves meet at a point on the abscissa, $H_{o,max}$ where acidity = bascity = 0 [24]. $H_{o,max}$ can be regarded as a practical parameter to represent the acid-base properties of solids, which is sensitive to the surface structure.

Fig. 17 Acid base strength distribution of $LaCrO_3$, $PrCrO_3$ & $SmCrO_3$

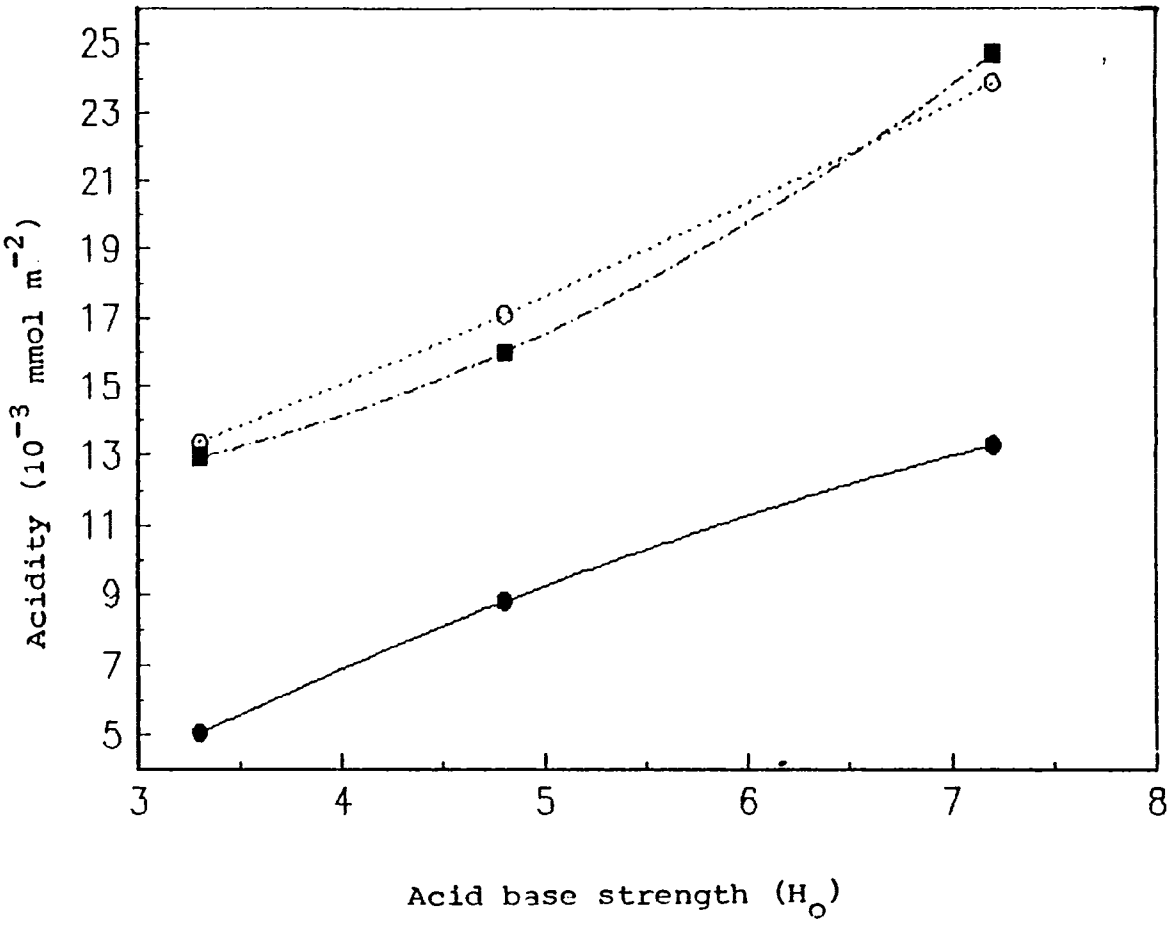

Fig. 18 Acid base strength distribution of
$LaMnO_3$ $PrMnO_3$ & $SmMnO_3$

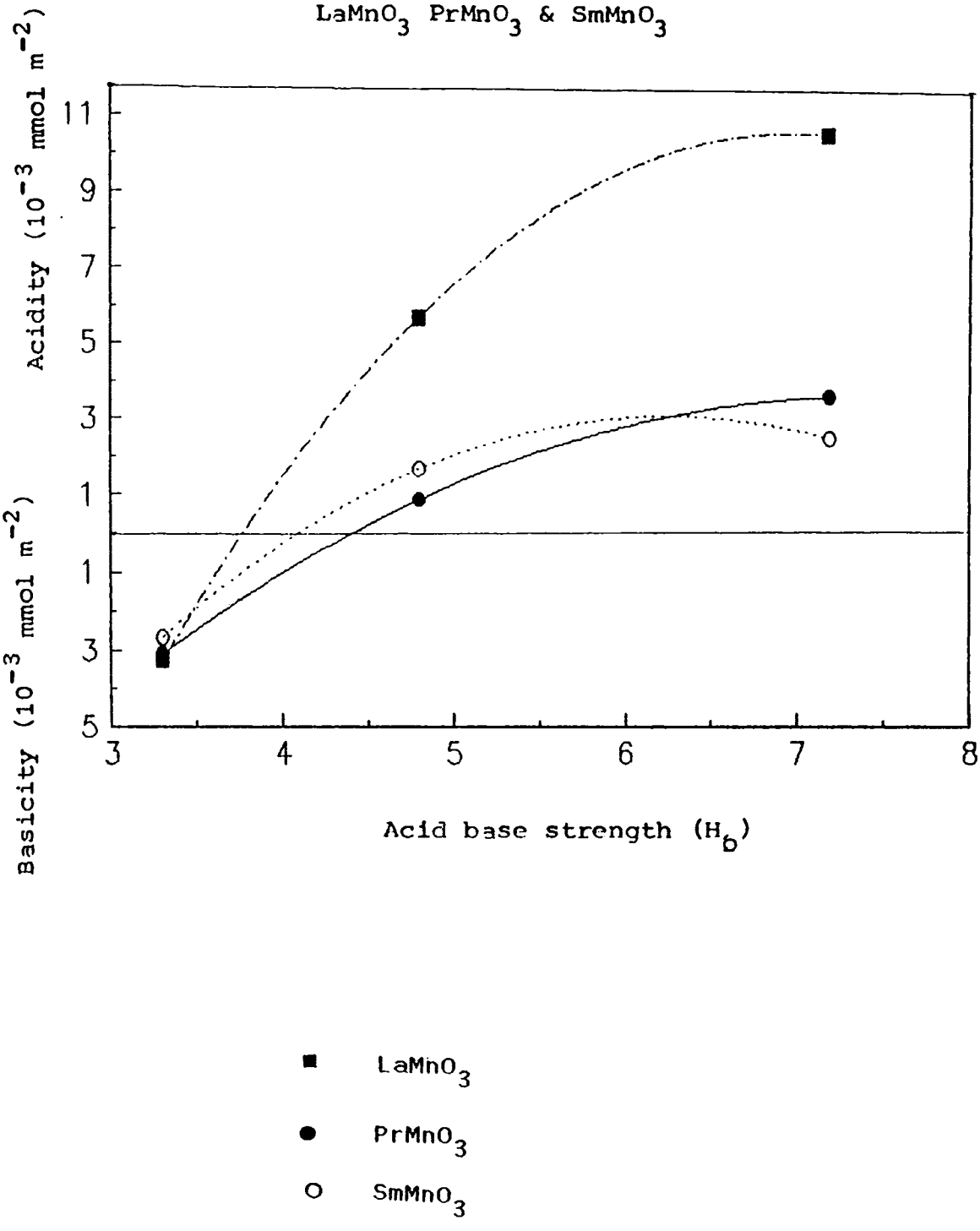

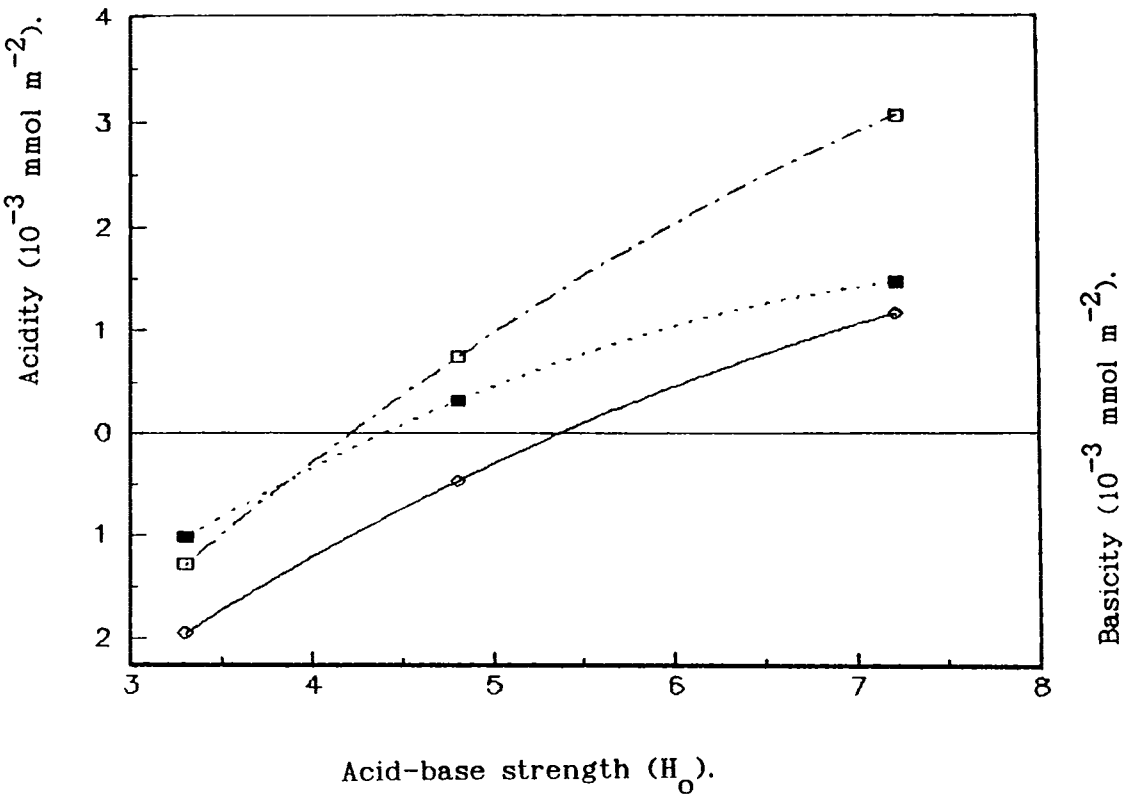

Fig. 19

Acid-base strength distribution curves for $LaFeO_3$, $PrFeO_3$, and $SmFeO_3$.

○ $LaFeO_3$

■ $PrFeO_3$

□ $SmFeO_3$

Fig. 20 Acid base strength distribution of $LaCoO_3$ $PrCoO_3$ & $SmCoO_3$

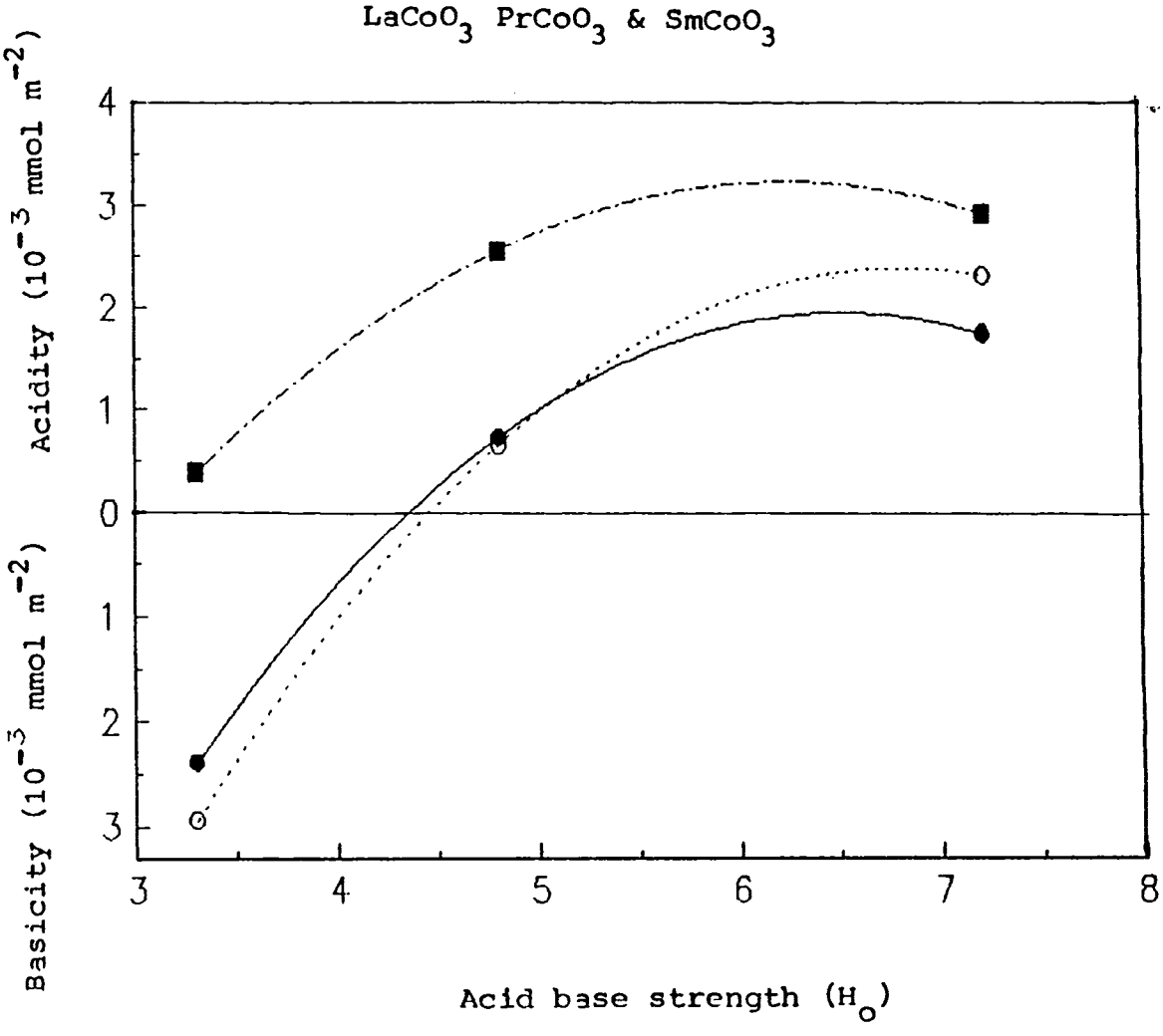

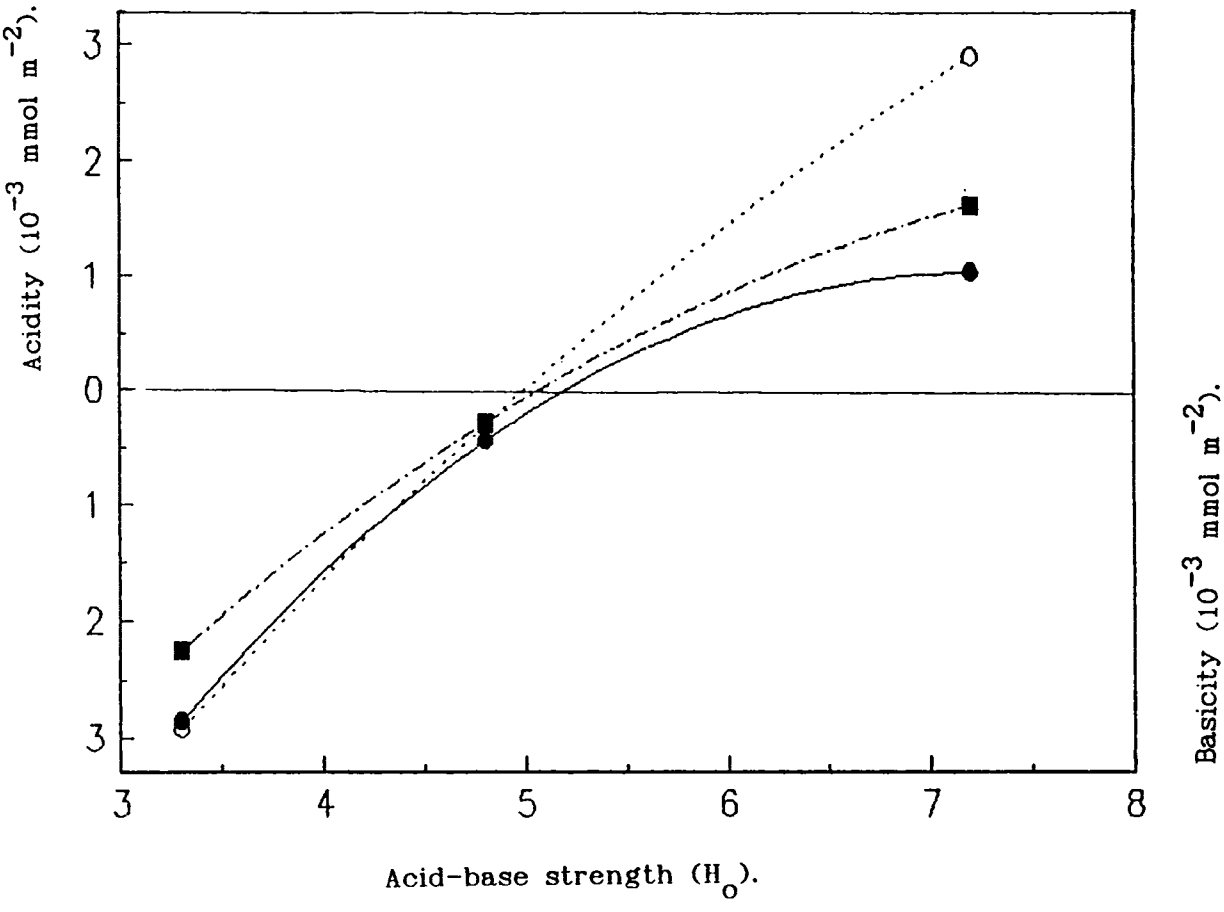

Fig. 21
Acid-base strength distribution curves for $LaNiO_3$, $PrNiO_3$, and SmNiO

● $LaNiO_3$
○ $PrNiO_3$
■ $SmNiO_3$

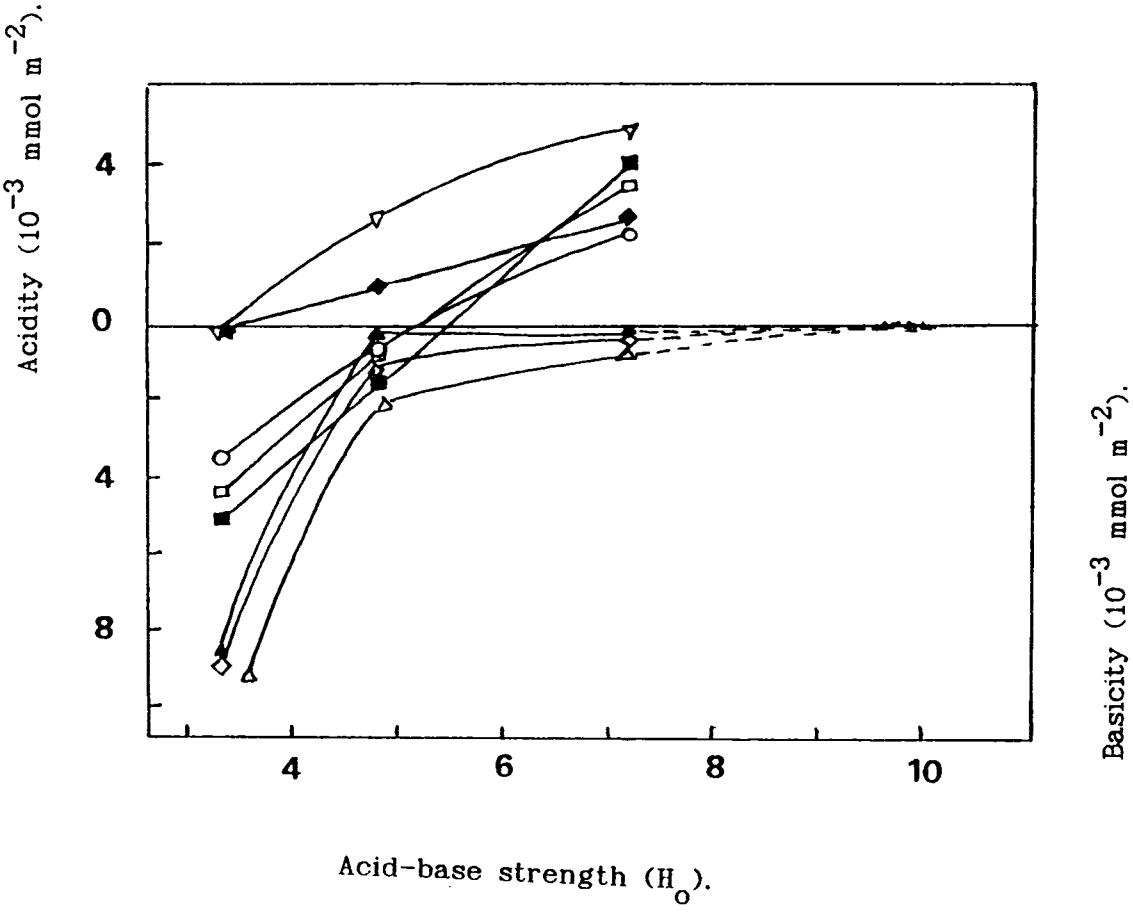

Fig. 22
Acid-base strength distribution curves for pure oxides

▽ Cr_2O_3
◆ MnO_2
□ Fe_2O_3
○ Co_3O_4
■ NiO
▲ La_2O_3
◇ Pr_6O_{11}
△ Sm_2O_3

Table- 48

Acidity / Basicity of $LaCrO_3$, $PrCrO_3$ and $SmCrO_3$.

Oxides	Basicity (10^{-3} meq m^{-2})			Acidity (10^{-3} meq m^{-2})			$H_{o,max}$
	H_o ≥3.3	H_o ≥4.8	H_o ≥7.2	H_o ≤3.3	H_o ≤4.8	H_o ≤7.2	
$LaCrO_3$	--	--	--	13.3	17.0	23.9	--
$PrCro_3$	--	--	--	12.9	16.0	24.7	--
$SmCro_3$	--	--	--	5.04	8.78	13.3	3.0

Table- 49

Acidity / Basicity of $LaMnO_3$, $PrMnO_3$ and $SmMnO_3$.

Oxides	Basicity (10^{-3} meq m^{-2})			Acidity (10^{-3} meq m^{-2})			$H_{o,max}$
	H_o ≥3.3	H_o ≥4.8	H_o ≥7.2	H_o ≤3.3	H_o ≤4.8	H_o ≤7.2	
$LaMnO_3$	3.27	--	--	--	5.63	10.6	3.6
$PrMnO_3$	3.09	--	--	--	0.84	3.54	4.8
$SmMnO_3$	2.67	--	--	--	1.64	2.44	4.0

Table- 50

Acidity / Basicity of $LaFeO_3$, $PrFeO_3$ and $SmFeO_3$.

Oxides	Basicity (10^{-3} meq m^{-2})			Acidity (10^{-3} meq m^{-2})			$H_{o,max}$
	H_o ≥3.3	H_o ≥4.8	H_o ≥7.2	H_o ≤3.3	H_o ≤4.8	H_o ≤7.2	
$LaFeO_3$	1.95	0.47	--	--	--	1.19	4.3
$PrFeO_3$	1.03	--	--	--	0.32	1.50	5.2
$SmFeO_3$	1.29	--	--	--	0.75	3.10	5.4

Table- 51

Acidity / Basicity of $LaCoO_3$, $PrCoO_3$ and $SmCoO_3$.

Oxides	Basicity (10^{-3} meq m^{-2})			Acidity (10^{-3} meq m^{-2})			$H_{o,max}$
	H_o ≥3.3	H_o ≥4.8	H_o ≥7.2	H_o ≤3.3	H_o ≤4.8	H_o ≤7.2	
$LaCoO_3$	2.39	--	--	--	0.72	1.72	4.2
$PrCoO_3$	2.94	--	--	--	0.63	2.31	4.3
$SmCoO_3$	--	--	--	0.38	2.55	2.91	3.1

Table-52

Acidity / Basicity of $LaNiO_3$, $PrNiO_3$ and $SmNiO_3$.

Oxides	Basicity (10^{-3} meq m^{-2})			Acidity (10^{-3} meq m^{-2})			$H_{o,max}$
	H_o ≥3.3	H_o ≥4.8	H_o ≥7.2	H_o ≤3.3	H_o ≤4.8	H_o ≤7.2	
$LaNiO_3$	2.85	0.45	--	--	--	1.03	4.8
$PrNiO_3$	2.92	0.31	--	--	--	2.90	5.1
$SmNiO_3$	2.25	0.29	--	--	--	1.61	4.9

Table-53

Acidity / Basicity of Pure Oxides.

Oxides	Basicity (10^{-3} meq m^{-2})			Acidity (10^{-3} meq m^{-2})			$H_{o,max}$
	H_o ≥3.3	H_o ≥4.8	H_o ≥7.2	H_o ≤3.3	H_o ≤4.8	H_o ≤7.2	
La_2O_3	8.3	0.21	0.10	--	--	--	9.8
Pr_6O_{11}	9.2	1.80	0.50	--	--	--	9.4
Sm_2O_3	9.3	2.50	1.80	--	--	--	9.6
Cr_2O_3	0.16	--	--	--	2.74	4.96	3.3
MnO_2	0.20	--	--	--	0.93	2.76	3.5
Fe_2O_3	4.38	0.82	--	--	--	3.50	4.8
Co_3O_4	3.47	0.66	--	--	--	2.31	4.8
NiO	5.09	1.55	--	--	--	4.07	5.2

It is known that a solid with a large negative $H_{o,max}$ value has weak basic sites and that a solid with a large positive $H_{o,max}$ value has strong basic sites [24]. From the Tables 48-53, it is clear that the mixed and transition metal oxides are more acidic than the rare earth oxides, as indicated by the lower $H_{o,max}$ values.

4.3 CATALYTIC ACTIVITY

In order to correlate electron donating and acid base properties of the oxides with their catalytic activity, the following reactions were studied.

1. Reduction of cyclohexanone in isopropanol medium

2. Oxidation of cyclohexanol in presence of benzophenone

3. Esterification of acetic acid with 1-butanol

When a ketone in the presence of a base is used as the oxidising agent, the reaction is known as Oppenauer oxidation. This reaction is the reverse of Meerwein-Ponndorf Verley type reduction of ketones. Oppenauer oxidation of secondary alcohols proceeds efficiently using benzophenone as the hydrogen acceptor [25]. It has high

ability for oxidising the alcohol and to resist aldol condensation [26]. The catalytic activity of these oxides can be rationalized in terms of the mechanism (Scheme 1) proposed by Shibagaki et al. [27] for oxidation and reduction using ZrO_2 as the catalyst.

It has already been established from primary kinetic isotope effect studies that k_3 is the rate determining step [27]. The mechanism involves hydride ion transfer from alcohol to the carbonyl carbon of the ketone. Lewis basicity of the catalyst surface favours the hydride ion transfer from alcohol to the carbonyl carbon of the ketone. ABO_3 type oxides alongwith the rare earth oxides are found to be effective catalysts for the oxidation-reduction reactions. Data are given in Tables 54 and 55.

A mechanism has been proposed for the esterification of acetic acid with 1-butanol (Scheme II) using ZrO_2 as catalyst [28]. It has already been reported that the rate determining step is the step subsequent to the adsorption of the carboxylic acid and alcohol on the catalyst. The data are given in Table 56. Rare earth oxides owing to their high basicity are not at all catalysing the reaction. But, perovskite type oxides,

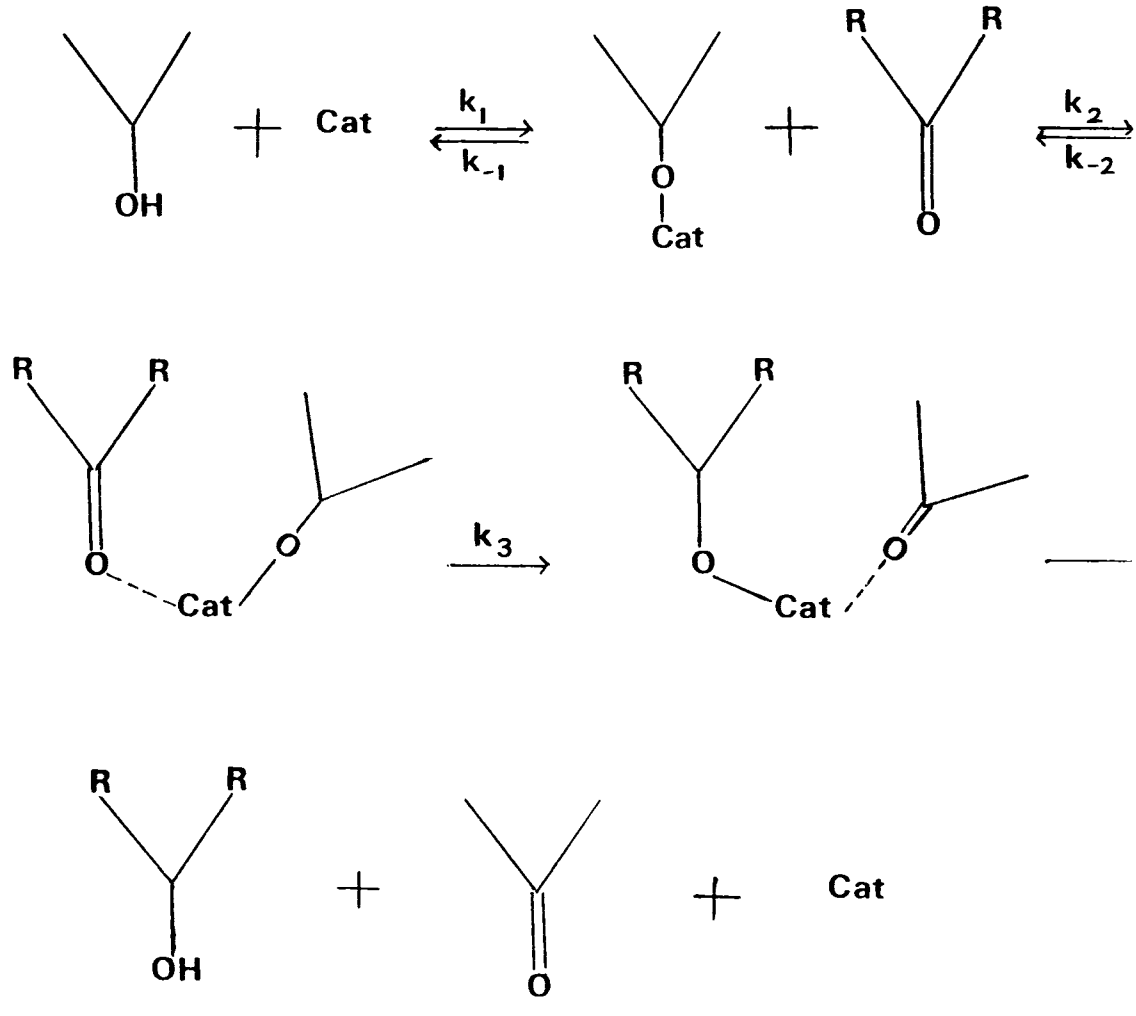

Scheme 1

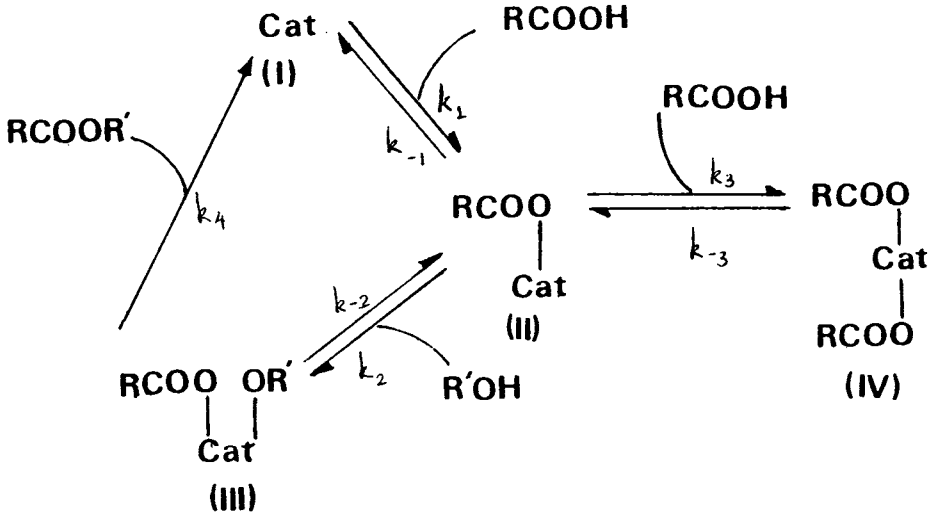
Cat
(I)
RCOOH
RCOOR'
k_1
k_{-1}
k_4
RCOOH
k_3
RCOO
Cat
(II)
k_{-3}
RCOO
Cat
RCOO
(IV)
k_{-2}
k_2
RCOO OR'
Cat
(III)
R'OH

Scheme II

Table- 54

Reduction of cyclohexanone to cyclohexanol in 2-propanol medium.

Oxide	Conversion %	Rate constant ($10^{-6}s^{-1}m^{-2}$)
$LaCrO_3$	—	—
$PrCrO_3$	—	—
$SmCrO_3$	—	—
$LaMnO_3$	—	—
$PrMnO_3$	—	—
$SmMnO_3$	—	—
$LaFeO_3$	87.44	2.67
$PrFeO_3$	14.84	0.16
$SmFeO_3$	20.14	0.24
$LaCoO_3$	40.14	1.92
$PrCoO_3$	32.68	2.48
$SmCoO_3$	31.70	3.13
$LaNiO_3$	3.0	0.01
$PrNiO_3$	0.96	0.03
$SmNiO_3$	3.31	0.06
Cr_2O_3	—	—
MnO_2	—	—
Fe_2O_3	2.12	0.01
Co_3O_4	—	—
NiO	—	—
La_2O_3	96.0	1.28
Pr_6O_{11}	90.13	2.76
Sm_2O_3	87.0	1.46

Table- 55

Oxidation of cyclohexanol to cyclohexanone with benzophenone.

Oxide	Conversion %	Rate constant ($10^{-6}s^{-1}m^{-2}$)
$LaCrO_3$	70.33	6.55
$PrCrO_3$	3.09	0.18
$SmCrO_3$	18.95	0.40
$LaMnO_3$	4.66	0.08
$PrMnO_3$	—	—
$SmMnO_3$	—	—
$LaFeO_3$	53.07	0.85
$PrFeO_3$	23.42	0.24
$SmFeO_3$	13.05	0.16
$LaCoO_3$	35.63	0.12
$PrCoO_3$	15.63	0.13
$SmCoO_3$	32.64	1.06
$LaNiO_3$	20.13	0.51
$PrNiO_3$	18.14	1.03
$SmNiO_3$	33.51	0.58
Cr_2O_3	61.60	0.86
MnO_2	8.50	0.04
Fe_2O_3	36.75	0.07
Co_3O_4	17.1	0.08
NiO	4.72	0.01
La_2O_3	97.23	1.34
Pr_6O_{11}	94.74	3.80
Sm_2O_3	93.69	1.78

Table- 56

Esterification of acetic acid with 1-butanol.

Oxide	Conversion %	Rate constant ($10^{-6}s^{-1}m^{-2}$)
$LaCrO_3$	17.39	2.48
$PrCrO_3$	37.20	5.68
$SmCrO_3$	18.95	0.44
$LaMnO_3$	29.40	1.35
$PrMnO_3$	20.81	0.57
$SmMnO_3$	12.01	0.66
$LaFeO_3$	35.30	1.25
$PrFeO_3$	18.96	0.45
$SmFeO_3$	19.76	1.68
$LaCoO_3$	11.92	1.35
$PrCoO_3$	16.14	2.72
$SmCoO_3$	9.27	0.63
$LaNiO_3$	3.14	—
$PrNiO_3$	16.25	1.31
$SmNiO_3$	9.19	0.67
Cr_2O_3	57.6	3.92
MnO_2	54.1	2.10
Fe_2O_3	14.09	0.84
Co_3O_4	1.92	0.01
NiO	36.03	4.33
La_2O_3	—	—
Pr_6O_{11}	—	—
Sm_2O_3	—	—

together with the component transition metal oxides are catalysing the reaction effectively.

The rare earth oxides have greater electron donor property and higher $H_{o,max}$ value compared to the perovskite oxides and transition metal oxides. The higher catalytic activity of these oxides for the oxidation/reduction reactions, which is a base-catalysed reaction, is in agreement with the above observation.

A distinct separation of the functions of the transition and rare-earth metal cations is observed for some perovskites [29]. The activities of the oxides are governed by the transition metal cations at high temperatures and by the rare-earth ions at low temperatures.

The perovskite oxides and the component transition metal oxides which were found to have lower $H_{o,max}$ value compared to the rare earth oxides are efficient catalysts for the esterification reaction, which is an acid catalysed reaction, while the rare earth oxides are not at all giving the reaction. The presence of co-ordinatively unsaturated cationic sites (Lewis acidity) on $LaCrO_3$ surface was

reported by Fierro et al. [30]. These sites which are unstable and of high reactivity should play an important role in catalysis.

The transition metal oxides have sufficient electron donor sites with various electron donor strength. But all of them are not effective in catalysing the reaction, which results in a low catalytic activity. By incorporating the rare earth oxide into it, the activity is increased by increasing the concentration of the active sites.

The activity of these oxides are in agreement with the electron donor and acid-base properties.

REFERENCES

1. D.B. Meadowcroft : *Nature*, 266, 847 (1970).

2. W.F. Libby : *Science*, 171, 499 (1971).

3. K.R.P. Sabu, K.V.C. Rao and C.G.R. Nair : *Bull. Chem. Soc. Jpn.*, 64, 1926 (1991).

4. K.R.P. Sabu, K.V.C. Rao and C.G.R. Nair : *Bull. Chem. Soc. Jpn.*, 64, 1920 (1991).

5. H. Nakabayashi : *Bull. Chem. Soc. Jpn.*, 65, 914 (1992).

6. S. Sugunan and K.B. Sherly : *React. Kinet. Catal. Lett.*, 51 (2), 533 (1993).

7. S. Sugunan and J.M. Jalaja : *Indian J. Chem.*, 34 A, 216 (1995).

8. S. Sugunan and J.M. Jalaja : *React. Kinet. Catal. Lett.*, (in press).

9. K. Esumi, K. Miyata and K. Meguro : *Bull. Chem. Soc. Jpn.*, 58, 3524 (1985).

10. K. Esumi, K. Miyata F. Waki and K. Meguro : *Bull. Chem. Soc. Jpn.*, 59, 3363 (1986).

11. K. Esumi, K. Miyata F. Waki and K. Meguro : *Colloids and Surfaces*, 20, 81 (1986).

12. M. Che, C. Naccache and B. Imelik : *J. Catal.*, 24, 328 (1972).

13. D.S. Acker and W.R. Hertler : *J. Am. Chem. Soc.*, 84, 328 (1962).

14. R.H. Boyd and W.D. Phillips : *J. Chem. Phys.*, 43, 2927 (1965).

15. R. Foster and T.J. Thomson : *Trans. Faraday Soc.*, 58, 860 (1962).

16. H. Hosaka, T.Fujiwara and K. Meguro : *Bull. Chem. Soc. Jpn.*, 44, 2616 (1971).

17. K.Esumi and K. Meguro : *J. Japan Color Material.*, 48, 539 (1975).

18. K. Meguro and K.Esumi : *J. Colloid Interface Sci.*, 59, 93 (1973).

19. M. Crespin and W.K. Hall : *J. Catal.*, 69, 359 (1981).

20. B.D. Flockhart, J.A.N. Scott and R.C. Pink : *Trans. Faraday Soc.*, 62, 730 (1966).

21. G.V. Fomin, L.A. Blyumenfield and V.I. Sukhorukov : *Proc. Acad. Sci.*, USSR, 157, 819 (1964).

22. M.L. Hair and W. Hertler : *J. Phys. Chem.*, 74, 91 (1970).

23. L.P. Hammett and A.J. Deyrup : *J. Am. Chem Soc.*, 54, 2721 (1932).

24. T. Yamanaka and K. Tanabe : *J. Phys. Chem.*, 80, 1725 (1976).

25. H. Kuno, T. Takahashi, M. Shibagaki and H. Matsushita : *Bull. Chem. Soc. Jpn.*, 63, 1943 (1990).

26. H. Kuno, T. Takahashi, M. Shibagaki and H. Matsushita : *Bull. Chem. Soc. Jpn.*, 64, 312 (1991).

27. M. Shibagaki, T. Takahashi, and H. Matsushita : *Bull. Chem. Soc. Jpn.*, 61, 328 (1988).

28. T. Takahashi, M. Shibagaki and H. Matsushita : *Bull. Chem. Soc. Jpn.*, 62, 2353 (1989).

29. L.A. Sazonov, Z.V. Moskvina and E.V. Artamonov : *Kinet.*

Catal., 15, 100 (1974).

30. J.L.G. Fierro and L.G. Tejuka : *J. Chem. Tech. Biotechnol.*, 34 A, 29 (1984).

CONCLUSIONS

The investigations carried out to study the electron donor, acid-base properties and the catalytic activity of ABO_3-type oxides (A = La, Pr and Sm and B = Cr, Mn, Fe, Co and Ni) along with the component rare earth and 3d transition metal oxides lead to the following conclusions

1. The amount of electron acceptors adsorbed on the oxide surface depends upon the basicity of the solvent and the electron affinity of the electron aceptors.

2. The limit of electron transfer in terms of the electron affinity (eV) of the acceptors is between 2.40 and 2.84 for mixed oxides and transition metal oxides, and between 1.77 and 2.40 for the rare earth oxides.

3. The mixed oxides and the component transition metal oxides are found to be more acidic than the component rere earth oxides, as indicated by the lower $H_{o,max}$ values.

4. Transition metal oxides are found to be poor catalysts for the Meerwein-Ponndorf-Verley type reduction of cyclohexanone and the reverse reaction (Oppneauer oxidation) of cyclohexanol. By incorporating the rare earth oxides, the mixed oxides are found to be more effective in catalysing both the reactions.

5. Rare earth oxides, owing to their high basicity, are not at all catalysing the esterification, which is an acid catalysed reaction, while, the ABO_3-type oxides, together with the 3d transition metal oxides are catalysing the reaction effectively.

6. Lewis acidity is proposed to play an important role in the catalytic activity of the mixed oxides.

LIST OF PAPERS PUBLISHED/COMMUNICATED

Journal Papers

1. S. Sugunan and V. Meera; "Electron donating property and catalytic activity of perovskite-type mixed oxides (ABO_3) consisting of rare earth and 3d transition metals", *J. Mater. Sci. Technol.*, 11, 229 (1995).

2. S. Sugunan and V. Meera; "Catalytic activity of some of the perovskite-type mixed oxides (ABO_3) consisting of rare earth and 3d transition metals", *Indian J. Chem.*, (in press).

3. S. Sugunan and V. Meera; "Electron donating, acid-base and catalytic properties of Perovskite-type mixed oxides of rare earths",*Collect. Czech. Chem. Commun.*, Vol 60, (1995, in press)

4. S. Sugunan and V. Meera; "Acid-base properties and catalytic activity of ABO_3 (perovskite-type) oxides consisting of rare earth and 3d transition metals", (communicated to *React. Kinet. Catal. Lett.*).

Symposium Papers

1. S. Sugunan and V. Meera; "Electron donating property and catalytic activity of Perovskite-type mixed oxides (ABO_3) consisting

of rare earth and 3d transition metals", *Proceedings of the 12th National Symposium on Catalysis,* p 63, 1994 (Organised by *Catalysis Society of India,* held in BARC, Bombay).